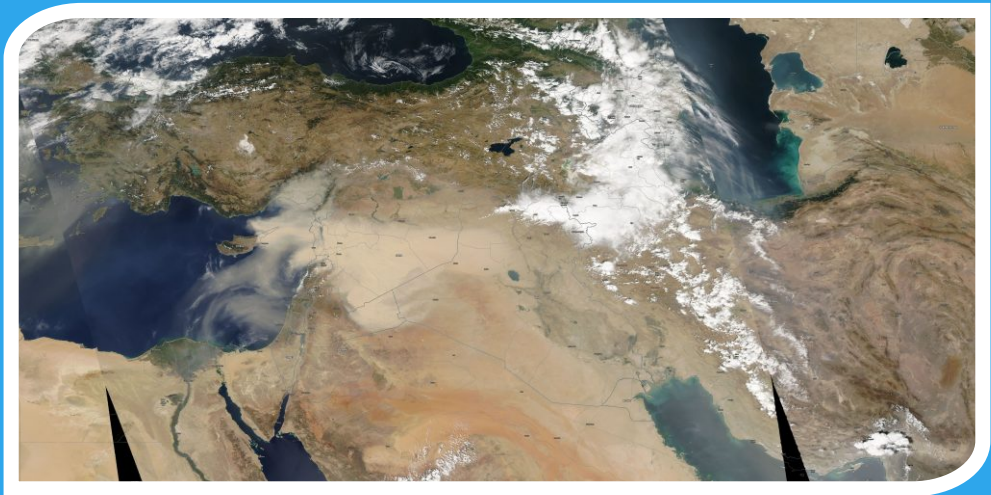




5th INTERNATIONAL WORKSHOP ON SAND AND DUST STORMS

(DUST SOURCES AND THEIR IMPACTS IN THE MIDDLE EAST)
23-25 October 2017, Istanbul, TURKEY

PROCEEDINGS



SUPPORTING ORGANIZATIONS



5th INTERNATIONAL WORKSHOP ON SAND AND DUST STORMS
(Dust Sources and their Impacts in the Middle East)
23-25 October 2017, Istanbul, TURKEY

October 23, 2017 - Monday

SDS, Dust Sources and Dust-Climate-Drought Interaction

TIME	SUBJECT	SPEAKER
08:30-09:30	Registration	
09:30-10:30	Opening Speeches <i>Introduction Films of TSMS and ÇEM</i> M. Mustafa GÖZÜKARA, <i>General Director of Combating Desertification and Erosion (ÇEM)</i> İsmail GÜNEŞ, <i>Director General of Turkish State Meteorological Service (TSMS)</i> Utchang KANG, <i>United Nations Convention to Combat Desertification (UNCCD)</i> Gemma SHEPHERD, <i>United Nations Environmental Programme (UNEP)</i> Enric TERRADELLAS, <i>World Meteorological Organization (WMO)</i> Prof. Dr. Mehmet KARACA, <i>Rector of Istanbul Technical University (ITU)</i> Prof. Dr. Veysel EROĞLU, <i>Minister of Forestry and Water Affairs</i>	
	SESSION I	MODERATOR - Dr. Emin ÖZSOY
10:30-10:50	SDS Warning Advisory and Assessment System (SDS-WAS)	Enric TERRADELLAS, <i>Spanish Meteorological Agency (AEMET)</i>
10:50-11:20	COFFEE BREAK	
11:20-11:40	SDS-WAS Regional Cooperation in the Middle East	Dr. Tareq HUSSEIN, <i>University of Jordan</i>
11:40-12:00	Drought Evaluation over the Middle East	Dr. Abdullah CEYLAN, <i>TSMS, Turkey</i>
12:00-12:20	Climate-Dust Interaction in the Middle East	Dr. Ali AL-DOUSARI, <i>Kuwait Institute for Scientific Research</i>
12:20-13:00	Group Discussion and Group Report	
13:00-14:00	LUNCH	

	SESSION II	MODERATOR - Dr. Ali AL-DOUSARI
14:00-14:20	Standard Aerosol Optical Depth Index (SAODI) and Application in the Middle East	Zekâi ŞEN, <i>Turkish Water Foundation (TWF)</i>
14:20-14:40	Methodology Framework for SDS Sources Identification	Dr. Ali DARVISHI, <i>University of Tehran, Iran</i>
14:40-15:00	Monitoring the Changes in the Mesopotamian Marshlands during Drought Periods	Dr. Orkan OZCAN, <i>ITU Eurasia Institute of Earth Sciences, Turkey</i>
15:00-15:30	COFFEE BREAK	
15:30-15:50	Sand and Dust Storm Sources in Kuwait	Dr. Mohamed F. YASSIN, <i>Kuwait Institute for Scientific Research</i>
15:50-16:10	Change of Water Masses-Dust Storms Interaction in Syria and Iraq	Dr. Halil GUNEK, <i>Firat University, Turkey</i>
16:10-16:30	Frequent Interval of Sand and Dust Storms in Jordan	Dr. Ziyad BALASMEH, <i>Jordan Meteorological Department</i>
16:30-17:30	Group Discussion and Group Report	

October 24, 2017 - Tuesday

Monitoring and Forecast of SDS

TIME	SUBJECT	SPEAKER
	SESSION III	MODERATOR - Dr. Murat TÜRKEŞ
09:00-09:20	Climatology and Spatiotemporal Variations of Synoptic Meteorological Dust Events Observed over the Middle East and Surrounding Regions during the 2003-2016 Period	Dr. Murat TÜRKEŞ, <i>Center for Climate Change and Policy Studies, Boğaziçi University, Turkey</i>
09:20-09:40	Ground Observation of Dust	Dr. Sergio RODRIGUEZ, <i>Spanish Meteorological Agency (AEMET)</i>
09:40-10:00	EUMETSAT SDS Products for the Middle East	José PRIETO, <i>EUMETSAT</i>
10:00-10:30	COFFEE BREAK	



10:30-10:50	Challenges and Perspectives in Dust Modeling	Dr. Carlos PEREZ, <i>Barcelona Supercomputing Center (BSC)</i>
10:50-11:10	High Resolution SDS Forecast Requirement for the Middle East	Dr. Sara BASART, <i>Barcelona Supercomputing Center (BSC)</i>
11:10-11:30	SDS-WAS: Ensemble Prediction of Airborne Dust	Gerardo García-CASTRILLO, <i>Spanish Meteorological Agency (AEMET)</i>
11:30-12:15	Group Discussion and Group Report	
12:15-13:30	LUNCH	
	SESSION IV	MODERATOR - Dr. Carlos PEREZ
13:30-13:50	Analysis of Sand and Dust Storms (SDS) between the years 2003 and 2016 in the Middle East	Cihan DÜNDAR, <i>TSMS, Turkey</i>
13:50-14:10	Analysis of DOD and Dust Emissions over the Middle East by using CAMS	Dr. Richard ENGELEN, <i>ECMWF</i>
14:10-14:30	Dust Variability in the Middle East Recorded in the Elbrus Mt. Ice Core.	Dr. Stanislav KUTUZOV, <i>Russian Academy of Sciences, Moscow</i>
14:30-15:00	COFFEE BREAK	
15:00-15:20	Contribution of Desert Dust Transport to Daily PM ₁₀ Concentrations in Aksaray, Istanbul: A long-term study	Dr. Rosa Maria FLORES, <i>Marmara University, Turkey</i>
15:20-15:40	Dust Sources and Monitoring the Changes on the Sources over the Middle East	Hassan HERSI, <i>Africa Nature Conservation Organization, Somalia</i>
15:40-16:00	15 Years View of Aerosol Dust over the Middle East	Dr. Saviz SEHATKASHANI, <i>Atmospheric Science and Meteorological Research Center, Iran</i>
16:00-17:00	Group Discussion and Group Report	

October 25, 2017 - Wednesday

Impacts of SDS

TIME	SUBJECT		SPEAKER
	SESSION V	MODERATOR-Dr. Moutaz Al-DABBAS	
09:00-09:20	Health Effects of SDS Focusing on the Middle East		Dr. Mazen MALKAWI, <i>World Health Organization (WHO)</i>
09:20-09:40	The Effects of SDS Events on the Chemical Composition of Particulate Matter in the Middle East		Dr. Najat SALIBA, <i>American University of Beirut, Lebanon</i>
09:40-10:00	Evaluation of the Effects of Settled Desert Dust on Socioeconomic Activities in Turkey on the Basis of Some Provinces in the SE Anatolian Region		Dr. Taner ŞENGÜN, <i>Firat University, Turkey</i>
10:00-10:30	COFFEE BREAK		
10:30-10:50	The Mineralogical and Micro-Organisms Effects of Regional Dust Storms over the Middle East		Dr. Moutaz AL-DABBAS, <i>University of Baghdad, Iraq</i>
10:50-11:10	Review of Dust Control Projects in Ahwaz, Iran and Solutions toward Sustainable Development		Ali HAMIDIAN, <i>University of Tehran, Iran</i>
11:10-11:30	Monitoring of Irrigable Agricultural Lands in Euphrates-Tigris River Basin (Syria-Iraq)		Dr. Ayhan ATEŞOĞLU, <i>Bartın University, Turkey</i>
11:30-12:00	Group Discussion and Group Report		
12:00-13:30	Preparation of Workshop Report and Closure	MODERATOR- Enric TERRADELLAS Chairs and Reporters Session	
13:30-14:30	LUNCH		

Sand and Dust Storm - Warning Advisory and Assessment System

Enric Terradellas

AEMET, Barcelona, Spain, eterradellasj@aemet.es

Abstract

Given the important impacts of airborne dust on human health, the environment and diverse socio-economic sectors, in 2007, the World Meteorological Organization endorsed the launching of the Sand and Dust Storm - Warning Advisory and Assessment System (SDS-WAS) with the mission to enhance the ability of countries to deliver timely and high-quality sand and dust storm forecasts, observations, information and knowledge to users. This paper describes SDS-WAS' mission, organization and objectives, highlights its transition from R&D to operational forecast services and postulates the implementation of future dust early warning systems.

1. Introduction

Sand and dust storms are common hazards in arid and semi-arid regions of the planet. They occur when strong or very turbulent winds blow over dry, sparsely vegetated soils and lift loose particles from the Earth's surface to the atmosphere. The concentration of airborne particles increases rapidly and the visibility drops to few meters. The sand and dust storms occur mostly on the belt of tropical and subtropical deserts of the northern hemisphere, stretching from the Sahara through the Middle East to the Great Indian Desert, as well as on the mid-latitude deserts of Central Asia and China-Mongolia (Terradellas et al., 2017).

Between 1,000 and 3,000 megatons of particles are emitted annually to the atmosphere, where the finer fraction may be transported downwind over long distances, even across continents (Prospero and Nees, 1986). Airborne sand and dust is detrimental to human health, ecosystems and diverse socio-economic sectors. Impacts on health include respiratory and cardiovascular problems, eye infections and, in some regions, infectious diseases such as meningitis and valley fever (Goudie, 2014). Dust also can carry irritating spores, bacteria, viruses and persistent organic pollutants. Other impacts include negative effects on ground transport, aviation, agriculture and solar power plants.

It is necessary to mention that dust, especially once deposited back to the Earth's surface, has also positive environmental impacts, since it provides nutrients to terrestrial and oceanic ecosystems, boosting primary productivity. Many ocean biota, such as phytoplankton, are iron limited, such that the supply of bioavailable iron by the dust deposition enhances ocean productivity (Jickells et al. 2005). Similarly, the long-term productivity of many land ecosystems, for example the Amazon rainforest, is limited by the availability of phosphorus (Chadwick et al., 1999, Okin et al. 2004), such that the deposition of dust-borne phosphorus is often critical for ecosystem productivity.

Airborne dust affects weather and climate through a wide range of interactions. These include scattering and absorbing radiation, lowering snowpack albedo, altering atmospheric CO₂ concentrations by modulating ecosystem productivity, and serving as cloud nuclei and thereby likely increasing cloud lifetime and reflectivity (Andreae and Rosenfeld, 2008). Since mineral dust therefore affects Earth's radiation balance, changes in the atmospheric dust loading can produce a substantial radiative forcing (Tegen et al., 1996; Sokolik and Toon, 1996; Mahowald et al., 2006, 2010). Conversely, the global dust cycle is also highly sensitive to changes in climate, as evidenced by the several times larger global dust deposition rate during glacial maxima than during interglacials (Rea 1994, Kohfeld and Harrison, 2001).

The scientific community is aware that a significant part of the dust emission is the consequence of human-induced factors such as poor agricultural practices or land and water mismanagement. However, there is a great deal of uncertainty about the percentage it represents versus the total emission. There are also contradictory conclusions about the long-term trend of dust emissions, especially in relation to land use and climate change. Conversely, it is necessary to clarify on how changes in dust emissions may impact the atmosphere, climate and oceans in the future.

Over the last decades, the social interest and the eagerness of the research community to better understand the physical processes associated with the dust cycle, to predict future events and to prevent their undesired impacts has increased rapidly. This paper describes the response of the World Meteorological Organization (WMO) to the problems associated with suspended dust. The trans-boundary nature of the dust cycle makes international co-operation essential. In addition, this is a multidisciplinary

phenomenon, and coordination with other United Nations agencies and programs is absolutely necessary.

2. Sand and Dust Storm – Warning Advisory and Assessment System

Recognizing the importance for multiple societal sectors around the world to better understand and monitor atmospheric sand and dust, in 2007, the WMO endorsed the launching of the Sand and Dust Storm - Warning Advisory and Assessment System (SDS-WAS) with the mission to enhance the ability of countries to deliver timely and high-quality sand and dust storm forecasts, observations, information and knowledge to users through an international partnership of research and operational communities (Terradellas et al., 2015).

The SDS-WAS works as an international network of research, operational centres and users, organized through regional nodes and coordinated by the SDS-WAS Steering Committee (Nickovic et al., 2015). Three regional nodes are currently in operation:

- Northern Africa, Middle East and Europe (NAMEE), coordinated by a Regional Center in Barcelona, Spain, hosted by the State Meteorological Agency (AEMET) and the Barcelona Supercomputing Center (BSC): <https://sds-was.aemet.es>.
- Asia, coordinated by a Regional Center in Beijing, China, hosted by the China Meteorological Administration (CMA): http://eng.nmc.cn/sds_was.asian_rc/.
- Pan-America, coordinated by a Regional Center in Bridgetown, Barbados, hosted by the Caribbean Institute for Meteorology and Hydrology (CIMH): <http://sds-was.cimh.edu.bb/>.
- The SDS-WAS Science and Implementation Plan (Nickovic et al., 2014) identifies the following objectives as the axis around which the activities of SDS-WAS shall be articulated during the period 2015-2020:
- Facilitating collaboration and coordination at regional and global scale between SDS-WAS partners and initiating joint research projects for improving dust observations and modelling.
- Encouraging experimental provision of near-real-time forecasts, models validation and models intercomparison.
- In collaboration with other WMO technical commissions, supporting

transfer of the SDS-WAS research observational and forecasting facilities to operational technology and to applications relevant for users.

- Providing training on use of the SDS-WAS research outcomes.
- Building bridges between SDS-WAS and other communities conducting aerosol-related studies (air quality, biomass burning, etc.).
- Participating in international multi-disciplinary research initiatives.
- Establishing links with the EU-funded Copernicus Atmosphere and Monitoring Services, satellite agencies and ground-based observing networks

3. Motivation for a Regional Center in West Asia

The Middle East is the second largest source of global dust after the Sahara desert, but, unlike North Africa, where large population centres are concentrated along the coasts of the Mediterranean and the Atlantic Ocean, relatively far away from dust sources, much of the population in West Asia lives inside, or in the vicinity of, dust sources. The dust impact on health, on ecosystems and on many economic and social activities is therefore of utmost importance. Furthermore, the usual coexistence of desert mineral dust with industrial aerosols from petrochemical activities constitutes an additional challenging problem (Cuevas, 2013).

The complex mixture of natural and anthropogenic sources is extensively described in Ginoux et al. (2012). Many of these sources are closely related to land degradation and overuse of water resources, so that many countries in the region have suffered a sharp increase in dust cases in recent years (Cuevas, 2013). The transport of airborne dust turns local changes in the soil conditions into a serious trans-boundary environmental problem that can only be addressed through international information exchange and cooperation to implement early warning systems, adopt preparedness and adaptation policies and take effective measures for mitigation.

The future is also worrisome, because global warming has the potential to cause major changes in dust emissions. The International Panel on Climate Change (Solomon, 2007; Stocker, 2014) suggests that, under most scenarios, many dry-land areas will suffer from lower rainfall regimes and drier terrains because of higher rates of evapotranspiration. Therefore,

there is a likelihood of increased dust storm activity, though this conclusion depends on how winds may change - a matter of great uncertainty.

All these particular circumstances encourage the creation of a SDS-WAS regional node for West Asia. National Meteorological and Hydrological Services (NMHS), environment protection agencies, health institutions, aviation authorities, energy departments, marine resources and fishery agencies, wildlife, forestry and agriculture agencies, disaster risk and civil protection agencies, research institutions and universities should participate in this SDS-WAS regional node as contributors and/or as specialized users.

The Turkish State Meteorological Service (TSMS) and the Islamic Republic of Iran Meteorological Organization (IRIMO) have recently expressed their willingness to host the SDS-WAS Regional Center for West Asia and the SDS-WAS Regional Center for NAMEE is ready to support its implementation.

4. Dust monitoring

There are many complementary ways of observing airborne dust. In this Section, we focus on the most suitable observational methods for monitoring and now-casting dust events, leaving aside techniques commonly used for data assimilation into numerical models, verification of dust predictions, investigation of the physical processes involved in the dust cycle or impact assessment.

The main objective of the SDS-WAS Regional Centers is to facilitate user access, particularly for NMHSs, to observational and forecast products. Operational meteorologists typically use products generated from measurements performed by instruments on board geostationary satellites for dust monitoring and now-casting. These products have the advantages of large spatial coverage (regional to global) and regular observations, which can be made available to weather centres in near-real-time. However, the application of satellite products (Figure 1) to monitor dust events faces several problems and must be complemented with in-situ measurements. In this sense, the air quality monitoring stations and the ordinary meteorological stations play a fundamental role. Unfortunately, there is still no protocol for the international exchange of air quality data, unlike that for meteorological data, which has been in force for more than 50 years.

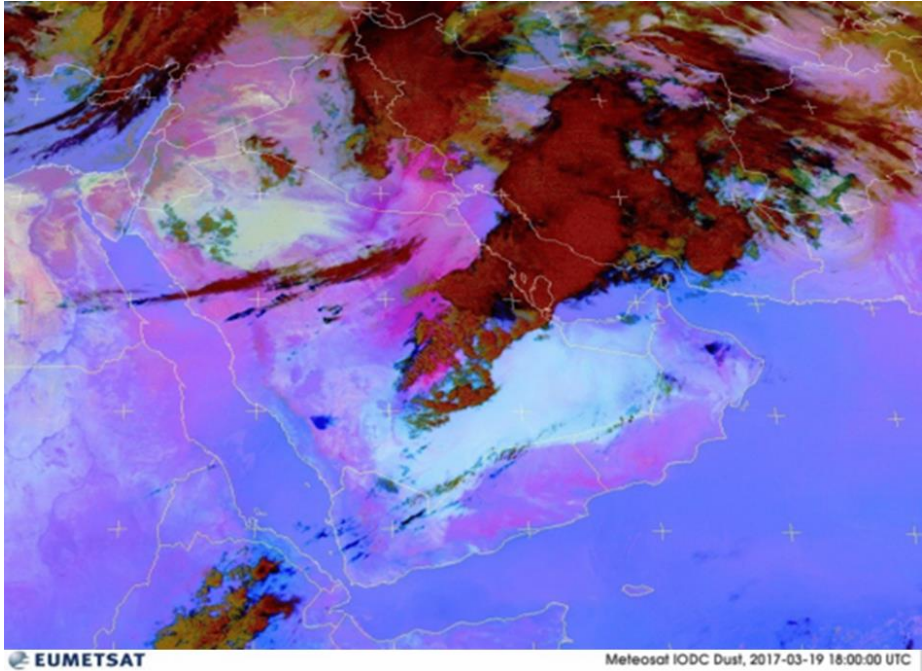


Figure 1. EUMETSAT RGB-Dust product of 19 Mar 2017 at 18:00 UTC. Sandstorm 'Madar' originated in Northern Africa disrupted life in West Asia

5. Dust forecasting

Numerical prediction of dust in Numerical Weather Prediction (NWP)-type models faces a number of challenges. First, the physical processes involved in the dust cycle, particularly in the dust emission, are not yet fully understood. Then, the range of scales required to fully account for all those processes is very wide. Dust production is a function of surface wind stress and soil conditions, but wind is an extremely variable parameter in both space and time and soil properties are highly heterogeneous and not always well characterized. Finally, the functional form of the emission parametrization is typically that of a power law in surface wind speed, making emissions highly sensitive to modelled wind fields. This section highlights the SDS-WAS initiatives related to dust prediction.

The SDS-WAS Regional Center for NAMEE daily collects and distributes through its website forecast products released by different numerical models. This initiative has grown significantly with the incorporation of more and more partners. At the time of writing this paper, twelve modelling groups provide three-hourly forecasts of dust surface

concentration and dust optical depth at 550 nm for a reference area, which is intended to cover the main source areas in Northern Africa and Middle East, as well as the main transport routes and deposition zones from the equator to the Scandinavian Peninsula. The action involves forecasts up to 72 h with a 3-hour frequency.

Ensemble multi-model products are also daily generated after bi-linearly interpolating all forecasts to a common grid mesh of 0.5 x 0.5 degrees. Multi-model forecasting intends to alleviate the shortcomings of individual models while offering an insight on the uncertainties associated with a single-model forecast. Centrality products (median and mean) are aimed at improving the forecasting skill of the single-model approach. Spread products (standard deviation and range of variation) indicate whether forecast fields are consistent within multiple models, in which case there is greater confidence in the forecast.

The SDS-WAS Regional Center for Asia conducts a similar exercise. It daily collects and publishes on the web dust forecasts from five numerical models. Its geographical domain covers the main dust sources in Central and Eastern Asia, and transport routes and deposition zones up to the central Pacific.

6. From R&D to operational dust forecast

In 2012, in view of the demand of many NMHSs and the good results obtained by the SDS-WAS, which prove the feasibility and the need to begin developing operational services beyond the scope of R&D, WMO designated the consortium formed by AEMET and the BSC to host the first Regional specialized Meteorological Center with activity specialization on Atmospheric Sand and Dust Forecasts. Since February 2014, the Center, called Barcelona Dust Forecast Center (BDFC, <https://dust.aemet.es>) operationally generates and distributes dust predictions for Northern Africa (north of equator), Middle East and Europe.

The BDFC prepares regional forecast fields using the NMMB/BSC-Dust model continuously throughout the year on a daily basis (figure 2). Forecasts cover the period from the starting forecast time up to a forecast time of 72 hours, with an output frequency of 3 hours. They cover the geographical domain with a horizontal resolution of 0.1° longitude x 0.1° latitude. The forecasts are disseminated through the Center's website, the WMO Global Telecommunications System and the EUMETCast service. EUMETCast is a multi-service dissemination system based on standard

digital video broadcast technology. It uses commercial telecommunication geostationary satellites to multi-cast files to a wide user community.

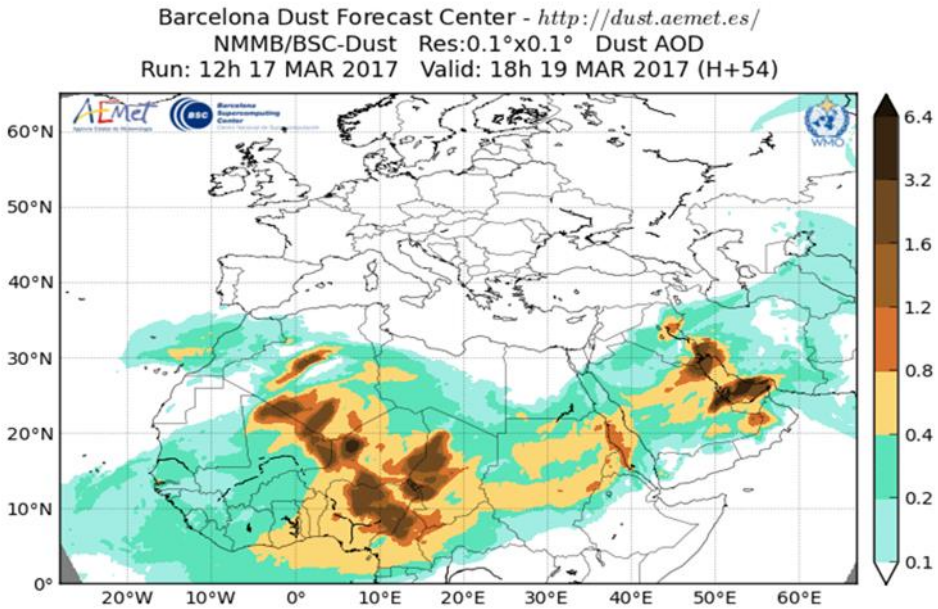


Figure 2. 54-hour forecast of dust optical depth for 19 Mar 2017 at 18 UTC. The dust prediction for West Asia was quite precise as observed after comparison with Figure 1

7. Towards Dust Early Warning Systems

Traditionally, many countries have been reactive to natural disasters. The Hyogo Framework for Action 2005–2015 led to a paradigm shift in disaster risk management from emergency response to a comprehensive approach that includes preparedness and preventive strategies to reduce risk. Early Warning Systems (EWS) are well recognized as critical tools for reducing negative impacts of natural hazards.

Although the negative impacts of airborne dust are well known and the necessary tools for its observation and prediction are available, very few countries have implemented EWSs for airborne dust. A complete and effective EWS comprises four inter-related elements, spanning knowledge of hazards and vulnerabilities through to preparedness and capacity to respond:

Risk knowledge - The impact of airborne dust on air quality, human health, weather and climate, the environment and different economic sectors is

generally known, although some aspects require further investigation. A clear case is the interaction between dust and climate, where there are still many uncertainties, as recognized by the International Panel on Climate Change. Also, though the impact of suspended particles on health is reasonably well known, the specific effect of mineral dust is highly uncertain. Thus, World Health Organization recently commissioned a report on this.

Monitoring and warning services - Warning services lie at the core of the system. Though the NMHS of a majority of countries has the ability to obtain and use the basic products of dust monitoring and prediction necessary to set up an EWS for dust operating 24 hours a day, such services have rarely been established. The cause probably lies in the lack of awareness that there is a sound scientific basis for predicting dust and that early warning can bring important benefits to the population and save economic costs to society. It is necessary to highlight that the inclusion of dust in a multi-hazard EWS could gain the benefit of shared institutional, procedural and communication networks.

Dissemination and Communication - Warnings must reach those at risk. Clear messages containing simple, useful information are critical to enable proper responses. Regional, national and community level communication systems must be pre-identified and appropriate authoritative voices established.

Response Capability - It is essential that communities understand their risks; respect the warning service and know how to react. Education and preparedness programmes play a key role. It is also essential that disaster management plans are in place, well practiced and tested.

8. WMO Airborne Dust Bulletin

Although the SDS-WAS Regional Centers provide information primarily through their respective websites, WMO has begun to publish an annual bulletin entitled 'WMO Airborne Dust Bulletin' (Terradellas et al., 2017) reporting on the atmospheric burden of mineral dust through the year, its geographical distribution and the inter-annual variation. The bulletin also includes descriptions of dust cases and dust-related news and events.

References

- Andreae, M. O., & Rosenfeld, D. (2008). Aerosol–cloud–precipitation interactions. Part 1. The nature and sources of cloud-active aerosols. *Earth-Science Reviews*, 89(1), 13-41.
- Chadwick, O. A., Derry, L. A., Vitousek, P. M., Huebert, B. J., & Hedin, L. O. (1999). Changing sources of nutrients during four million years of ecosystem development. *Nature*, 397(6719), 491-497.
- Cuevas, E. (2013). Establishing a WMO Sand and Dust Storm Warning Advisory and Assessment System Regional Node for West Asia: Current Capabilities and Needs. WMO No. 1121, Geneva, Switzerland
- Ginoux, P., Prospero, J. M., Gill, T. E., Hsu, N. C., & Zhao, M. (2012). Global-scale attribution of anthropogenic and natural dust sources and their emission rates based on MODIS Deep Blue aerosol products. *Reviews of Geophysics*, 50(3).
- Goudie, A. S. (2014). Desert dust and human health disorders. *Environment international*, 63, 101-113.
- Jickells, T. D., An, Z. S., Andersen, K. K., Baker, A. R., Bergametti, G., Brooks, N., ... & Kawahata, H. (2005). Global iron connections between desert dust, ocean biogeochemistry, and climate. *Science*, 308(5718), 67-71.
- Kohfeld, K. E., & Harrison, S. P. (2001). DIRTMAP: the geological record of dust. *Earth-Science Reviews*, 54(1), 81-114.
- Mahowald, N. M., Yoshioka, M., Collins, W. D., Conley, A. J., Fillmore, D. W., & Coleman, D. B. (2006). Climate response and radiative forcing from mineral aerosols during the last glacial maximum, pre-industrial, current and doubled-carbon dioxide climates. *Geophysical Research Letters*, 33(20).
- Mahowald, N. M., Kloster, S., Engelstaedter, S., Moore, J. K., Mukhopadhyay, S., McConnell, J. R., ... & Flanner, M. G. (2010). Observed 20th century desert dust variability: impact on climate and biogeochemistry. *Atmospheric Chemistry and Physics*, 10(22), 10875-10893.
- Nickovic, S., Cuevas Agulló, E., Baldasano, J. M., Terradellas, E., Nakazawa, T., & Baklanov, A. (2015). Sand and Dust Storm Warning Advisory and Assessment System (SDS-WAS) Science and Implementation Plan: 2015-2020, WWRP 2015-5, WMO, Geneva, Switzerland.
- Okin, G. S., Mahowald, N., Chadwick, O. A., & Artaxo, P. (2004). Impact of desert dust on the biogeochemistry of phosphorus in terrestrial ecosystems. *Global Biogeochemical Cycles*, 18(2).
- Prospero, J. M., & Nees, R. T. (1986). Impact of the North African drought and El Nino on mineral dust in the Barbados trade winds. *Nature*, 320(6064), 735-738.
- Rea, D. K. (1994). The paleoclimatic record provided by eolian deposition in the deep sea: The geologic history of wind. *Reviews of Geophysics*, 32(2), 159-195.
- Sokolik, I. N., & Toon, O. B. (1996). Direct radiative forcing by anthropogenic airborne mineral aerosols. *Nature*, 381(6584), 681.

Solomon, S. (Ed.). (2007). *Climate change 2007-the physical science basis: Working group I contribution to the fourth assessment report of the IPCC* (Vol. 4). Cambridge University Press.

Stocker, T. (Ed.). (2014). *Climate change 2013: the physical science basis: Working Group I contribution to the Fifth assessment report of the Intergovernmental Panel on Climate Change*. Cambridge University Press.

Tegen, I., Lacis, A. A., & Fung, I. (1996). The influence on climate forcing of mineral aerosols from disturbed soils. *Nature*, 380(6573), 419.

Terradellas, E., Nickovic, S., & Zhang, X. (2015). Airborne dust: a hazard to human health, environment and society. *WMO Bulletin*, 64, 42-46.

Terradellas, E., Zhang, X. Y., Farrell, D., Nickovic, S., & Baklanov, A. (Eds.) (2017). *WMO Airborne Dust Bulletin No. 1*, WMO, Geneva, Switzerland, ISBN 2520-2928.

New approach for characterization, mapping and controlling active and potential sources of dust and sands in Kuwait

Ali Al-Dousari

Institute for Scientific Research, Kuwait, adousari@kisir.edu.kw

Summary

The purpose of this proposal is to identify and control active and potential sources of dust and sands in Kuwait. The anticipated end results of the proposal are recent maps for the sources of dust and sands as well as scenarios for controlling these sources. The duration of the project is 30 months. The total anticipated budget is KD **165,000**.

Approaches for identification and mapping sources of dust and sands in Kuwait include:

- Analyses and interpretation of recent satellite images (Landsat of August 2017 and SPOT-7 Satellite Image) Fig.1

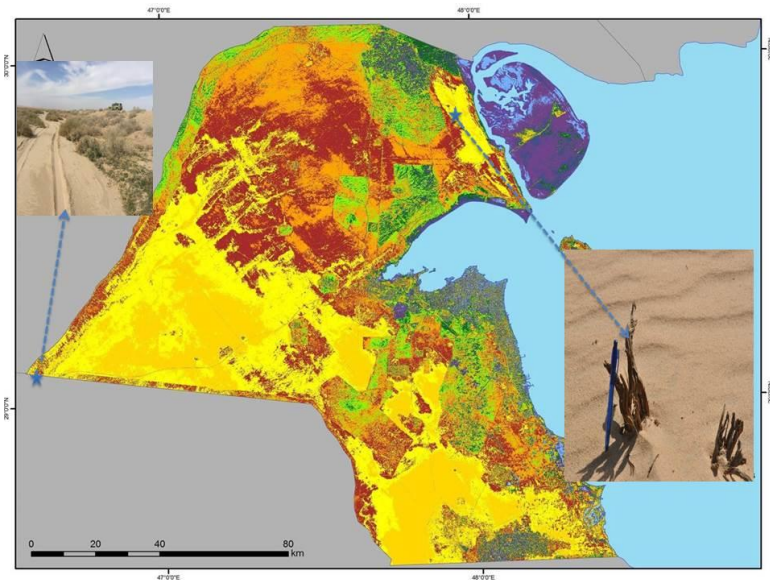


Figure 1. Recent Landsat image (2017) for Kuwait showing different surface sediments classes including sources of dust and sands (under finalization)

- Based on previous experience and recent satellite images, the potential sources of dust (mainly fluvial, aeolian and sabkhas deposits) will be delineated.
- Selection of 250-300 observation points (GPS records) for ground truth and field investigations for surface morphology and sedimentology as well as conditions of local sources of dust.
- Collection of representative samples (700-800 samples) from dust sources (top, 20 cm, and 50 cm depth)
- Lab Analyses (grain size and chemical analyses)
- Producing final map for sources of dust in Kuwait (Landsat 2017)
- Produce 7 maps for seven geographic areas in Kuwait (SPOT-7 Satellite Image) Fig.2

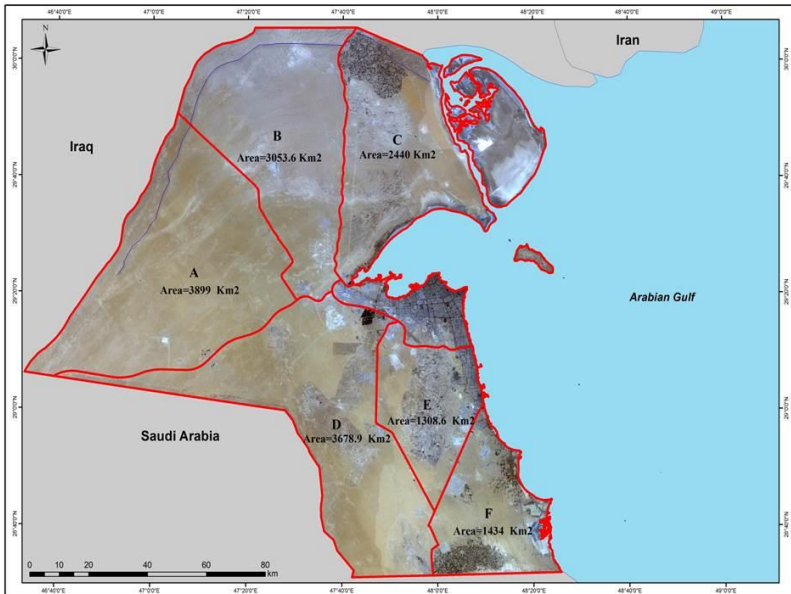


Figure 2. Geographic areas in Kuwait (A-F)

After identification and mapping the sources of sand and dust, several scenarios for controlling these sources will be proposed. Pilot sites for controlling sources of dust and sands will be selected for field experiments and tests.

1. Introduction

Dust in Kuwait has a major negative impact on air quality. In extreme cases (the case of the huge dust storm of March 25, 2011), dust storms result in loss of human life and severe disruption of social and economic activities. In the last decade, Kuwait experienced a number of severe dust storms. Examples were July- September, 2007, April 2008, April 2010, March 2011, May-July 2012, September 2015, September 2016 and May – June 2017.

In Kuwait, SDS (Sand and Dust Storms) represent the most common natural hazards. SDS have negative impact on several sectors in Kuwait. These are public health & environment, oil and industry, agriculture & animal production, water & electricity, defence and transportation /communications.

As stated by Tozer et al 2017, accumulated data of dust storms in Kuwait for the past 14 years (2001–2014) showed that the month of March had the highest number of dust storms (total 19), which is rather unusual, with an average of 8 dust storms per year (year 2008 had the highest dust storms of total 22). The rainfall of the year 2008 was less than 30 mm, while the annual average is 110mm. So dust storms of year 2008 were the highest.

Identification, characterization, mapping and control active and potential sources of dust in Kuwait are main challenges for managing dust storms in Kuwait.

Reliable maps for active and potential sources of dust and sands in Kuwait are not available. The ultimate goal of the current study is to develop a map for sources of dust and sand (State level) and 7 detailed maps (area level).

2. Needs/Problems

Currently no reliable recent maps for the sources of dust and sands in Kuwait. So, no real control measures were adopted to control these sources.

The proposed study will identify and map the active and potential sources of dust and sands in Kuwait. So, control measures could be adopted to minimize sand and dust amounts by at least 25 %. This will positively reflect on the quality of life in Kuwait.

3. Goals/Objectives

- Goal 1: Analyses and interpretation of recent remote sensing data followed by ground truth and field sampling
- Goal 2: Producing set of maps for sources of dust and sands (state level) and area level (7 maps)
- Goal 3: Proposing scenarios for controlling active sources of sand and dust in Kuwait
- Goal 4: Identification the specifications and cost of control measures for sources of sand and dust in Kuwait

Key benefits

- Enhancement of the quality of life in Kuwait as a direct result of controlling sources of sands and dust
- Safe at least 30 % of maintenance costs for facilities subject to sand encroachment and dust
- Enhancement the Kuwaiti Experience in managing SDS

4. Procedures/Scope of Work

- Analyses and interpretation of recent satellite images (Landsat of August 2017 & **SPOT-7 Satellite Image recent archive after (Nov 2017)**)
- Based on previous experience and recent satellite images, the potential sources of dust (mainly fluvial, aeolian and sabkhas deposits) will be delineated.
- Selection of ground observation sites (250-300 points) for ground truth and field investigations for sources of sands and dust.
- Collection of representative samples from dust and sands sources
- Lab Analyses (grain size and chemical analyses)
- Producing final map for sources of dust in Kuwait (Landsat image of 2017)
- Producing 7 maps for seven geographic areas in Kuwait (SPOT-7 Satellite Image recent archive after (Nov 2017))

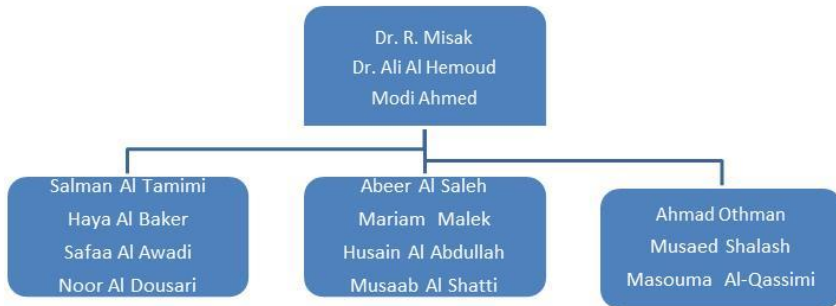
5. Timetable

	Description of Work	Start and End Dates
Phase One	Analyses of recent remote sensing data(Landsat and Spot 7) & ground truth	March 2018 – August. 2018
Phase Two	Field sampling and investigations & Lab. analyses	Sep. 2018 to August 2019
Phase Three	Setting up scenarios for controlling sources of sand and dust& pilot field tests	Sep.2019 to May 2020
Phase Four	Producing maps & reporting	June – August 2020

6. Budget

	Description of Work	Anticipated Costs (KD)
Phase One	Analyses & interpretation of satellite images (Landsat and Spot 7) & ground truth	30,000
Phase Two	Field work including sampling of sources of dust and sands& Laboratory analyses	50,000
Phase Three	Field tests and experiments on controlling dust and sand sources (6-8 pilot sites)	60,000
Phase Four	Producing maps for sources of dust and sands & Reporting	25,000
Total		165,000

7. Key Personnel



8. Evaluation

3399 - 1308 km². Progress will be evaluated throughout the project by time of mapping completion & pilot site experiments of 25 %, 50 %, 75% and 100% of the country (at the end of the project).

9. Endorsements

EPA (Environment Public Authority)

PAAFR (Public Authority for Agriculture Affairs and Fish Resources)

KISR (Kuwait Institute for Scientific Research)

Civil society (Kuwait Environment Protection Society)

KFAS (Kuwait Foundation for the Advancement of Sciences)

10. Next Steps

Specify the actions required of the readers of this document:

- Next Step 1: Critically evaluate the document
- Next Step 2: Suggesting any modifications, if any
- Next Step 3: Support the project

11. Appendix

SPOT-7 Satellite Image recent archive after (Nov 2017)

Multispectral Imagery (4 bands) Pan-Sharpned(ortho)	Blue (0.455 μm – 0.525 μm) Green (0.530 μm – 0.590 μm) Red (0.625 μm – 0.695 μm) Near-Infrared (0.760 μm – 0.890 μm)
Resolution	1.5 m
Area	17750 km ²

References

Tozer,P., Al-Hemoud, A. and Al-Dousari, A. 2017. Economic impact of sand and dust storms in Kuwait, COP13 China.



Remote sensing-based Land Degradation Index for Sand and Dust Storm Sources (LDISDS)

Ali Darvishi Bolorani, Mohsen Bakhtiari and Yasin Kazemi

University of Tehran, Faculty of Geography, Dpt. of Remote Sensing and GIS,
ali.darvishi@ut.ac.ir, m.bakhtiari_rs@ut.ac.ir and y.kazemi94@gmail.com

Abstract

Land degradation will reduce food production in next decades while population growth will dictate more demand for food. These demands will require millions of hectares of additional agricultural lands. In fragile ecosystems of arid and semi-arid areas like Iran the situation because of its climate is even more severe. This paper offering an integrated modeling based on remote sensing imagery. Here a Wind Erosion Index (WEI), Normalized Environmental Health Index (NEHI) and Modified Vegetation Water Supply Index (MVWSI) are developed using the available time-series products of MODIS and the point meteorological data. These indices were used as inputs for developing and introducing the Land Degradation Index for Sand and Dust Sources (LDISDS). This new index is adapted using Artificial Neural Network (ANN) for Sand and Dust Sources (SDS) sources in Khuzestan province of Iran from 2000- 2014. The findings show that the average of LDISDS is able to model the spatiotemporal behavior of dust sources sources in Khuzestan as beneficial evidence to assist in better investments and management of resources.

Keywords: Land Degradation Index for Sand and Dust Sources (LDISDS), MODIS products, Time Series Data, Artificial Neural Network (ANN)

1. Introduction

Land degradation refers to any form of deterioration of the land productivity that affects the integrity and usual cycle of the environment; this phenomenon is most pronounced in drylands, which cover more than 40% of the earth's surface (Dobie, 2001). In arid and semiarid climates with unsustainable development conditions, land degradation phenomenon is related to vegetation cover destructions caused by drought, deforestation, overgrazing and etc. (Eckert et al., 2015; Li et al., 2016). According to UNCCD, land degradation in arid, semi-arid, and dry sub-humid areas, drylands, may result from various factors, including climatic variations and human activities. It includes diverse processes, ranging from changes in plant species composition to soil erosion phenomenon, and reduces the land's productive potential (Hill et al., 1995; Reynolds, 2001; Reynolds et al., 2007). Land degradation encompasses the whole environment but includes individual factors concerning soils, water resources (surface, ground), forests (woodlands), grasslands (rangelands), croplands (rain fed, irrigated) and biodiversity (animals, vegetative cover, soil) (FAO, 2005), but generally the phenomenon is most pronounced in the drylands. Land degradation will reduce food production up to 12% globally in next 25 years and population growth will dictate 50% more demand for food in 2030. These demands will require millions of hectares of additional agricultural lands. In fragile ecosystems of arid and semi-arid areas like Iran the situation is even more severe. In recent years many studies about the applications of remote sensing indices in land degradation have been done based on parameterization and quantification of environmental phenomena and features. Modified Vegetation Water Supply Index, MVWSI, to monitor drought based on NDVI and LST parameters has been introduced by Men-xin and Hou-quan (2015). Temperature Condition Index, TCI, (Kogan, 2000), vegetation health index, VHI, (Kogan, 2002), LST/NDVI ratio (McVicar and Bierwirth, 2001), Vegetation Temperature Condition Index, VTCI, (Wang, 2001), Temperature Vegetation Drought Index, TVDI, (Sandholt et al., 2002) and Perpendicular Drought Index, PDI, (Zhan et al. 2006) are some of remote sensing indices useful for drought, land degradation and desertification monitoring. Some studies that have applied MODIS data have reached relative useful results on drought, land degradation and desertification monitoring; for instance, Alexakis and Tsanis (2016) studied two multiple linear regression and artificial neural network models for downscaling TRMM precipitation products using MODIS data, the downscaling procedure performed significant im-

provements for monthly estimation of precipitation. Yang and Leys (2014) studied wind erosion hazard in Australia using MODIS derived land cover, soil moisture and climate data. They made time series using wind erosion hazard maps, generally time series data provide detailed and useful information in better targeting regions for investments and continuous monitoring, evaluation and reporting that will lead to reduced wind erosion and improved soil condition.

This paper introduces a Remote sensing-based Land Degradation Index for Sand and Dust Sources, LDISDS, which integrates MODIS products and meteorological data. LDISDS is including three input indices as Wind Erosion Index (WEI), Normalized Environmental Health Index (NEHI) and Modified Vegetation Water Supply Index (MVWSI). These indices are combined using training the Artificial Neural Network (ANN) with randomly selected dust sources to assess the LDISDS. The used remote sensing data are time-series products of MODIS, meteorological data within Khuzestan province (Fig. 1) for sources of dust storms from 2000 to 2014. Results demonstrate that the integrated time series of MODIS-products and meteorological data can be used to monitor land degradation within the desired extent and in association with dust sources. The produced time-series LDISDS maps provide detailed and beneficial evidence to assist in better investments for managing and controlling the progressive trend of dust storms in sources.

2. Methodology

As illustrated in Fig. 1, the LDISDS is developed in three main steps: (i) selecting and develop the most suitable satellite based indices for modeling soil, water and vegetation behaviors, i.e. MVWSI, NEHI, and WEI; (ii) design and develop an ANN algorithm to model the relationship between the indices and Sand Dust Storm (SDS) sources to assess LDISDS and (iii) extracting weights of ANN between input layers and the first hidden layer's neurons for combining the input indices from 2000 to 2014.

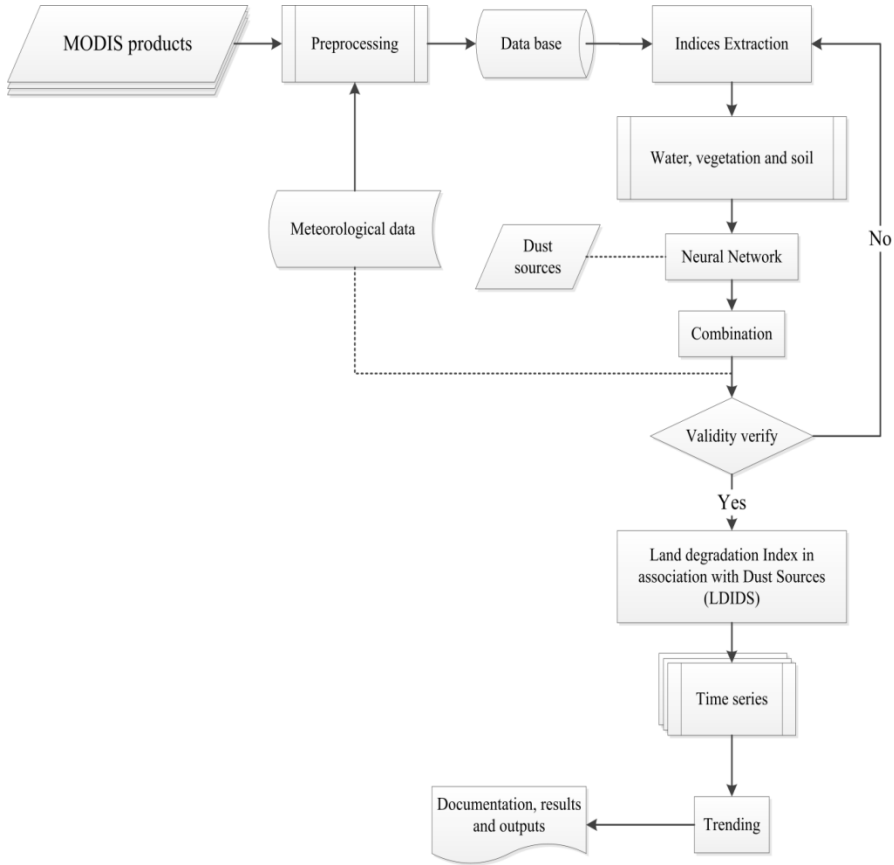


Figure 1. Stepwise procedure of LDIDS

MVWSI, was developed for drought monitoring by Men-xin and Hou-quan (2015) as following:

$$MVWSI = (RNDVI/RLST^2) \quad (1)$$

$$RLST = (LST/\overline{LST}) \quad (2)$$

$$RNDVI = (NDVI/\overline{NDVI}) \quad (3)$$

Where, RNDVI, RLST, \overline{LST} and \overline{NDVI} are relative normalized difference vegetation index, relative land surface temperature, and averages of LST and NDVI in a specific time period, here is for the past twenty years, respectively. The range of MVWSI is between 0 and 1 and the smaller the value, the less vegetation water supply and the more severe drought. In contrary, the greater the value, the less severe drought (Men-xin and Hou-quan, 2015). Wind Erosion Index, WEI, was developed for wind erosion potential modeling by Chepil et al., (1963) as follows:

$$WEI = W (P - E)^2 \tag{4}$$

$$P - E = \frac{R + 1}{T + 2} \tag{5}$$

Where, WEI, W, P-E, R and T are the wind erosion potential, mean monthly speed of wind (km/h) at 10 meter above ground, evapotranspiration index of Thornthwaite, mean monthly of precipitation (mm) and mean monthly of air temperature (°C), respectively. In current study,

Some modifications are carried out on the WEI parameters as follows: (i) reducing the averages of \overline{LST} and \overline{NDVI} to ten years, instead of twenty years, for prevent the increase of Nan-pixels in the time series dataset; (ii) to add a small constant to denominator in equation (5) to avoid the zero value in the denominator. Generally, the greater the WEI, the more potential of wind erosion and vice versa (Chepil et al., 1963). NEHI, developed for modeling health environment in regional scale as follows:

$$NHEI = -1 \times \left(\frac{LST_{(0-255)} - NDVI_{(0-255)}}{LST_{(0-255)} + NDVI_{(0-255)}} \right) \tag{6}$$

Where, LST and NDVI are standardized to 0 to 255 for better comparison. The range of NEHI is between of -1 to 1. The smaller the value, the more critical condition of the environment and ecosystem for arid and semiarid ecosystems. MODIS products are used in MVWSI and NEHI, while, point meteorological ground data are used for WEI by spatial interpolation function. Then, MVWSI, NEHI and WEI are converted into raster format on a monthly base from February 2000 to December 2014 (Table 1).

Table 1. LDISDS input data

Input data	Description	Source	Data type
LST	Land surface temperature	MODIS products	Surface
NDVI	Normalized difference vegetation index	MODIS products	Surface
R	Mean precipitation	Meteorological data	Point
T	Mean air temperature	Meteorological data	Point
W	Mean wind speed	Meteorological data	Pont

After preparing the time series of indices on a monthly base, the ANN algorithm is adapted for mapping LDISDS. In the procedure, %50 of randomly selected dust sources were imported to ANN algorithm as targets class of SDS sources, were mapped by Geological Survey & Mineral Explorations of Iran (GSI) using Landsat Imagery and field data in 2014 (Fig. 2). The map of LDISDS for 2014 is produced by ANN algorithm using the %50 of randomly selected dust sources for training ANN (Fig. 3). Results shows the land degradation happens in the areas that are corresponding to dust sources identified by GSI.

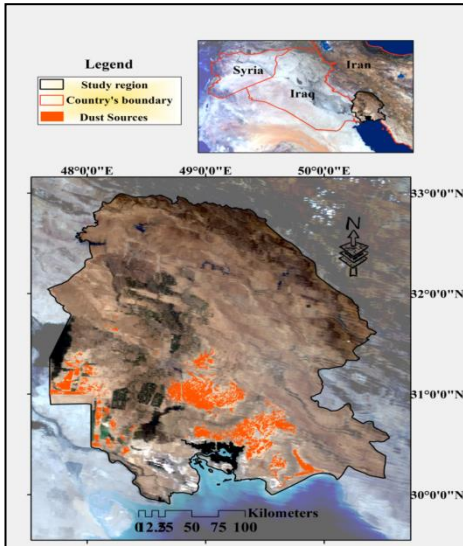


Figure 2. SDS sources in Khuzestan province of Iran

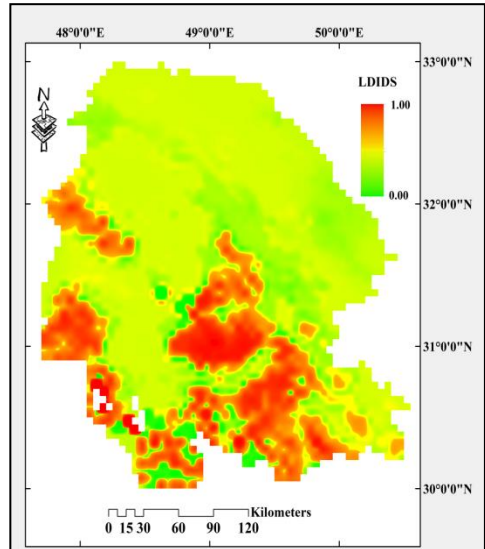


Figure 3. LDISDS for 2014, red color presents more degraded lands in relation to dust sources

In the next step, using the extracted average weights of ANN between input layers and the first hidden layer's neurons, the combination of input indices for mapping LDISDS over time series data was done. These weights were produced during running the parallel computations of ANN based on internal relationships between input pixels and SDS sources (Table 2). Finally, the process of temporal trending was carried out in the mentioned time period. In order to evaluate the usefulness and robustness of LDISDS, Khuzestan province (Fig. 1) in the southwest of Iran is selected. This province experiencing the highest frequency and intensity of dust storm events in the last decades because of its location in the pathway of dust corridor, started from Syrian Desert and ending in Oman Sea. Furthermore, Khuzestan province is suffering from mismanagement of soil/water re-

sources and drought. Consequently, land degradation and dust emissions are becoming an integrated part of the ecosystem in this province.

3. Results and Discussion

After running ANN algorithm and producing the initial outputs including LDISDS map, for validating and verifying results the remained %50 of dust sources that have not been used for training were validated. The accuracy of LDISDS for 2014, is presented in table 2 in which the value of left and right cells, below overall accuracy, indicate degraded and not degraded lands respectively.

Table 2. Accuracy of ANN results

Parameter	Percent	
Overall accuracy	0.8531	
Kappa Coefficient	0.5482	
	Degraded lands	Not degraded lands
User's accuracy	0.2813	0.9911
Commission error	0.7186	0.0088
Producer error	0.8843	0.8511
Omission error	0.1156	0.1488

Then using the average weights between the first and second layers, LDISDSs for other time points, from February 2000 to December 2014 are mapped. In the study period from 2000 to 2014, 179 maps of LDISDS were produced using overlaying of 537 input maps of MVWSI, NEHI, and WEI, and optimization procedure of inter-layers weights in the accomplished ANN.

Temporal analysis of LDISDS maps was done by calculating the average of randomly selected pixels in distinct and variable dimensions, e.g. from 1*1 to n * m where n and m present the number of pixels in each row and column of input raster respectively (Fig. 4), then for better understanding of spatiotemporal dynamics of LDISDS values within study area, average of randomly selected pixels along time period were calculated (Fig. 5). Finally, for evaluating the general trend of LDISDS during 2000 to 2014, a linear regression fitted within the monthly average values of LDISDS (Fig. 6), based on 179 time points, and annually, based on 15 time points, was calculated (Fig. 7).

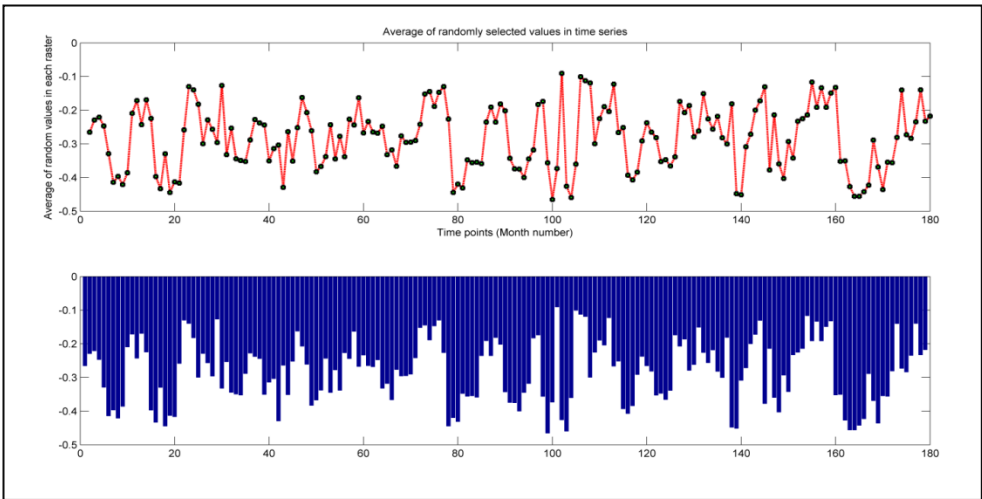


Figure 4. Average monthly of randomly selected LDISDS values in time series

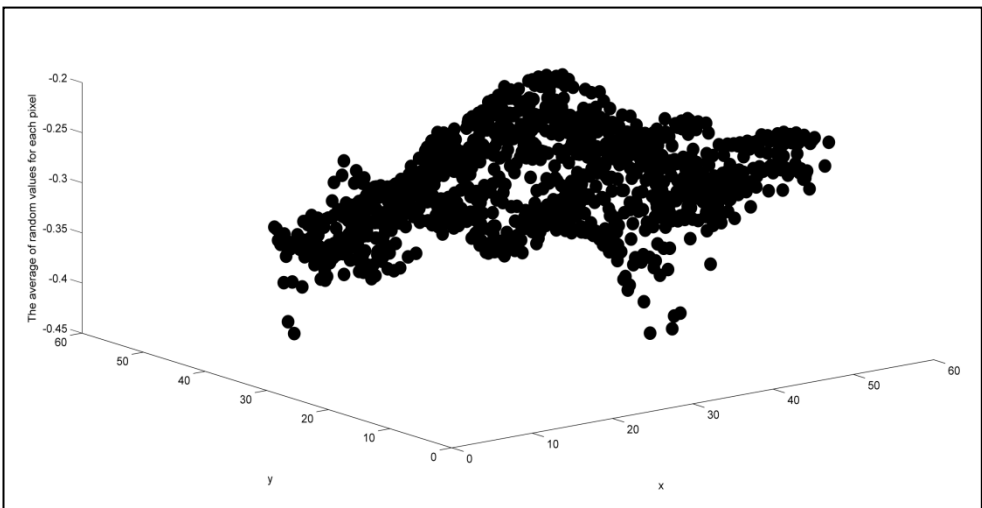


Figure 5. The average of random values for each pixel within study period time

Generally, in term of spatial, the southwest and south of study region indicates the more degraded lands along the studied time range based on assessed LDISDS. While in term of temporal changes, average values of LDISDS have a subtle greater than zero slope. In other words, generally average values of LDISDS within 179 months have been increased, although this increment was discontinuous, and subtle, but it is enough to tell us that along these 15 years degraded lands in association with dust sources have been increased. The findings of this research can be used in distinguish and

identify general spatial extent of dust sources that can decrease costs considerably in primary sectors of attempts. Although spatiotemporal modeling of land degradation encompasses many aspects but current study can be considered a start point in this field. Generally, the results of this study are opening a new horizon in the field of land surface variables modeling and investigation by developing new remote sensing indices.

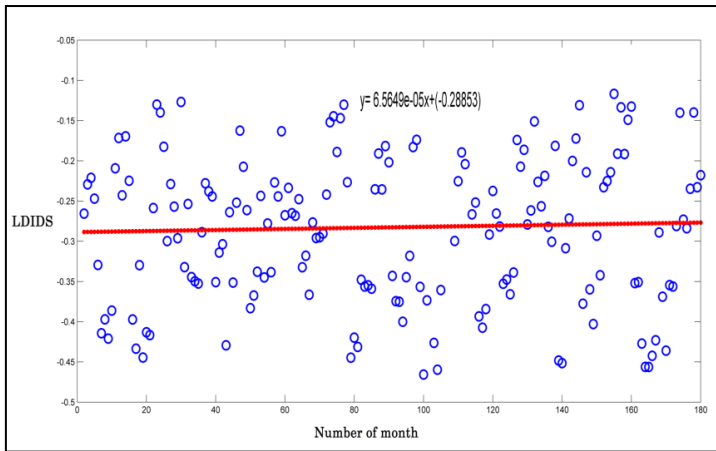


Figure 6. Monthly Trend of changes LDISDS

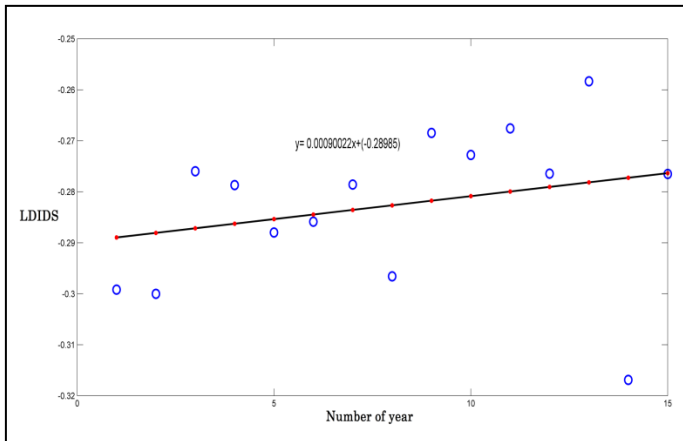


Figure 7. Annually Trend of changes LDISDS

4. Conclusion

The modeled land degradation maps demonstrated that the time series of MODIS-products and point meteorology data can be integrated and used to identify land degradation within the SDS sources. Generally, the time-series LDISDS maps provide detailed and beneficial evidence to assist in better investments and management of resources that will lead to SDS emission. The southwest and south of the study area indicates the more degraded lands along the studied time period. While average values of LDISDS have been increased in association SDS sources dust emission pattern. The findings of this research can be used in distinguish and identify general spatial extent of dust sources that can decrease costs considerably in primary sectors of attempts. Although spatiotemporal modeling of land degradation encompasses many aspects but current study can be considered a start point in this field.

References

- Alexakis, D. D., & Tsanis, I. K. (2016). Comparison of multiple linear regression and artificial neural network models for downscaling TRMM precipitation products using MODIS data. *Environmental Earth Sciences*, 75(14), 1-13.
- Dobie P. (2001). Poverty and the drylands. United Nations Development Programme, Dryland Development Centre. Nairobi, Kenya.
- Eckert, S., Hüsler, F., Liniger, H., & Hodel, E. (2015). Trend analysis of MODIS NDVI time series for detecting land degradation and regeneration in Mongolia. *Journal of Arid Environments*, 113, 16-28.
- FAO. (2005). Agro-Ecological Zoning and GIS application in Asia with special emphasis on land degradation assessment in drylands (LADA). Proceedings of a Regional Workshop, Bangkok, Thailand 10–14 November 2003. FAO, internet website: <ftp://ftp.fao.org/agl/agll/docs/misc38e.pdf>, accessed July 1, 2008.
- Hill, J., Sommer, S., Mehl, W., Megier, J., (1995). Use of Earth observation satellite data for land degradation mapping and monitoring in Mediterranean ecosystems: towards a satellite-observatory. *Environmental Monitoring and Assessment* 37, (1–3), 143–158.
- Li, J., Liu, Z., He, C., Tu, W., Sun, Z., (2016). Are the drylands in northern China sustainable? A perspective from ecological footprint dynamics from 1990 to 2010. *Sci. Total Environ.* 553, 223–231.
- Kogan, F. N. (2000). Satellite-observed sensitivity of world land ecosystems to El

Nino/La Nina. Remote Sensing of Environment, 74, 445-462.

Kogan, F. N. (2002). World droughts in the new millennium from AVHRR based vegetation health indices. Eos, Transactions, American Geophysical Union, 83, 557-564.

Chepil, W. S., Siddoway, F. H., & Armbrust, D. (1963). Climatic index of wind erosion conditions in the Great Plains. Soil Science Society of America Journal, 27(4), 449-452.

McVicar, TR, Bierwirth PN. (2001). Rapidly assessing the 1997 drought in Papua New Guinea using composite

Men-xin, W. U., & Hou-quan, L. U. (2015). A modified vegetation water supply index (MVWSI) and its application in drought monitoring over Sichuan and Chongqing. China, 15(9), 2132-2141.

Organization of Geological survey and mineral exploration, (2015). The recognition of dust sources within Khuzestan province.

Reynolds, J.F. (2001). Desertification. In S. Levin (Ed.), Encyclopedia of Biodiversity, (vol. 2, pp. 61– 78). San Diego: Academic Press.

Reynolds, J. F., Smith, D. M. S., Lambin, E. F., Turner, B. L., II, Mortimore, M., Batterbury, S. P. J., et al. (2007). Global desertification: Building a science for dryland development. Science, 316, 847–851.

Sandholt I, Rasmussen K, Andersen J. (2002). A simple interpretation of the surface temperature/vegetation index space for assessment of surface moisture status. Remote Sensing of Environment, 79, 213

Secretary General's Report on Land Chapter of Agenda 21 to Commission on Sustainable Development (CSD8, UN, New York 2000), UNCCD Agenda 21, Rio de Janeiro, 1992 and UNCCD Paris, 1994.

Wang P, Gong J, Li X. (2001). Vegetation temperature condition index and its application for drought monitoring. Geomatics and Information Science of Wuhan University, 26, 412-417.

Yang, X., & Leys, J. (2014). Mapping wind erosion hazard in Australia using MODIS-derived ground cover, soil moisture and climate data. In IOP Conference Series: Earth and Environmental Science (Vol. 17, No. 1, p. 012275). IOP Publishing.

Zhan Z, Qin Q, Ghulam A. (2006). A new method of soil moisture monitoring based on NIR-red spectral space. Science in China (D Earth Sciences), 36, 1020-1026.

Monitoring the Changes in the Mesopotamian Marshlands during Drought Periods

Orkan Özcan^{1,*}, Murat Türkeş² and Nebiye Musaoğlu³

^{1,*}(Corresponding author) Istanbul Technical University, Eurasia Institute of Earth Sciences, ozcanork@itu.edu.tr

²Bogazici University, Center for Climate Change and Policy Studies

³Istanbul Technical University, Civil Eng. Faculty, Geomatics Eng. Department

Abstract

The Mesopotamian marshlands constitute the largest wetland ecosystem in the Middle East and Western Eurasia, which were formed by the confluence of the Tigris and Euphrates rivers. The scale and speed of land cover change in the Mesopotamian marshlands have been extraordinary since they were devastated by damming and river channelization during the late 1980s. Large scale ecosystem degradation such as the loss of the Mesopotamian marshlands may have serious impacts on climate characteristics by means of water scarcity, and large temperature and soil moisture variations very likely leading potential dust and sand storms. Remote sensing can be implemented as an effective tool to monitor and assess/quantify ongoing changes taking place on a near real-time basis so as to advise rapid restoration actions. Recent researches have shown that remotely sensed data can provide a synoptic and repeatable source of information to overcome difficulties in multi-temporal characterization of marshlands. The main aim of this study is to characterize the change in spatial and temporal distributions of marshland and near surroundings that took place due to drying operations and the consequences on the environment. To map the evolution of the marshlands, a multistage approach using low- and medium-scale resolution satellite imagery was followed to obtain a comprehensive coverage and analysis. MODIS and Landsat data were used to map the extent of changes in the Mesopotamian marshes from 1988 to 2017. Normalized difference vegetation index (NDVI) and modified normalized difference water index (MNDWI) series were calculated for the region to determine the marshlands and the extent of open water. Further, both indices were applied in order to monitor the

changes in Mesopotamian marshlands within two time periods in which the marshes were exposed to significant droughts during 30 years.

Keywords: *Mesopotamia, Sand and dust storms (SDS), Normalized difference vegetation index (NDVI), Modified normalized difference water index (MNDWI), droughts.*

1. Introduction

The term sandstorm is a meteorological phenomenon common in arid and semi-arid regions, where sand is a more prevalent soil type than dirt or rock. Iraq is one of the countries in the world where dust storms hit and last for days. The World Health Organization (WHO) reported that annually more than 800,000 deaths were attributed to air pollution and approximately 150,000 cases of these deaths happened in southern Asia (Goudarzi et. al., 2017). The results of the Kutiel and Furman (2003)'s study presented the Middle East as one of the regions most affected by dust, in the world, next to Africa. In some seasons in certain regions of the Middle East and North Africa and for about 30% of the time on average, the dust conditions in the lower troposphere fall into one of these three categories. Thus, in these regions, dust storms are a very frequent phenomenon and a better knowledge of their spatial and temporal distribution is of prime importance (Kutiel and Furman, 2003). Shimali winds, which can occur when dust storms are driven by a northwest wind, can last for several days in a row, strengthening during the day and weakening at night, and creating devastating dust storms (Sissakian et al. 2013). Ganor et al. (2010) observed 966 dust days in the eastern Mediterranean during 1958-2006. They showed that the total incidence of dust days in the region increased in recent decades with an average rate of an additional 2.7 dust-storm days per decade (Barlow et al., 2015). In Iraq, a dust storm has the potential to occur when high winds at a threshold speed blow over areas with minimal vegetation cover, soils that lack snow and/or soil moisture content (NRL, 2009), or soils that are vulnerable to surface disturbance (Wilcox, 2012). In 2013, the Ministry of Environment in Iraq recorded 122 dust storms and 283 dusty days, and sources suggest that within the next ten years Iraq could witness 300 dusty days and dust storms per year (Kobler 2013). In recent years, because of the middle eastern dust (MED) storms, especially from the Arabian Peninsula and Iraq, the areas of south, west and southwestern Iran have been affected by exposure to PM₁₀ (Nourmoradi et. Al., 2016). In addition findings of Nourmoradi et al. 2016 study indicated

that pollution peaks associated with disastrous dust storm, have a remarkable adverse impacts on public health in Kermanshah.

Mesopotamian marshlands, the largest wetland in the Middle East and one of the most outstanding freshwater ecosystems in the world are located at the confluence of the Tigris-Euphrates river system at Shatt-ul Arab in southern Iraq, and partially extend into Iran. Dust-storm-related activity in the Tigris and Euphrates basin begins in May, reaches a maximum in July, and generally subsides by September–November (Middleton 1986; Al-Dabbas et al., 2012; Prospero et al., 2002). Drying the marshes prior 2003 and the obstacles encountered in restoring them is a factor contributing to the generation of these storms, which had led to enormous decrease in the agricultural lands. The main reason for the degradation of marshlands is the massive drainage works implemented by Iraq during the 1990's. A huge canal, which is known as “The Third River”, between the Tigris and Euphrates rivers was constructed to drain the waters of the marshes into the Persian Gulf. United Nations defines this degradation of the marshlands as “environmental and human disaster”. Several rehabilitation projects have been developed with the assistance of several countries as well as United Nations Environment Program (UNEP) since 2004 (Url-1). In addition, the large-scale development of upstream water regulation and dam structures, together with the drainage of the Mesopotamian Marshes have caused severe salinization of the river. Recent researches have shown that remotely sensed data can provide a synoptic and repeatable source of information to monitor marshlands. The Iraqi Marshland Observation System (IMOS) is one of the project which is conducted a preliminary analysis using satellite images between January 2003 and December 2005. It found dramatic changes in the vegetation cover (UNEP 2005), with 42 % of the original marshland recovered by November 2005. Some other attempts were made to investigate marshland recovery using remote sensing instruments like Moderate Resolution Imaging Spectroradiometer (MODIS) and/or Landsat (Despini et al. 2009; Muhsin et al. 2011; Al-Handal and Hu 2015). Those studies investigated the changes in Mesopotamian marsh vegetation and water coverage, and discussed potential drivers, including human activities and climate variability.

The main aim of this study is to assess aspects of the response of the Iraqi Marshes during the period of 1988–2017. This period directly follows the intensive localized human intervention that occurred during the 1990s through roughly 2002, and continues to be subject to ongoing human activities at a greater distance (dam construction and increased water

retention in the upper portions of the T-E basin). This period also shows responses to changes in water available due to changes in weather and climate.

2. Study area

The Mesopotamian marshlands constitute the most important and the largest wetland ecosystem in the Middle East and Western Eurasia, which were formed by the confluence of the Tigris and Euphrates rivers (Fig.1). The Mesopotamian marshes located on Lower Mesopotamia, are a complex of freshwater and brackish water lakes and impoundments constituting several sedimentary sub-environments.

The scale and speed of land cover change in the Mesopotamian marshlands, which suffered from rapid damage that caused severe ecological impacts, have been extraordinary since they were devastated by damming and river channelization during the late 1980s. Large-scale ecosystem degradation such as the loss of the Mesopotamian marshlands may have serious impacts on climate characteristics by means of water scarcity, extreme temperature variations that may lead potential dust storms.

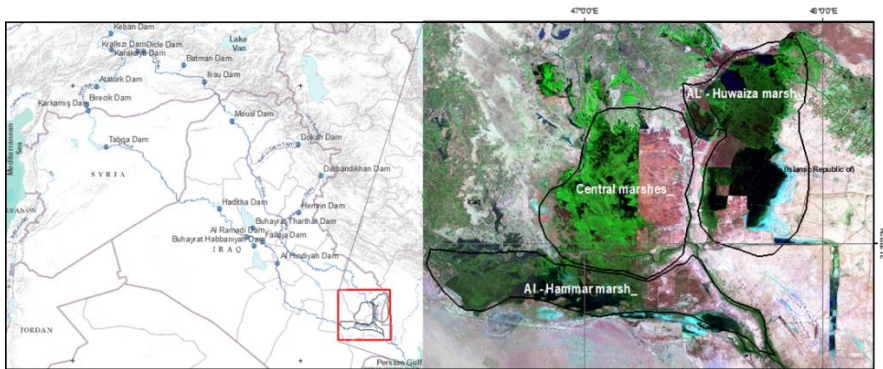


Figure 1. Shaded relief map of the Tigris-Euphrates basin (left) and Iraq marshlands (right).

The study area mainly focuses on three major marshes (Jones et al. 2008; Al-Ansari et al. 2012). The Al-Hammar marsh, which is located on the southern Lower Mesopotamia, is fed from the Euphrates and overflowing water from the Tigris through the Central marshes. The Central marshes with a coverage of 2,400 km², receive water mainly from the Tigris and to a lesser extent from the Euphrates. The Al-Huwaiza marsh lies on the border between Iraq and Iran and receives water from the Tigris.

3. Methodology

A multistage approach using low- and medium-scale resolution satellite imagery was followed to obtain a comprehensive coverage and analysis in order to map the evolution of the marshlands. In the study, MODIS and Landsat data were used to map the extent of changes in the Mesopotamian marshes from 1988 to 2017. To assess the surface extent of this change over the marshes, MODIS 8 day, 500 m, surface reflectance image composite scenes (MOD09A1) was used to examine the trends of open water recovery throughout the 1988–2017 time period. MODIS and Landsat (TM, 30m) scenes for each year were selected as of second week in March to coincide with maximum surface water extent.

Normalized difference vegetation index (NDVI) was used to determine marshland and irrigated land extent (Rouse et al. 1973). This most known and used vegetation index is a simple, but effective VI for quantifying green vegetation. It normalizes green leaf scattering in the Near Infra-red wavelength and chlorophyll absorption in the red wavelength (Eq.1).

$$\frac{(NIR-R)}{(NIR+R)} \quad (1)$$

A threshold value should be applied on NDVI images to separate vegetation from other land surfaces which is equivalent to a binary classification method in the sense that a pixel is treated as either 100 % vegetated or 100 % non-vegetated land pixel. In the study the threshold value was determined to be 0.16 to minimize the effect of arbitrary or subjective selection (Al-Handal and Hu 2015). The modified normalized difference water index (MNDWI) images were calculated for the region to determine the marshlands and the extent of open water. It is possible to achieve reliable quick discrimination of open water features by MNDWI (Xu 2006; Ouyang et al. 2014). This index is defined as:

$$\frac{(GR-MIR)}{(MIR+GR)} \quad (2)$$

In the study, MODIS bands 4 (0.545–0.565 microns), and 6 (1.63–1.65 microns) were used for Green (GR) and mid-infrared (MIR), respectively. A uniform threshold was also applied to MNDWI and NDVI images to identify the areal coverage of the wetlands. In some research, MNDWI was used to achieve reliable quick discrimination of open water features and it was found to provide an estimate of open water extent accurate to between 0.5% and 1.5% of the open water area derived from high resolution

images (Ouyang et al. 2014; Becker 2014). In our study, the accuracy was calculated by taking average difference percentages of MNDWI and NDVI values for the three marshes through the time period of 2001-2017 (Fig.2). As a result, MNDWI provided an estimate of open water extent accurate to 3%.

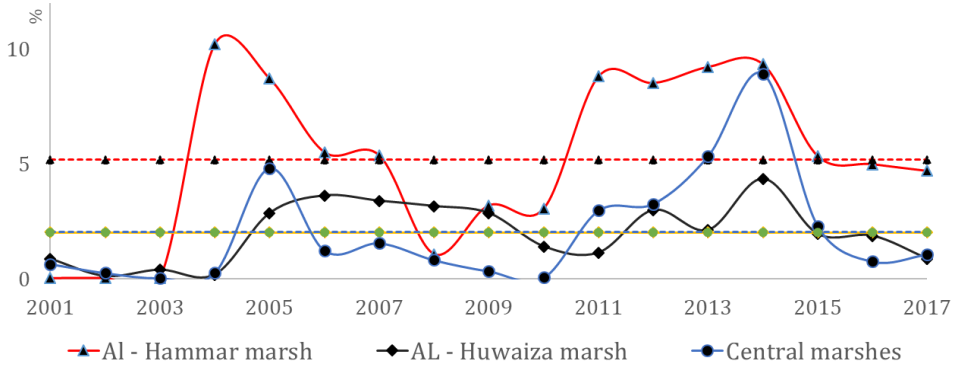


Figure 2. Inter-annual variations of average difference percentages of MNDWI and NDVI values for the three marshes.

Furthermore, precipitation and temperature data were obtained from Climatic Research Unit (CRU) of the University of East Anglia in the same time period on half-degree gridboxes of the study region to show responses to changes in water available due to changes in weather and climate (Harris et al. 2014). NDVI and MNDWI images were calculated for the period of 2000-2017 (Fig.3). Highly vegetated areas are shown in green and open water is blue where MNDWI is larger than zero. Colour in brownish indicates the low vegetated soil or sand areas.

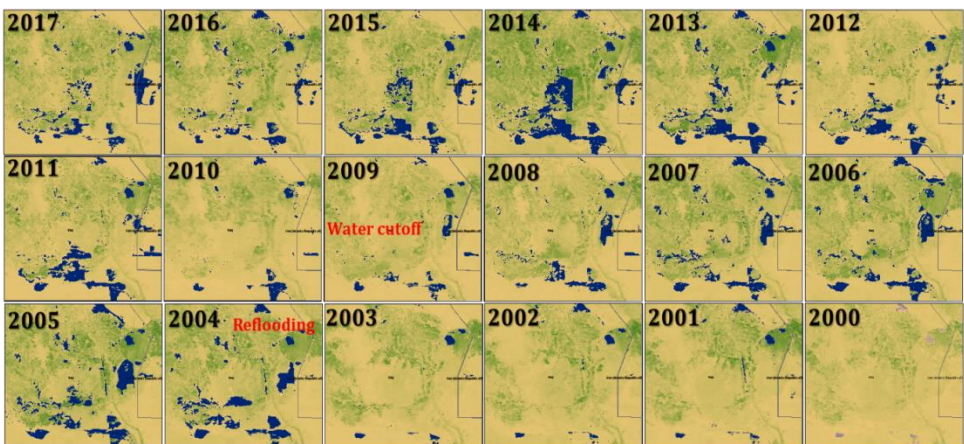


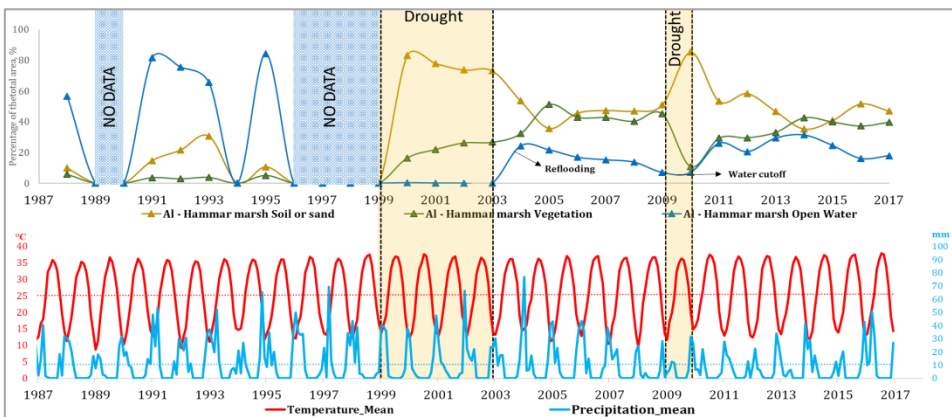
Figure 3. Geographical variations in combined MODIS NDVI-MNDWI images for 2000-2017 over three marshes.

4.Results

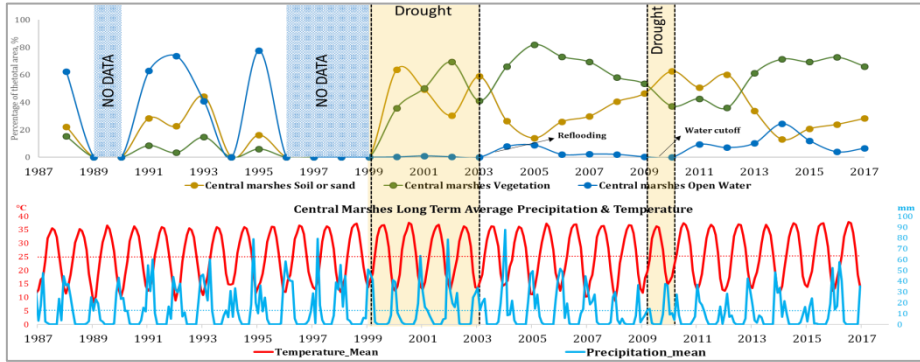
MODIS and Landsat data were used to map the extent of changes in the marshlands from 1988 to 2017. In the study, changes in vegetation, water and soil or sand coverage in three marshes investigated separately along with the associated climate data (Fig.4).

In the drought period of the region between 1999 and 2003; prior to the alterations from the Second Gulf War, a decrease in both water coverage and vegetated areas are clearly seen in 2003. Before that period, an increase in soil or sand areas is obviously seen in 2000 along with an increase in vegetation cover. In the period of 2004–2006, both open water and vegetated areas are increased.

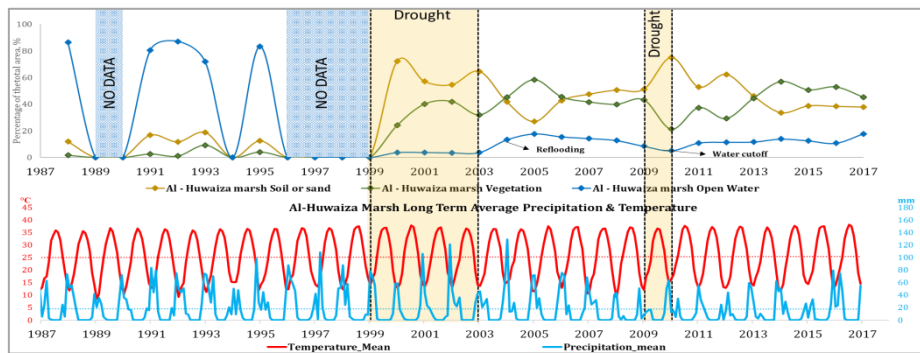
To rehabilitate the Mesopotamian marshes, a restoration program was initiated by national and international efforts through reflooding by 2003 (UNEP 2005). During the period from 2004 to 2009, water from the Tigris and Euphrates was redirected to flow towards these three marshes, which caused the highest water coverage resulting from marsh reflooding. This falls off between 2008 and 2009, reaching a decrease in open water in 2009, and vegetation in 2010 in the drought period. The area covered by water together with recovery of vegetation expanded after 2012. However, the observations also elicited continuous reductions between the 2004–2008 and 2009–2012 in all three regimes.



(a)



(b)



(c)

Figure 4 .Inter-annual variations of monthly changes in vegetation, water and soil or sand coverage in (a) Al-Hammar marsh, (b) Central marshes and (c) Al-Huwaiza marsh along with precipitation and temperature.

Figure 5 also shows the time series of the calculated areas of each class of the associated marshlands between 1988 and 2017. As seen in the figure, the vegetation coverage in all three marshes are coincide with those for the water coverage, contrary to the soil or sand coverage.

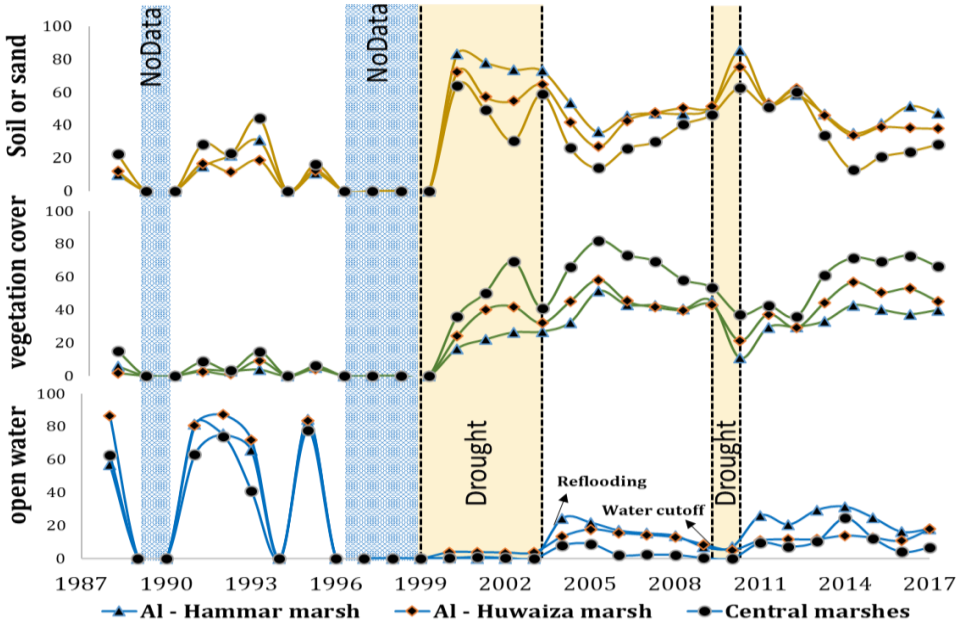


Figure 5. Inter-annual variations in time series of each class of the associated marshlands.

Before 2003, in the drought period, the marshes extent was minimized by active drainage and water diversion. Due to the increase in water storage, the marshes areal extent and mass experienced a great increase in the period of 2003 to 2005. In contrary, a sharp decline appears in water for the period of 2006–2009.

5. Conclusion

MODIS derived wetlands extent were used to determine the extent of changes in the three most important marshes from 1988 to 2017. Further, both indices were applied in order to monitor the changes in Mesopotamian marshlands within two time periods in which the marshes were exposed to significant droughts during the last 30 years.

Since almost all the waters of the Tigris river and more than half of the waters of the Euphrates river flow into Iraq, the negative impact of human activities on marshlands causes dramatic changes in vegetation coverage between 2003 and 2004 and 2009–2010. For the period of 2010 – 2017, the extent of changes in the marshlands show that the marshes may recover to a sustainable size. In conclusion, ecosystem rehabilitation and

sustainable management of these marshlands should be assessed with a continuous monitoring program. This will be required to fully understand the effects of anthropogenic actions on Mesopotamian marshlands and to evaluate the long-term and short-term changes in the marshes in response to changes in policies and management efforts.

References

- Al-Ansari, N.; Knutsson, S.; Ali, A.A. (2012). Restoring the Garden of Eden, Iraq. *J. Earth Sci. Geotech. Eng.*, 2, 53–88.
- Al-Dabbas M.A., A.M. Ayad, and R.M. Al-Khafaji. (2012). Dust storms loads analyses—Iraq Arabian Journal of Geosciences. 5:121–131.
- Al-Handal, A. & Hu, C. (2015). MODIS Observations of Human-Induced Changes in the Mesopotamian Marshes in Iraq, *Wetlands*, 35: 31. <https://doi.org/10.1007/s13157-014-0590-6>.
- Barlow, M., B. Zaitchik, S. Paz, E. Black, J. Evans, and A. Hoell, 2015: A Review of Drought in the Middle East and Southwest Asia. *J. Climate*. doi:10.1175/JCLI-D-13-00692.1
- Becker, R. H. (2014). The Stalled Recovery of the Iraqi Marshes. *Remote Sensing*, 6(2), 1260-1274. Doi:10.3390/rs6021260.
- Despini F, Teggi S, Bovio L, Immordino F (2009). Applications of Terra MODIS data for Iraq marshland monitoring. SPIE Europe Remote Sensing. Proceedings of the SPIE Europe's International Symposium on Remote Sensing (ERS09), Berlin.
- Ganor, E., Osetinsky, I., Stupp, A. and Alpert, P. 2010. Increasing trend of African dust, over years, in the eastern Mediterranean. *J. Geophys. Res.*, 115, D07201. doi:10.1029/2009JD012500.
- Goudarzi, S.M. Daryanoosh, H. Godini, P.K. Hopke, P. Sicard, A. De Marco, H.D. Rad, A. Harbizadeh, F. Jahedi, M.J. Mohammadi, J. Savari, S. Sadeghi, Z. Kaabi, Y. Omidi Khaniabadi, 2017. Health risk assessment of exposure to the Middle-Eastern Dust storms in the Iranian megacity of Kermanshah, *Public Health* Volume 148, July 2017, Pages 109-116.
- Harris, I., Jones, P.D., Osborn, T.J. and Lister, D.H. (2014). Updated high-resolution grids of monthly climatic observations - the CRU TS3.10 Dataset. *International Journal of Climatology* 34, 623-642 doi:10.1002/joc.3711
- Jones, C., Sultan, M., Yan, E. Milewski, A., Hussein, M., Al-Dousari, A., Al-Kaisy, S., Becker, R. (2008). Hydrologic impacts of engineering projects on the Tigris-Euphrates system and its marshlands. *J. Hydrol*, 353, 59–75.
- Kobler, M. (2013) Dust storms of Iraq, UN Secretary General for Iraq, A ministerial

meeting in Nairobi, Kenya.

Kutiél, H. and Furman, H. 2003. Dust Storms in the Middle East: Sources of Origin and their Temporal Characteristics, *Indoor Built Environ* 12:419–426.

Middleton, N. (1986). Dust storms in the Middle East. *J. Arid Environ.* 10:83–96.

Muhsin I, Fouad J, Mashe K, Rafid JT (2011). Monitoring the vegetation and water content of Al-Hammar marsh using remote sensing techniques. *Bag Sci J* 8:646–650.

Nourmoradi H, Omid Khaniabadi Y, Goudarzi G, Daryanoosh S M, Khoshgoftar M, et al. Air Quality and Health Risks Associated With Exposure to Particulate Matter: A Cross-Sectional Study in Khorramabad, Iran, *Health Scope.* 2016 ;5(2):e31766. doi: 10.17795/jhealthscope-31766.

NRL, (2009). Description of NAAPS (Navy Aerosol Analysis and Prediction System) Global Aerosol Model. Naval Research Laboratory. http://www.nrlmry.navy.mil/aerosol/Docs/globaer_model.html (accessed 24.10.17).

Ouyang, Z.; Becker, R.; Shaver, W.; Chen, J. (2014). Evaluating the sensitivity of wetlands to climate change with remote sensing techniques. *Hydrol. Process*, 28, 1703–1712.

Prospero, J.M., P. Ginoux, O. Torres, S.E. Nicholson, and T. E. Gill. (2002). Environmental characterization of global sources of atmospheric soil dust identified with the NIMBUS 7 Total Ozone Mapping Spectrometer (TOMS) absorbing aerosol product. *Rev. Geophys.* 40(1):1002. doi:10.1029/2000RG000095

Rouse JW, Haas HR, Schell JA, Deering DW (1973). Monitoring vegetation systems in the Great Plains with ERTS. Third ERTS Symposium, NASA SP-351 I: 309–317

Sissakian, V. , Al-Ansari, N. and Knutsson, S. (2013). Sand and dust storm events in Iraq. *Natural Science*, 5, 1084-1094. doi: 10.4236/ns.2013.510133.

UNEP (2005) Project to Help Manage and Restore the Iraqi Marshlands.

Url-1. Republic of Turkey Ministry of Foreign Affairs. <http://www.mfa.gov.tr/the-mesopotamian-marshlands.en.mfa> (accessed 14.11.2017)

Wilcox, B., (2012). Dust Storms Roll Across America. United States Geological Survey Science Features. http://www.usgs.gov/blogs/features/usgs_top_story/dust-storms-roll-across-arizona-2/ (accessed 24.10.17).

Xu, H. (2006). Modification of normalised difference water index (NDWI) to enhance open water features in remotely sensed imagery. *Int. J. Remote Sens.*, 27, 3025–3033.

Sand and Dust Storm Sources in Kuwait

Mohamed F. Yassin^{1*}, Sarah K. Almutairi²

¹Environment & Life Sciences Center, Kuwait Institute for Research and Science

²College for Graduate Studies, Kuwait University

mohamed_f_yassin@hotmail.com

Abstract

Sand and Dust storms are among the most severe environmental problems in certain regions of the World, such as Kuwait. To assess the impact on air quality, this study concerns to investigate the dust storms sources in Kuwait over a 12-year period from 2000 to 2012 at different latitudes. The HYSPLIT model is used to create seasonal climatologies of air parcel trajectories. Monitored visibility levels during the twelve years for each transport pattern will be collected from the meteorological stations. The analysis of visibility levels is presented and discussed. Daily trajectories are computed backward for five days from an origin centered over Kuwait at 1000, 3000 and 5000 m above the ground surface. The present work provides evidence of the mean region of dust storm sources over Kuwait. Furthermore, it is expected to help in establishing guidelines to assist people to protect themselves from the dust.

Keywords: Meteorological data; Visibility; Dust storm; Numerical model

1. Introduction

Dust and sand storms are meteorological phenomena driven by gusty winds that occur when strong pressure gradients develop across arid or semi-arid regions where loose sands or soils are more prevalent (Glickman 1999). Essential conditions for the occurrence of dust storms include an immense dust/sand source, strong surface winds, and an unstable atmosphere (Zhao and Yu 1990; Yu et al. 2002). Dust storms (DS) may cause reduction of visibility that limits various activities such as air and sea navigation movement and increase traffic accidents. In addition, the environmental impacts of DS include reduced soil fertility and damage to crops, a reduction of solar radiation and in consequence the efficiency of solar devices, damage to telecommunications and mechanical systems, dirt, air pollution, increase of respiratory diseases and many other

environmental and health impacts. (Hagen 1973; Mitchell 1996; Nihlen 1995).

The identification of territorial dust and sand sources plays an important role in fighting the effects of these phenomena; several approaches have been used to recognize these sources based on various sources of data, such as Prospero et al. (2002), Kutiel and Furman (2003), Lin et al. (2004, 2007), Liu et al. (2004), Kaskaoutis et al. (2008), Dementeva et al. (2008), McGowan and Clark (2008), Baddock et al. (2009), Igarashi et al. (2009), Yasunari and Yamazaki (2009), Yu et al. (2010), Lee et al. (2010), Prasad et al. (2010), and Desouza et al. (2011). They found that the largest and most persistent sources are located in the Northern Hemisphere, mainly in a broad “dust belt” that extends from the west coast of North Africa, over the Middle East, Central and South Asia, to China. Pineda-Martinez et al. (2011) investigated the regional impact of extreme wind-induced dust transport in the central-northern part of Mexico by numerical modeling of a strong dust storm during the passage of a cold front on 18 March 2008. They estimated roughly that the fraction of PM₁₀ emitted during this event was 9162.72 ton. Wang et al. (2011) simulated the global dust distribution for 2008 by HYSPLIT model using two different dust emission schemes. The model reproduces the dust storm frequency for most of the regions for the two emission approaches. Sai-Chun and Guang-Yu (2012) examined the characteristics of dust storms between 1997 and 2007 Based on daily observation data at 222 meteorological stations in China. Results showed that, Dust storms were positively correlated to wind speed and temperature, and they were negatively correlated to relative humidity and air pressure. Indoitu et al. (2012) monitored and assessed the spatial and temporal distribution of dust storms over the Central Asian region during the last seven decades. The results of the analysis show a significant decrease in dust/sand storm frequency during the last decades and considerable changes in the active source areas. Recently, Wang et al. (2016) proved that dust storms are the direct cause of the variations in the number of acid rain days and acid rain ratio, as well as the changes in atmospheric particulate pollution, in spring by using the Granger Causality Test and correlation analysis methods based on 1993 to 2007 data, including the number of days of dust storms, atmospheric particulate pollution, and acid rain. Broomandi et al. (2016) studied the features of an intense dust storm and its transport characteristics during June 7th to June 9th 2010 in Ahvaz city. The model results were found to well reproduce temporal and spatial distribution of mineral dust concentrations according

to in-situ measurements.

Various studies on dust and sand characteristics and sources have been performed in the State of Kuwait, e.g. Draxler et al. (2001), Saeed and Al-Dashti (2010), Sabbah. (2010), and Bu-Olayan and Thomas. (2011, 2012). A.Alolayan. et al. (2013) investigated source apportionment of fine particles in Kuwait city between February 2004 and October 2005. The results indicated that the PM_{2.5} levels in Kuwait were 35µg/m³ and more than half of the PM_{2.5} appears due to crustal material originated outside of the country. In this study, we used a combination of surface observations, remote sensing and meteorological data to study the variability and temporal and synoptic characteristics of sand and dust cases over northern Saudi Arabia. The main goal of this study is to identify the key geographical regions responsible for dust storms in Kuwait over a 12 year period from 2000 to 2012 at different latitudes. To accomplish this objective, the HYSPLIT model was used to create seasonal climatologies of air parcel trajectories. The results of the model were validated using extensive satellite data.

2. Materials and Methods

2.1. Site Description

Kuwait is a small country with total land area 17818 km² located in the northwestern sector of the northwestern sector of the Persian Gulf and bordered by Saudi Arabia and Iraq. It is located between altitude 29° 30' north and longitudes 45° 45' east. Topography of Kuwait characterized by: a) high frequency of blowing sand, b) raising dust due to the high wind speeds and sandy soil, c) long hot and dry summer, and d) short, cool and sometimes rainy winters.

2.2. Data Collecting

For this study, Kuwait meteorology data provided by the Meteorology Department of Kuwait Directorate General of Civil Aviation which is located in the vicinity of Kuwait International Airport, 15 km west of Kuwait City. The meteorological data for 12 years from 2000-2012 include visibility, wind speed, wind direction, air temperature, and humidity. To determine the dust storm days, wind speed at the surface should be 8 m/s or greater to metabolize dust and the visibility equal or less than 1000m.

2.3. HYSPLIT Model

HYSPLIT (Hybrid Single-Particle Lagrangian Integrated Trajectory) model is a complete system for computing simple air parcel trajectories, complex dispersion and deposition simulations. It was developed in National Oceanic and Atmospheric Administration (NOAA) and in the Atmospheric Research Laboratory (ARL), USA (Draxler and Hess, 1998). The model updated and developed several times the initial version of the model was in 1982. HYSPLIT has previously been used extensively to compute both forward and back air parcel trajectories for periods ranging from several hours to 14 days (see Draxler and Hess, 1998; Pace et al., 2006; Rousseau et al., 2006; McGowan and Clark, 2008). The forward and backward trajectories of the HYSPLIT model have been recognized as a powerful tool for the analysis of dust cloud transport (Nee et.2007; Yuh Yu et. 2010). On the map the path of air mass trajectory is presented as series points drawn either backwards or forwards in time. Hysplit trajectory model use a formula to calculate the position based on wind velocity vectors and time. The model was configured to compute backward trajectories starting daily at 20:00 UTC (11:00 Kuwait LT). The Trajectory calculation is achieved by the time integration of the position of an air parcel as it is transported by the 3-D winds (Draxler and Hess, 1998; McGowan and Clark, 2008), with each trajectory having duration of five days. The trajectories were run for randomly day from each season during 12 years started from 2000 to 2012 and selected three levels to analyze the trajectory paths. These levels were 1000, 3000, 5000m agl (above ground level).

3. Results and Discussions

The HYSPLIT model was applied for a case study data selected on 25 March 2011 during a heavy dust storm covered Kuwait around 18:00KWT (15:00 UTC) of that day . It was one of the most severe dust storms recorded on Kuwait and Arabian Peninsula due to both large scale and severity of this storm event. Storm was originating on 25 March 2011, impacting several cities in northwest, west, southwest, and central parts of Iraq and Kuwait. The fast moving storm decrease visibility to near zero in Kuwait with wind speed of 17.7m/s. Storm lasted for 7hr started from 18:00KWT (15:00UTC) to 24:00KWT (21:00 UTC). Figures 1-2 are showing that there is an inverse relation between wind speed and visibility. The highest wind speed was in 25th March with lowest visibility.

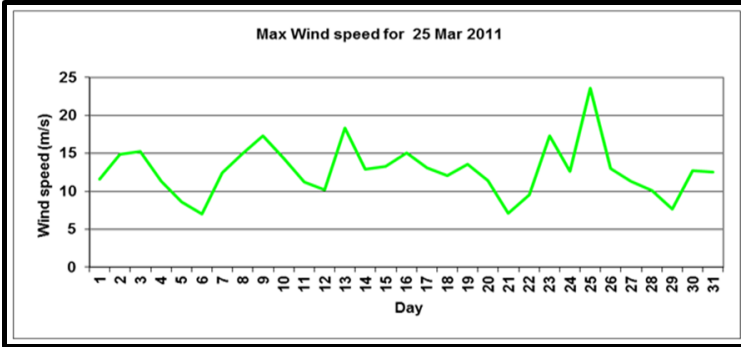


Figure 1. Maximum wind speed for 25th March 2011.

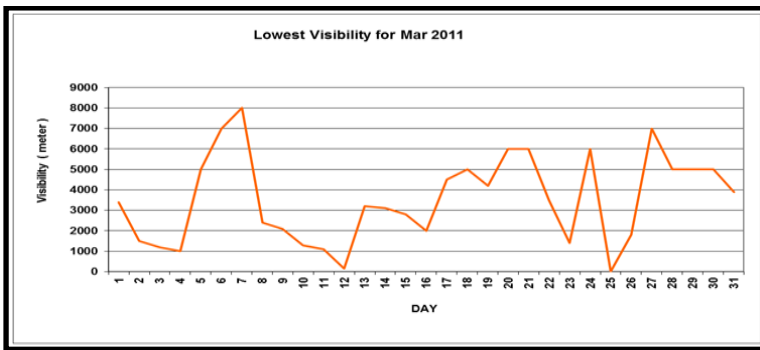


Figure 2. Lowest visibility for March 2011.

A low pressure system moved eastward from Western Red Sea into North East of Saudi Arabia with velocity of more than 35 km/hr. It carried dust and sands from North Africa and loft it. The surface low was reflection of an upper trough centered over Turkey and the Black Sea, which then moves into the southeastern direction (Fig.3).

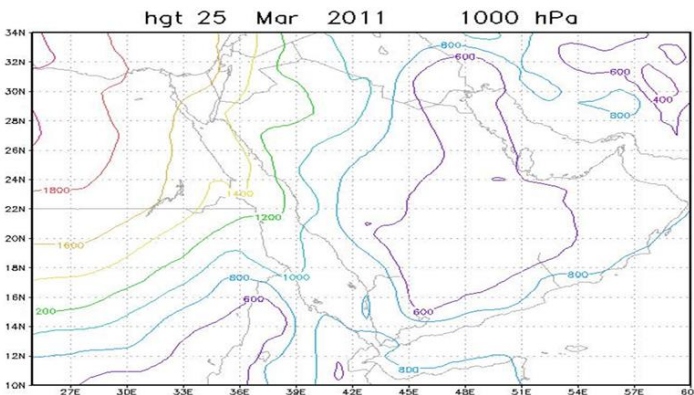


Figure 3. Pressure system for the case study (25 Mar 2011) at surface (1000hpa).

The low pressure system was stretched from north of the Mediterranean to its central parts and resulted as dust storm over Kuwait. The isotach (wind arrows) was sharpened with ridge of the wave centered over the depression. The wind field relating to 25 March dust storm over Kuwait is shown in (Fig.4).

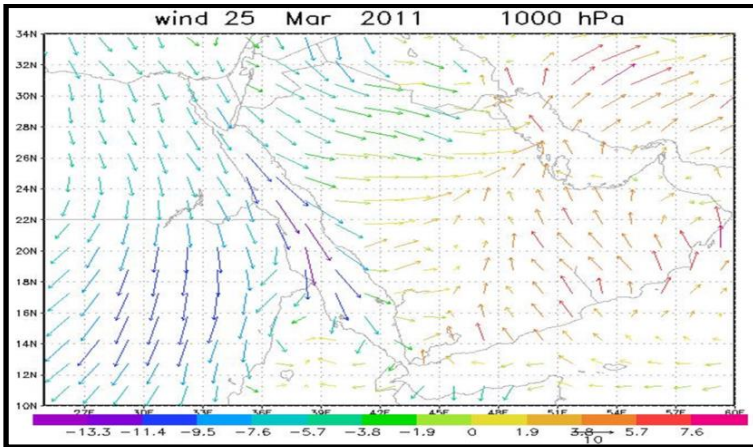


Figure 4. Wind system for the case study (25 Mar 2011) at surface (1000hpa).

The isotachs are plotted at different geopotential heights. The plot shows an area of convergence takes place over central east of Saudi Arabia. The cold wind blowing from the Mediterranean was intersected with warm air stream blowing from southern Saudi Arabia resulting in a strong upward motion over Kuwait, the dust storm then generated. The severity of the dust storm and the high density of fine dust carried by the wind from south of Saudi Arabia had caused a thick suspension of fine dust into atmosphere that lasted for the following 24 hours.

Fig. 5 shows dust storm blow in northwest Kuwait. With 1000 m altitude it was started on 21 March 2011 from Mediterranean Sea close to Lebanon and passing to Syria, Iraq then reach Kuwait on 25 March 2011. The direction of dust storm change with different altitude on 3000 m it was started on 21 March 2011 from Bay of Biscay (located off the north coast of Spain and the west coast of France in the Atlantic Ocean, south of the Celtic Sea) to pass through Portugal, Spain, Mediterranean Sea close to Tunisia, Libya, Egypt and move to Saudi Arabia then arrived Kuwait from southwest on 25 March 2011. At 5000 m altitude dust storm before 5 days

of 25 March 2011 started from North Atlantic Ocean passing west Morocco, Algeria, Tunisia, and Libya, Egypt then west Saudi Arabia and end in Kuwait.

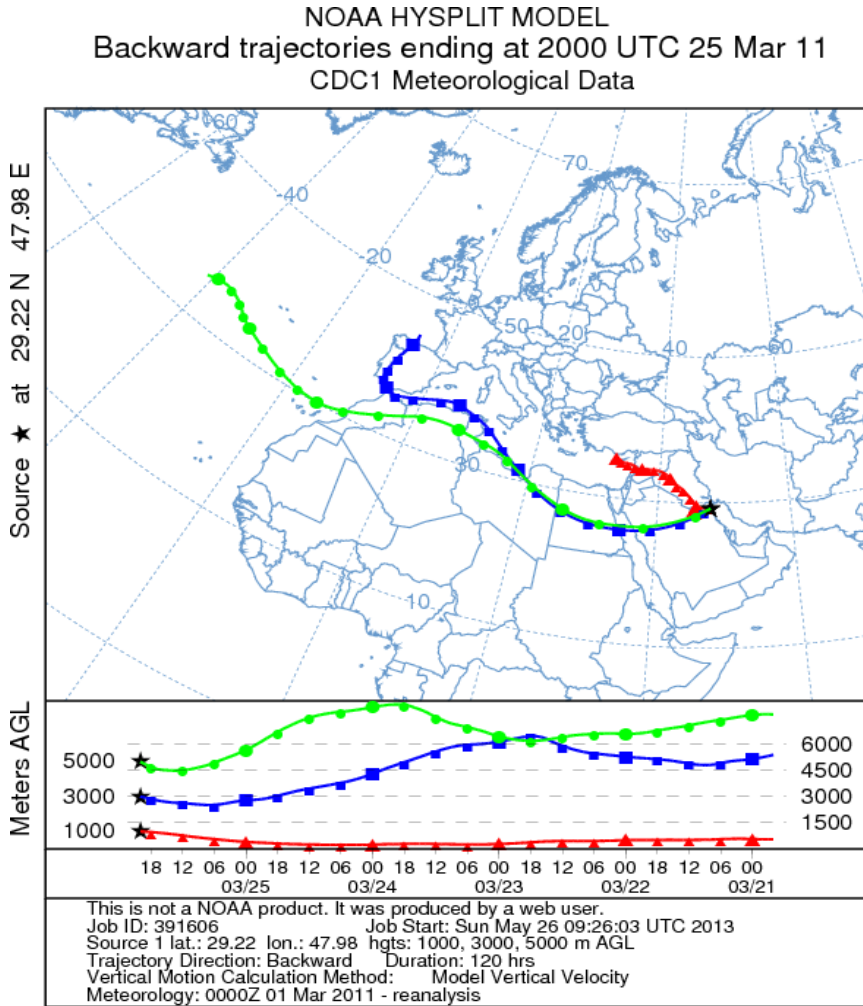


Figure 5. Five days backward trajectory analysis started at altitudes of 1000, 3000, and 5000 m at 20:00 UTC (23:00 KWT) on 25 March 2011 at Kuwait.

4. Conclusion

A back trajectory method based on HYSPLIT model, and climate conditions were used to study the source of the dust storms over Kuwait in each season during 2000 to 2012. The current study clearly indicates that there is significant influence of the climate conditions on the dust storms sources in Kuwait. The result indicated that influencing the visibility come from the west and northwest direction. Kuwait air quality was influence strongly by

North West winds which caused by the huge Indian monsoon from the east of the country together with the west high pressure “Mediterranean ride”. The air mass trajectories were originated from Mediterranean Sea, North Africa and North Atlantic Ocean mainly from west- southwest sector. For Winter Season: Influencing the visibility come from the northwest direction. Air mass trajectories demonstrate that Kuwait air quality was influence strongly by North West winds “Shamal wind”. The air mass trajectories for were originated from south Iraq, north Saudi Arabia, Europe, North Atlantic Ocean, North Africa and Sahara Desert mainly from west- North West sector. During 12 years from 2000 to 2012 in Kuwait, almost all dust sources have been Sahara Desert and Arabian Desert.

References

- A.Alolayan, Mohammad., Brown, Kathleen W., Evans, John S., Bouhamra, Walid S., Koutrakis, Petros.(2013). Source Apportionment of Fine Particles in Kuwait City, *Science of the Total Environment*, 448, 14-2.
- Baddock, Matthew C., Bullard, Joanna E., and Bryant, Robert G. (2009). Dust source identification using MODIS: A comparison of Techniques Applied to the Lake Eyre Basin, Australia. *Remote Sensing of Environment*, 113, 1511–1528.
- Brown, K. W., Bourhamra, W., Lamoureux, D.P., Evans J.S., and Koutrakis, P. (2008). Characterization of Particulate Matter for Three Sites in Kuwait, *Journal of the Air Waste Management Association*, 58(8), 994-1003.
- Bu-Olayan, A.H., Thomas, B.V. (2011). Monitoring the Dust Deposition Rate and Trace Metals Levels in PM_{1.0} from Industrial Areas of Kuwait, *ARCH. ENVIRON. SCI.*, 5, 11-16.
- Bu-Olayan, A.H., Thomas, B.V. (2012). Dispersion Model on the PM_{2.5} Fugitive Dust and Trace Metals Levels in Kuwait Governorates, *Environ Monit Assess*, 184, 1731-1737.
- Dementeva, Ayuna L., Zhamsueva, Galina S., Zayahanov, Alexander S., Tsydypov, Vadim., Ayurzhanayev, A.A. (2008). Particularities of Circulation and the Analysis of Dust Storm in Sharp- Continental Climate Conditions of Mongolia, *Proc. of SPIE* Vol. 6936 69360Z-1.
- Desouza, Nirmala D., Simon, Baby. , Qureshi, Muhammmad S. (2011). Evolutionary Characteristics of A dust storm over Oman on 2 February 2008, *Met. Atmos Phys*, 114:107–121.
- Draxler, R.R. and Hess, G.D. (1998). An overview of the HYSPLIT_4 Modeling System for Trajectories, dispersion and deposition. *Aust. Metero. Mag.*, 47, 295-308.

Draxler, R.R., Gillette, D. A., Kirkpatrick, J. S., and Heller, J. (2001). Estimating PM₁₀ Air Concentrations from Dust Storms in Iraq, Kuwait and Saudi Arabia, *Atmospheric Environment*, 35, 4315-4330.

Glickman, T. S. (1999). *Glossary of Meteorology*, American Meteorological Society, 850 pp.

Hagen, L.J. , Woodruff, N.P. (1973). Air Pollution from Dust Storms in the Great Plains, *Atmos Environ*, 7, 323–332.

Igarashi, Yasuhito. , Inomata, Yayoi. , Aoyama, Michio. , Hirose, Katsumi, Takahashi, Hiroshi., Shinoda, Yoshihiro., et al. (2009). Possible Change in Asian Dust Source Suggested by Atmospheric Anthropogenic Radionuclides during the 2000s, *Atmospheric Environment*, 43, 2971–2980.

Indoitu, R., Orlovsky, L., Orlovsky, N. (2012). Dust Storms in Central Asia: Spatial and Temporal Variations, *Journal of Arid Environments*, 85, 62-70.

Kaskaoutis, D.S., Kambezidis, H.D., Nastos, P.T., Kosmopoulos, P.G. (2008). Study on an Intense Dust Storm over Greece, *Atmospheric Environment*, 42, 6884–6896.

Kutiel, Haim., and Furman, Hadar. (2003). Dust Storms in the Middle East: Sources of Origin and their Temporal Characteristics, *Indoor Built Environ*, 12, 419–426.

Lee, Y.C., Yang, Xun., and Wenig , Mark. (2010). Transport of Dusts from East Asian and non-East Asian sources to Hong Kong during dust storm related events 1996-2007, *Atmospheric Environment*, 44, 3728-3738.

Liu, Xiaodong., Yong Yin, Zhi., Zhang, Xiaoye., and Yang, Xuchao. (2004). Analyses of the Spring Dust Storm Frequency of Northern China in Relation to Antecedent and Concurrent wind, Precipitation, Vegetation, and Soil moisture Conditions, *Journal of Geophysical Research* , 109, D16210, doi: 10.1029/2004JD004615.

Lin, C.-Y. , Wang, Z., Chen, W.-N. , Chang, S.-Y., Chou, C.C.K., Sugimoto, N., and Zhao, X. (2007). Long-range Transport of Asian dust and Air Pollutants to Taiwan: Observed Evidence and Model Simulation, *Atmos. Chem. Phys.*, 7, 423–434, 2007.

McGowan, Hamish and Clark, Andrew. (2008). Identification of Dust Transport Pathways from Lake Eyre, Australia using Hysplit, *Atmospheric Environment* ,42, 6915–6925.

Nihlen T, Lund SO. (1995). Influence of Aeolian Dust on Soil formation in the Aegean Area, *Zeitschrift fur Geomorphologie*, 393, 341–361.

Pineda-Martinez, Luis F., Carbajala, Noel., Campos-Ramosb, Arturo A., Noyola-Medrano, Cristina., and Aragón-Piña, Antonio. (2011). Numerical Research of Extreme Wind-induced Dust Transport in a Semi-arid Human-impacted Region of Mexico, *Atm. Env.*, 45, 4652- 4660.

Prasad, Anup K., El-Askary, Hesham., and Kafatosa, Menas. (2010). Implications of High Altitude Desert Dust Transport from Western Sahara to Nile Delta During

Biomass Burning Season, *Environmental Pollution*, 158, 3385-3391.

Prospero, Joseph M., Ginoux, Paul., Torres, Omar., Nicholson, Sharon E., and Gill, Thomas E. (2002). Environmental Characterization of Global Sources of Atmospheric Soil Dust Identified with the Nimbus 7 Total Ozone Mapping

Sabbah, I. (2010). Impact of Aerosol on Air Temperature in Kuwait, *Atm. Res.*, 97, 303–314.

Saeed, Thuraya M. and Al-Dashti, Hassan. (2011). Optical and physical characterization of “Iraqi freedom “dust storm, a case study, *Theor Appl Climatol*, 104, 123–137.

Sai-Chun, TAN. and Guang-Yu, SHI. (2012). Correlation of Dust Storms in China with Chlorophyll *a* Concentration in the Yellow Sea between 1997–2007, *Atmospheric and Oceanic Science Letters*, 5(2), 140-144.

Wang, Yaqiang., Stein, Ariel F., Draxler, Roland R., De la Rose, Jesus, D., and Zhang, Xiaoye. (2011). Global Sand and Dust Storms in 2008: Observation and HYSPLIT model Verification, *Atmospheric Environment*, 45, 6368-6381.

Yasunari, Teppei J., and Yamazaki, Koji. (2009). Impacts of Asian Dust storm Associated with the Stratosphere-to-troposphere Transport in the spring of 2001 and 2002 on Dust and Tritium Variations in Mount Wrangell ice core, Alaska, *Atmospheric Environment*, 43, 2582–2590.

Yu, Jia-Yuh., Wang, Yi-Wen., and Chang, Cheng-Wei. (2010). Asian Dust Storm Activity and Its Association with Atmospheric Circulation from 1995 to 2006, *Terr. Atmos. Ocean. Sci.*, 21(2), 375-391.

Zhao, B. and X. Yu. (1990). On eastern Asian dust storm, *Adv. Atmos. Sci.*, 7, 11-26.

The Change in Water Masses in Syria and Iraq Relating to Sand and Dust Storms

Dr. Halil GÜNEK

Firat University, Department of Geography, Elazığ, Turkey

Abstract

Remote sensing data have been used for a long time to assess coastal management and water resources. The large source of dust creates natural resources. However, there is a certain extent of influence in human resources. The most prominent of human resources correspond to the areas of temporary water masses. The Euphrates and Dicle ridges, which arise from relatively humid regions in our study and which are arid regions, are based on determining the areal changes in the water masses formed by the dams and lakes established in the catchment areas and investigating their effect on the dust storms. The changes in the water masses in the study were dealt with in two ways. The first is how the water masses changed over the long term. In order to determine this change, Landsat TM 5 images belonging to 1989 or 1990 and Landsat 8 OLI images belonging to September or October 2016 were used to identify the changes and occurrences in the fields of Syrian and Iraqi water bodies. In the study, differences were made using methods such as NDWI, MNDWI, NDVI, IP and land classification, water bodies and land areas were differentiated. Surfaces that are classified by satellite images are transformed into areal computations.

In the study, it is seen that new water masses were formed especially in the high sections in Iraq and Syria. However, artificial lake surfaces, which have been formed very early in Iraq, have been found to have been reduced to large areas, even in most places because the salinity in these areas has increased considerably.

Keywords: AWEI, MNDWI, NDWI, Iraq, Syria, Dust and Sandstorms

Recent Spatiotemporal Variations of Synoptic Meteorological Sand and Dust Storm Events Observed over the Middle East and Surrounding Regions

Murat Türkeş

*The Center for Climate Change and Policy Studies and the Department of Physics,
Boğaziçi University, Istanbul, Turkey*

Abstract

The study investigated the climatology and spatiotemporal variations of synoptic meteorological sand and dust storms (SDS) observed over the Middle East and surrounding regions during 2003-2016 period. Time-series data from total 172 stations was used in station- and country-based climatological analysis, whereas 134 of 172 stations were used for the station-based and country-based time-series analysis. We also made use of the Aerosol Optical Depth/Optical Thickness (AOD) time-series data in addition to the station-based observational weather sand and dust events.

Statistically significant positive relations between inter-annual variations of numbers of the SDS weather events and the country-based AOD time-series revealed clearly that synoptic meteorological surface SDS weather events data and remotely-sensed atmospheric data are well correlated, proving that both data sets can be used for the observational SDS studies including temporal and spatial variability. According to the $u(t)$ test statistics calculated for the Mann-Kendall rank correlation coefficient, annual number of synoptic SDS weather events in Turkey, Saudi Arabia, Iran and the regionally averaged annual totals of the Eastern Mediterranean and the Southwest Asia increased significantly at the 5 per cent level. Among the 11 countries selected for the study only Egypt's annual total SDS series indicated significant decreased trend at the 5 per cent level. Based on the resultant $u(t)$ test statistics from the Mann-Kendall analysis, even though 94 (40) of all 134 stations used in the trend analysis is characterised with an increasing (a decreasing) trend, 34 (16) stations tended to increase significantly at the 5 (1) per cent level, while 12 stations indicated a decreasing trend at the 5 per cent level of significance.

Keywords: *Turkey, Southwest Asia, Eastern Mediterranean; SDS and Aeresol Opti- cal Depth (AOD) data; Mann-Kendall $u(t)$ test, Pearson's correlation coefficient.*

1. Introduction

Aerosols, which would be of either natural or anthropogenic origin, may influence climate in several ways: directly through scattering and absorbing radiation, and indirectly by acting as cloud condensation nuclei or ice nuclei, modifying the optical properties and lifetime of clouds. Atmospheric aerosols originate from two different pathways: emissions of primary particulate matter (PM), and formation of secondary PM from gaseous precursors. The bulk of aerosols are of natural origin. Some scientists use group labels that refer to the chemical composition, namely: sea salt, organic carbon, black carbon, mineral species (mainly desert dust), sulphate, nitrate, and ammonium (IPCC, 2014). Another important term for the topic is sand and dust storms (SDS). Sand and dust storms are officially defined by the World Meteorological Organization (WMO) as the result of surface winds raising large quantities of dust into the air and reducing visibility at eye level (1.8 m) to less than 1000 m (UNEP, WMO, UNCCD, 2016). The most frequent and severe dust storms are commonly associated with surface and upper atmospheric specific synoptic meteorological conditions that vary according to region. These conditions essentially include: (i) steep atmospheric pressure gradients around subtropical anticyclones, (ii) surface cyclones and frontal cyclones (e.g. mid-latitude and Mediterranean originated frontal low pressure systems, (iii) direct or circulation-based monsoonal airflows, (iv) local winds associated with strong temperature and pressure gradients in topography, (v) dust devils and convective plumes as a result of daytime turbulence in the planetary boundary layer, (vi) near-surface cold-air outflows associated with thunderstorms (e.g. haboobs), and low-level jets.

Synoptic meteorological SDS events have a number of positive and negative effects on the environment through the various interactions that are complex and not yet fully understood (Knippertz, 2014). Dust affects atmospheric, oceanic, biological, terrestrial and human processes and systems (Washington and Wiggs, 2011). For instance, dust plays a major role in the Earth's biogeochemical cycles, fertilizing and sustaining both oceans and forests (Goudie, 2009; Goudie and Middleton, 2001). Dust affects the climate system, modifying tropical storm and cyclone intensities (Evan et al., 2006) and changing the Earth's radiative balance, which can cause drought intensification (Han et al., 2008; Highwood and Ryder 2014). On the other hand, dust can enhance precipitation by acting as droplet nuclei (Nenes et al., 2014). The magnitude of dust emissions to the atmosphere depends on the surface wind speed, many soil-related factors

(e.g. soil texture and moisture) and vegetation cover (Boucher et al., 2013). Drought and wind contribute to the emergence of dust storms, as do poor farming and grazing practices or inadequate water management by exposing the dust and sand to the wind (WMO, 2014). Prospero et al. (2002) indicated based on the NIMBUS 7 Satellite data analysis that most major dust sources are located in arid regions in topographic depressions where deep alluvial deposits have been accumulated. Although SDS have a wide geographical extent, as they occur in all world regions and are trans-boundary in nature, the largest and most persistent sources are located in the Northern Hemisphere (NH), mainly in a well-known broader dust belt extending from the west coast of North Africa, over the Middle East, Central and South Asia, to China. Dust sources, regardless of size or strength, can usually be associated with topographic lows (geomorphologic depressions) located in arid regions with annual rainfall under 200–250 mm (Prospero et al., 2002). On the other hand, the anthropogenic sources contributes with 25% to global dust emissions (Ginoux et al., 2012), and dust load may have doubled in the 20th century over much of the world due to anthropogenic activities (Mahowald et al., 2011). A factor of a significant influence on dust emissions and dust impacts to society and environment is the dust grain size distribution (WMO, 2014). SDS weather events and associated mineral aerosol transport are driven primarily by meso- and synoptic-scale atmospheric processes (Nickovic et al. 2012). Some recent works on detailed global mineralogy of arid soils also produced an important input for studying processes affected by the dust mineralogy, such as radiation, health, cloud formation and marine productivity (Nickovic et al. 2012; Journet et al. 2014).

Sand and dust storms are mostly associated with arid and semi-arid (dry-land) areas, but can occur anywhere where there are dry unprotected sediments, sands and dusts, etc. Impacts of the SDS on achieving sustainable development are therefore significant at the local, regional and global levels and require for joint efforts at all of these scales. Consequently, this study investigated the climatology and spatial and temporal variations of synoptic meteorological sand and dust storms (SDS) events observed over the Middle East and surrounding regions during 2003-2016 period via followings: climatology of SDS weather events and their spatial and temporal variations and patterns; some examples for the major atmospheric drivers and controls; inter-annual variations and long-term trends in the station-

and country-based and regional time-series; statistically significance and spatial distribution patterns of long-term trends in the SDS series.

2. Data and Methodology

- Study period: 1981-2010 for the climatology, and the main study period of 2003-2016;
- Geographical regions included in study area: Eastern Mediterranean Basin and the South-west Asia (Middle East, Iran, Arabian Peninsula);
- Number of surface synoptic meteorological stations: Total 172 was used in general country- and regional-based analysis, and 134 of all stations were used for station-based and country-based time-series analysis (e.g. analysis of correlation, temporal variations and trends etc.) (Figure 1). Stations in the Figure 1 labelled with a triangle symbol in Turkey were used both for the basic climatology and other correlation, trend and some anomalous surface and upper atmospheric pattern analyses (results of the later not given in the present paper), while the rest of the stations mostly characterised with a small number and rare SDS events in Turkey was used only for the basic climatology.

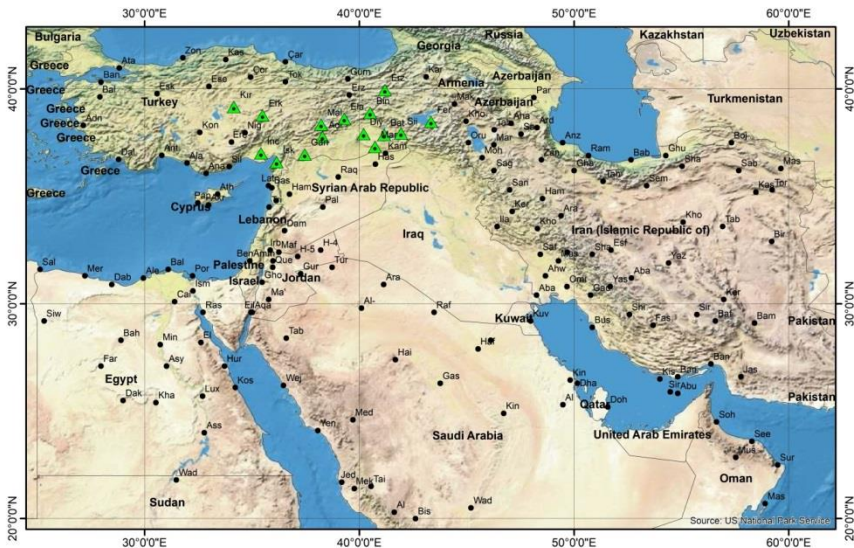


Figure 1. Geographical locations and distributions of the traditional climatological/ meteorological and automatic weather observation stations over the study region. Stations labelled with a triangle (green) symbol in Turkey were used both for the basic climatology and other trend, relationship and some anomalous surface and upper atmospheric pattern analyses.

- Daily synoptic data source for the WMO [(WMO Code 6677): “Present weather reported from a manned weather station”] Present Weather Dust/Sand Related Weather Events: www.ogimet.com;
- Data limit: The study period is relatively short to be analysed, however stations used in the analysis were characterised with a continuous and sufficient number of daily data. For instance almost all stations had about 90 per cent of all daily data that should be observed during the period from 1st January 2003 to 31 December 2016.

Synoptic meteorological dusty and/or sandy weather events based on the WMO Present Weather (WMO Code 6677) consist of following 11 present weather events with WMO code numbers: **06** - Widespread dust in suspension in the air, not raised by wind at or near the station at the time of observation; **07** - Dust or sand raised by wind at or near the station at the time of observation, but no well-developed dust whirl(s) or sand whirl(s), and no dust storm or sandstorm seen; **08** - Well developed dust whirl(s) or sand whirl(s) seen at or near the station during the preceding hour or at the time of observation, but no dust storm or sandstorm; **09** - Dust storm or sandstorm within sight at the time of observation, or at the station during the preceding hour; **30-32**: Slight or moderate dust storm or sandstorm has decreased during the preceding hour (**30**), no appreciable change during the preceding hour (**31**), begun or has increased during the preceding hour (**32**); **33-35**: Severe dust storm or sandstorm has decreased during the preceding hour (**33**), no appreciable change during the preceding hour (**34**), begun or has increased during the preceding hour (**35**); and **99** - Thunderstorm, heavy, with hail at time of observation.

Many recent studies have shown that remotely sensed data can provide a reliable and useful surface climatological, atmospheric, synoptic and repeatable source of information and data to investigate and monitor SDS and related synoptic weather vents. Consequently we have also used the Aerosol Optical Depth/Optical Thickness (τ , tau) time-series data for the study region in addition to the station-based observational synoptic weather sand and dust events. ‘Aerosol Optical Depth’ (AOD) is defined as “the degree to which aerosols prevent the transmission of light by absorption or scattering of light.” The optical thickness along the vertical direction is also called normal optical thickness. We have accessed the Aerosol Total Optical Thickness data through Giovanni at 550 nm from MODIS; at 865 and 869 nm from SeaWiFs; at 443, 555, 670, and 865 nm from MISR; and at a number of wavelengths between 342 and 500 nm from Aura/OMI. OMI

also provides Aerosol Absorption Optical Depth for near-UV wavelengths (<https://giovanni.gsfc.nasa.gov/giovanni/>).

Pearson correlation coefficient r analysis are performed for detecting possible statistical relationships between monthly and annual variations of number of synoptic dust and sand storm events and variations of AOD, and between AOD and other SDS weather related time-series, etc. Mann-Kendal rank correlation coefficient $u(t)$ test and Student's t test of the X (β) coefficient of Least Squares Linear Regression equation are used for detecting whether there is a long-term significant trend in the time-series of number of synoptic meteorological SDS events. Statistical significance levels (i.e. hypothesis tests) are determined for the test statistics r , $u(t)$ and t , etc.

3. Results of the Analysis

3.1 SDS Climatology

Maximum number of SDS events is seen mostly over the Arabian Peninsula, southern part of the Middle East countries and Sudan, and southern regions of Iran, according to the long-term averages of number of annual total synoptic meteorological SDS weather events observed during the time period from 2003 to 2016. Maximum values reach to 100 over the central Saudi Arabia along with Qatar and western parts of the United Arab Emirates (Figure 2).

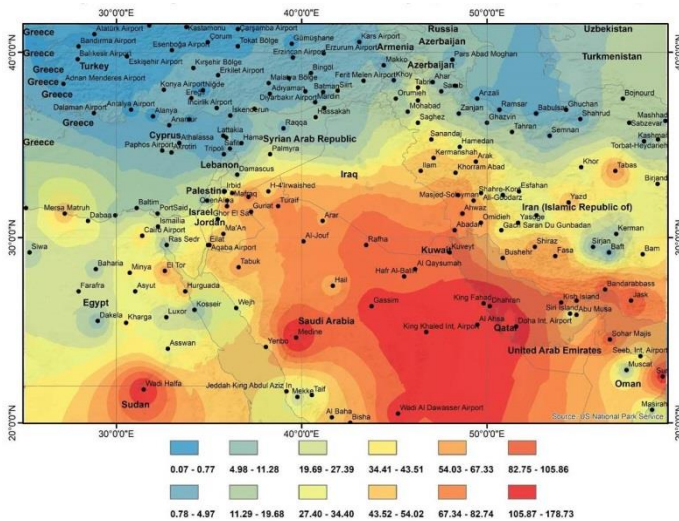


Figure 2. Spatial distribution of the long-term averages of annual total numbers of synoptic meteorological SDS weather events observed over the study region.

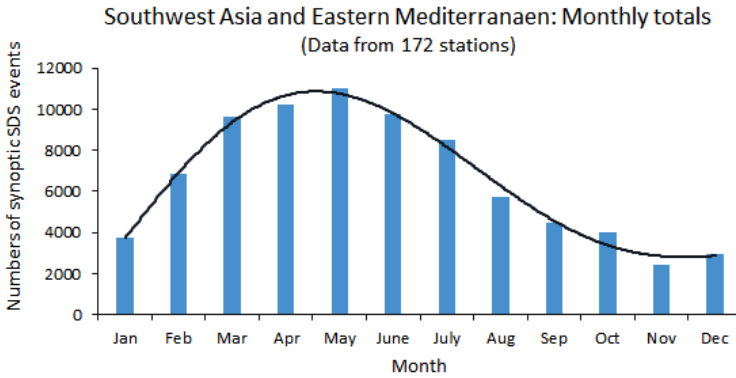


Figure 3. Monthly variations of the regional total numbers of synoptic meteorological SDS weather events.

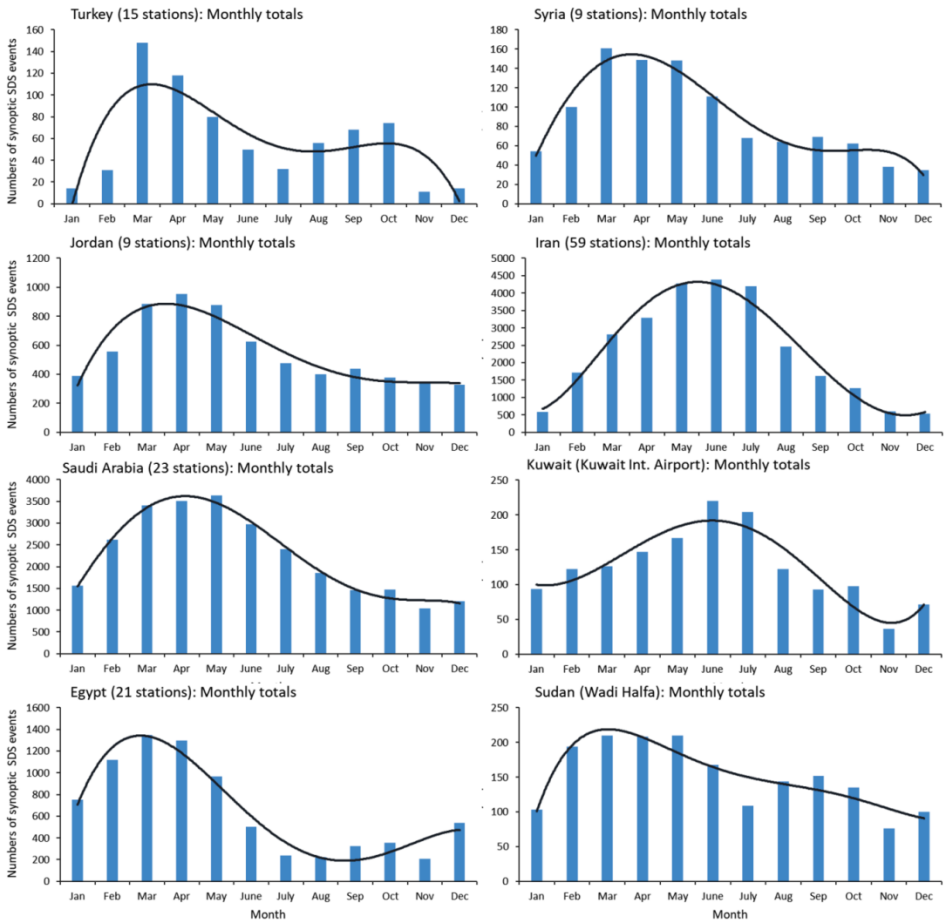


Figure 4. Monthly variations of the country-based total numbers of synoptic meteorological SDS weather events for the selected 8 countries.

Monthly variations of the regional total numbers of monthly SDS weather events (i.e. yearly SDS regime or climatology) are characterised generally with a unimodal monthly distribution for a large area including the south-west Asia and the Eastern Mediterranean (Figure 3). Regionally averaged numbers of the monthly SDS weather events also give the same monthly variation pattern within the year (not given here). The greater numbers of SDS weather events occur evidently during the 6 months from February to July with a maximum in May, and the lower numbers of SDS weather events is seen during the months from September to January with a lowest number of events in the November (Figure 3).

On the other hand, Turkey has evidently different yearly SDS event regime from other countries and regionally averaged monthly climatology, which is characterised with a marked seasonality showing bimodal monthly variation (Figure 4). The greater number of SDS events occur in the March of the high value period from March to May. The second period is seen in October within the second higher value period of August to October.

Table 1. Relationships between number of synoptic meteorological SDS weather events and AOD based country time-series.

		Turkey-AOD	Cyprus-AOD	Syria-AOD	Israel-AOD	Jordan-AOD	Saudi Arabia-AOD	Kuwait-AOD	Iran-AOD	Qatar-AOD	Oman-AOD	Egypt-AOD	Sudan-AOD
Turkey	Pearson Cor. r	0.402	0.393	0.528	0.534	0.444	0.366	0.464	0.375	0.347	0.075	0.299	0.151
	Sig. (2-tailed)	0.000	0.000	0.000	0.000	0.000	0.000	0.000	0.000	0.000	0.333	0.000	0.051
	N	167	167	167	167	167	167	167	167	167	167	167	167
Cyprus	Pearson Cor. r		0.460	0.325	0.355	0.178	0.032	0.189	0.193	-0.006	-0.187	0.140	-0.106
	Sig. (2-tailed)		0.000	0.000	0.000	0.021	0.680	0.015	0.012	0.934	0.015	0.071	0.174
	N												
Syria	Pearson Cor. r			0.686	0.624	0.568	0.497	0.667	0.620	0.485	0.175	0.360	0.176
	Sig. (2-tailed)			0.000	0.000	0.000	0.000	0.000	0.000	0.000	0.024	0.000	0.023
	N												
Israel	Pearson Cor. r				0.462	0.276	0.102	0.221	0.241	0.148	-0.130	0.215	-0.061
	Sig. (2-tailed)				0.000	0.000	0.190	0.004	0.002	0.056	0.095	0.005	0.431
	N												
Jordan	Pearson Cor. r					0.576	0.429	0.472	0.493	0.380	0.133	0.505	0.231
	Sig. (2-tailed)					0.000	0.000	0.000	0.000	0.000	0.088	0.000	0.003
	N												
Saudi Arabia	Pearson Cor. r						0.484	0.449	0.456	0.427	0.291	0.243	0.201
	Sig. (2-tailed)						0.000	0.000	0.000	0.000	0.002	0.009	0.031
	N												
Kuwait	Pearson Cor. r							0.794	0.757	0.705	0.626	0.569	0.531
	Sig. (2-tailed)							0.000	0.000	0.000	0.000	0.000	0.000
	N												
Iran	Pearson Cor. r								0.828	0.739	0.644	0.581	0.511
	Sig. (2-tailed)								0.000	0.000	0.000	0.000	0.000
	N												
Qatar	Pearson Cor. r									0.753	0.681	0.567	0.566
	Sig. (2-tailed)									0.000	0.000	0.000	0.000
	N												
Oman	Pearson Cor. r										0.748	0.598	0.578
	Sig. (2-tailed)										0.000	0.000	0.000
	N												
Egypt	Pearson Cor. r											0.306	-0.077
	Sig. (2-tailed)											0.000	0.322
	N												
Sudan	Pearson Cor. r												0.263
	Sig. (2-tailed)												0.001
	N												

3.2 Relationships between Synoptic Meteorological SDS Events and AOD based Country Time-series

Statistically significant positive relations between inter-annual variations of numbers of the SDS related synoptic weather events and the country-based AOD time-series revealed clearly that surface synoptic meteorological observational SDS time-series and remotely-sensed atmospheric time-series data are positively well correlated (Table 1). This result indicated that both data sets can be used in the observational SDS studies. All Pearson’s correlation coefficients calculated for the countries over the study area are significant at the 0.0001 significance level except Sudan with a 0.001 significance level. The greater correlation coefficients are detected between the inter-annual variations of the station-based surface SDS weather events and the AOD based series in Iran with a Pearson’s r of 0.828 along with the correlation coefficients of 0.794 in Kuwait, 0.753 in Qatar, 0.748 in Oman and 0.686 in Syria, respectively (Table 1).

Table 2. Resultant test statistics for the Mann-Kendal rank correlation coefficient ($u(t)$) test and the Student’s t test for the significance of the $X(\beta)$ coefficient of least squares linear regression equation.

Country	Trend test statistics	
	Linear regression t	Mann-Kendall rank correlation $u(t)$
SW Asia-E. Med.	1.05	0.6
Turkey	2.42*	2.19*
Cyprus	0.51	0.55
Syria	-0.61	-0.93
Lebanon	0.89	0.11
Israel	-1.18	-0.93
Jordan	-2.11	-1.70
Saudi Arabia	2.91**	2.57**
Kuwait	-0.45	-0.44
Iran	2.28*	1.15
Egypt	-2.58	-2.03*
Sudan	-1.83	-1.34

(*) and (**): Statistically significant test statistics at the 0.05 and 0.01 levels of significance, respectively.

3.3 Inter-annual Variations and Trends in Regional and Country Time-series

According to the Mann-Kendall rank correlation coefficient $u(t)$ test and the Student's t test for the significance of the $X(\beta)$ coefficient of least squares linear regression equation, annual number of synoptic SDS weather events in Turkey, Saudi Arabia and Iran increased significantly at the 5 per cent level (Table 2 and Figure 5). Among the 11 countries selected for the study because they have continuous time-series data for the 2003-2016 study period, only Egypt's annual total SDS series indicated significant decreased trend at the 5 per cent level with respect to both two trend analyses performed here (Table 2).

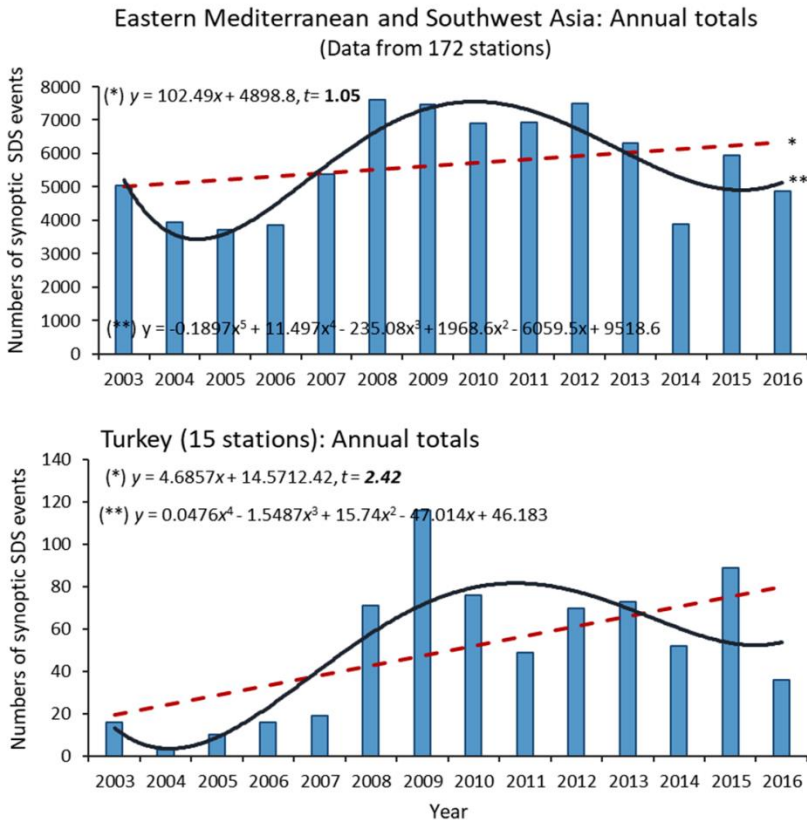


Figure 5. Inter-annual variations and trends in the annual SDS time-series data for the regionally averaged numbers of synoptic meteorological SDS weather events observed over the Eastern Mediterranean Basin and the South-west Asia and in the country based annual SDS time-series of Turkey.

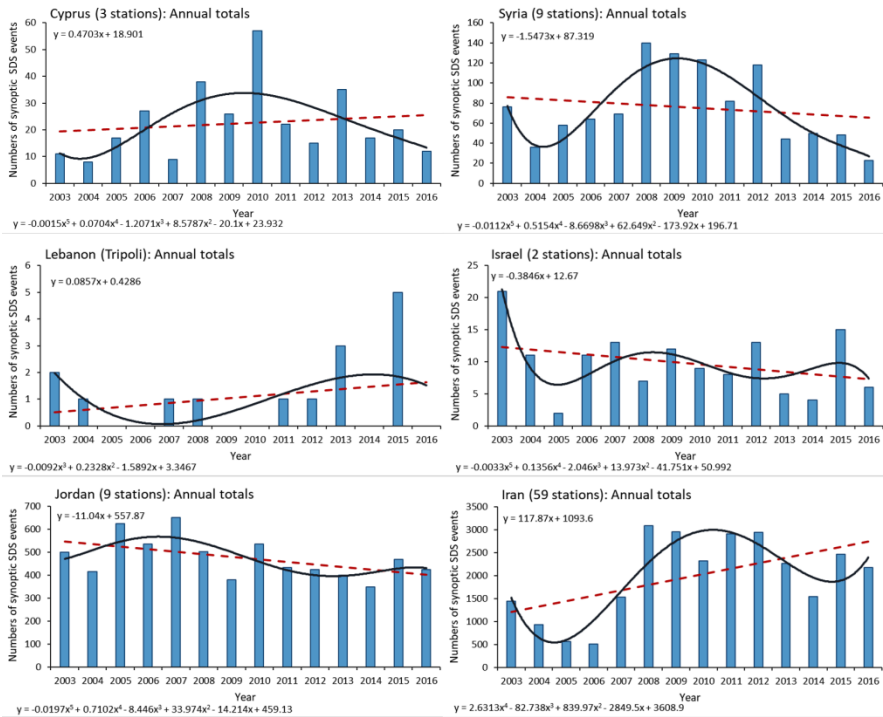


Figure 6-1. Inter-annual variations and trends in the annual SDS time-series data from the country-based averages of numbers of synoptic meteorological SDS weather events for 6 countries.

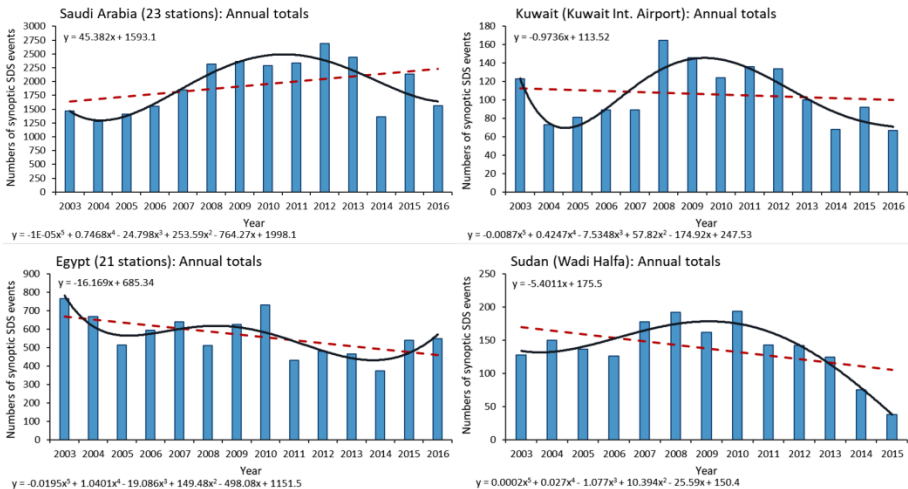


Figure 6-2. Inter-annual variations and trends in the annual SDS time-series data from the country-based averages of numbers of synoptic meteorological SDS weather events for 4 countries.

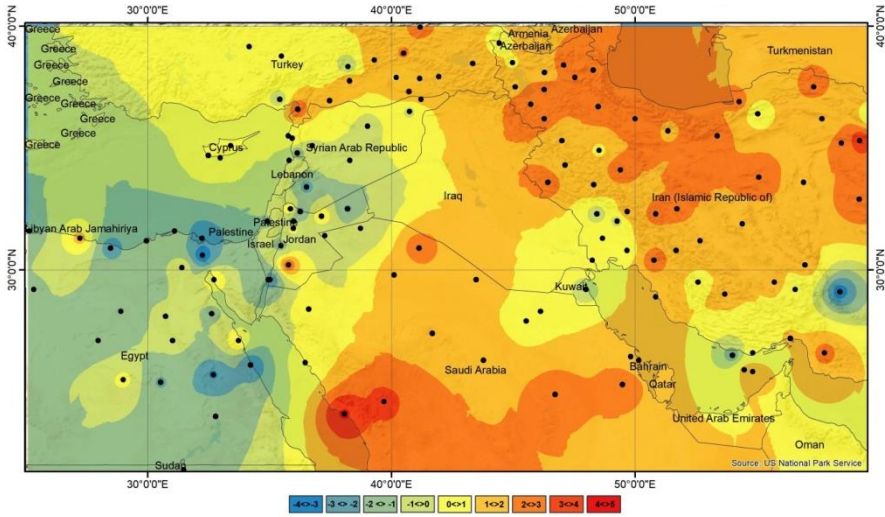


Figure 7. Spatial distribution pattern of the resultant test statistics $u(t)$ of the station-based annual numbers of synoptic meteorological SDS weather events over the study region according to the Mann-Kendall rank correlation coefficient.

Spatially coherent significant increased trends dominated over the eastern and south-eastern regions of Turkey, central, north and northwest Iran, and over the central and south-eastern regions of Saudi Arabia (Figure 7). The resultant $u(t)$ test statistics from the Mann-Kendall $u(t)$ analysis depicted that the 94 stations (70 per cent) and 40 stations (30 per cent) of the total 134 stations used in the study are characterised with positive and negative trends, respectively. Based on these results, 34 (16) of 94 stations tended to increase significantly at the 5 (1) per cent level, while 12 of 40 stations indicated to decrease significantly at the 5 per cent level.

4. Conclusions

Main findings of the study are as follows:

- (1) Maximum number of weather events related with the sand and dust storms (SDS) is detected mostly over the Arabian Peninsula, southern part of the Middle East countries and Sudan, and southern regions of Iran. Maximum values reach to 100 over the central Saudi Arabia along with Qatar and western parts of the United Arab Emirates.
- (2) Yearly SDS regime (climatology) generally reveals with a unimodal monthly distribution for a large area including the south-west Asia and the Eastern Mediterranean. The greater numbers of SDS events occur markedly

during the 6 months from February to July with a maximum in May, and the lower numbers of SDS events is seen during the months from September to January with a lowest number of events in the November.

(3) Turkey is characterised with evidently different yearly SDS event regime from other countries and regionally averaged monthly climatology, which is characterised with a marked seasonality showing bimodal monthly variation. The greater number of SDS events occur in the March of the high value period from March to May. The second period is seen in October within the second higher value period of August to October.

(4) Statistically significant correlation coefficients detected between the numbers of the SDS events and the country-based AOD time-series show clearly that surface synoptic meteorological SDS and remotely-sensed atmospheric time-series data are positively well related. This result also indicates that both data sets can be used in the observational SDS studies. All Pearson's correlation coefficients calculated for the countries over the study area are significant at the 0.0001 significance level except Sudan with a 0.001 significance level. The greater correlation coefficients are found between the station-based surface SDS weather events and the AOD based series in Iran with a Pearson's r of 0.828.

(5) The Mann-Kendall $u(t)$ test and the Student's t test for the $X(\beta)$ coefficient of least squares linear regression equation indicated that the annual number of the SDS events in Turkey, Saudi Arabia and Iran increased significantly at the 5 per cent level. Among the 11 countries selected for the study, only Egypt's annual total SDS series indicated significant decreased trend at the 5 per cent level. Spatially coherent significant increased trends dominated over the eastern and south-eastern regions of Turkey, central, north and northwest Iran, and over the central and south-eastern regions of Saudi Arabia. The Mann-Kendall $u(t)$ test showed that the 94 and 40 stations of the total 134 stations used are characterised with positive and negative trends, respectively, and 34 (16) of 94 stations tended to increase significantly at the 5 (1) per cent level, while 12 of 40 stations indicated to decrease significantly at the 5 per cent level.

Acknowledges

I would like to thank Cihan Dündar (Head of the Atmospheric Modeling Division, Turkish Meteorological Service) to assist me in accessing the original number of the SDS data, which was derived from the daily synoptic meteorological dusty and/or sandy weather events based on the related WMO Present Weather information.

References

- Boucher, O., D. Randall, P. Artaxo, C. Bretherton, G. Feingold, P. Forster, V.-M. Kerminen, Y. Kondo, H. Liao, U. Lohmann, P. Rasch, S.K. Satheesh, S. Sherwood, B. Stevens and X.Y. Zhang (2013). Clouds and Aerosols. In: *Climate Change 2013: The Physical Science Basis. Contribution of Working Group I to the Fifth Assessment Report of the Intergovernmental Panel on Climate Change* [Stocker, T.F., D. Qin, G.-K. Plattner, M. Tignor, S.K. Allen, J. Boschung, A. Nauels, Y. Xia, V. Bex and P.M. Midgley (eds.)]. Cambridge University Press, Cambridge.
- Evan, A.T., Dunion, J., Foley, J.A. et al. (2006). New evidence for the relationship between Atlantic tropical cyclone activity and African dust outbreaks. *Geophysical Research Letters* 33, L19813
- Ginoux, P.; J.M. Prospero, T.E. Gill, C. Hsu, M. Zhao (2012). Global scale attribution of anthropogenic and natural dust sources and their emission rates based on MODIS Deep Blue aerosol products. *Reviews of Geophysics*, doi: 10.1029/2012RG000388.
- Goudie, A.S. (2009). Dust storms: recent developments. *Journal of Environmental Management* 90, 89–94
- Goudie, A.S., Middleton N.J. (2001). Saharan dust storms: nature and consequences. *Earth Science Reviews* 56, 179–204
- Han, Y., Dai, X., Fang, X., Chen, Y. Kang, F. (2008). Dust aerosols: a possible accelerant for an increasingly arid climate in North China. *Journal of Arid Environments* 72, 1476–1489
- Highwood, E.J. and Ryder, C.L. (2014). Radiative effects of dust. In *Mineral Dust: A key Player in the Earth System* (ed. Knippertz, P. and Stuut, J.B.W.). pp.267–286, Springer.
- IPCC (2014). *Climate Change 2014: Mitigation of Climate Change. Contribution of Working Group III to the Fifth Assessment Report of the Intergovernmental Panel on Climate Change* [Edenhofer, O., R. Pichs-Madruga, Y. Sokona, E. Farahani, S. Kadner, K. Seyboth, A. Adler, I. Baum, S. Brunner, P. Eickemeier, B. Kriemann, J. Savolainen, S. Schlömer, C. von Stechow, T. Zwickel and J.C. Minx (eds.)]. Cambridge University Press, Cambridge.
- Journet, E., Balkanski, Y., Harrison, S. P. (2014). A new data set of soil mineralogy for dust-cycle modeling, *Atmos. Chem. Phys.*, 14, 3801-3816, <https://doi.org/10.5194/acp-14-3801-2014>
- Knippertz, P. (2014). Meteorological aspects of dust storms. In *Mineral Dust: A key Player in the Earth System* (ed. Knippertz, P. and Stuut, J.B.W.). pp.121–147. Springer.
- Mahowald, N., K. Lindsay, D. Rothenberg, S.C. Doney, J.K. Moore, P. Thornton, J.T. Randerson, C.D. Jones (2011) Desert dust and anthropogenic aerosol interactions

in the Community Climate System Model coupled-carbon-climate model, Biogeosciences, 8, 387-414, doi: 10.5194/bg-8-387-2011.

Nenes, A., Murray, B. Bougiatioti, A. (2014). Mineral dust in microphysical interactions with clouds. In Mineral Dust: A key Player in the Earth System (ed. Knippertz, P. and Stuut, J-B.W.). pp.287–325, Springer.

Nickovic, S., Vukovic, A., Vujadinovic, M., Djurdjevic, V., Pejanovic, G. (2012) Technical Note: High-resolution mineralogical database of dust-productive soils for atmospheric dust modeling, Atmos. Chem. Phys., 12, 845-855. <https://doi.org/10.5194/acp-12-845-2012>, 2012.

Prospero, J.M., P. Ginoux, O. Torres, S.E. Nicholson, T.E. Gill (2002). Environmental characterization of global sources of atmospheric soil dust identified with the NIMBUS 7 Total Ozone Mapping Spectrometer (TOMS) absorbing aerosol product. Review of Geophysics 40(1), 1002, doi:10.1029/2000RG000095.

UNEP, WMO, UNCCD (2016). Global Assessment of Sand and Dust Storms. United Nations Environment Programme (UNEP). Editor: Gemma Shepherd, UNON, Publishing Services Section, Nairobi, ISO14001:2004-Certified. It is available through UNEP Live (live.unep.org), UNEP website (<http://www.unep.org/publications>)

Washington, R., Wiggs, G.F.S. (2011). Desert dust. In Arid Zone Geomorphology: Process, Form and Change in Drylands (ed. Thomas, D.S.G.) pp. 517–538. 3rd Edition, Wiley.

WMO (2014). Sand and Dust Storm Warning Advisory and Assessment System (SDS-WAS) Science and Implementation Plan 2015-2020. Nickovic, S., Cuevas, E., Baldasano, J., Terradellas, E., Nakazawa, T. and Baklanov, A. (main cont. authors). World Meteorological Organization (WMO) Research Department, Atmospheric Research and Environment Branch, WWRP- No. 2015-5, Geneva, 37 pp. Available online: https://library.wmo.int/opac/doc_num.php?explnum_id=3383

EUMETSAT SDS Products for the Middle East

José Prieto

Training Officer, EUMETSAT

Abstract

The advent of Meteosat second generation (MSG) almost accidentally introduced the possibility of detecting dust storms and in general monitoring for dust across seas and continents. For the Middle East, two Meteosat satellites offer complementary perspectives of dust in the atmosphere, from 0 and 41.5 degrees East in the geostationary orbit.

Keywords: *AOD, dust composite, red-green-blue, RGB, albedo, brightness temperature (BT), sand and dust storms (SDS)*

1. Introduction

Channel combination through RGB products offer excellent capabilities for the identification of dust in the atmosphere. Better in the infrared domain as in the solar spectrum, Meteosat channels provide a continuous and reliable description of the presence of aerosol in the air, with a chance to determine the type, whether dust, pollen, ash from volcano eruptions or even smoke from raging fires.

Even a triplet of variables (AOD, temperature of upper dust layer and ground temperature) can be retrieved at pixel level in areas with SDS, providing statistically an indication of size. Further on,

In addition to RGBs, the most direct product for dust detection, cloud masks from the Nowcasting SAF involving decision trees are available from the EUMETSAT catalogue at navigator.eumetsat.int

Some examples of satellite analysis follow, as a demonstration of the synoptic capability of satellite in recognising dusty areas. More can be found at [1].

2. The Case of a Dust Transformation

The Meteosat-8 Dust composite with the ECMWF 10m-wind and mean sea level pressure overlaid, Figure below of 01 February 2017 00:00 UTC–02 February 12:00 UTC (MP4, 10 MB) indicate the presence of a weak circulation in the Middle East area, close to northern Iraq.

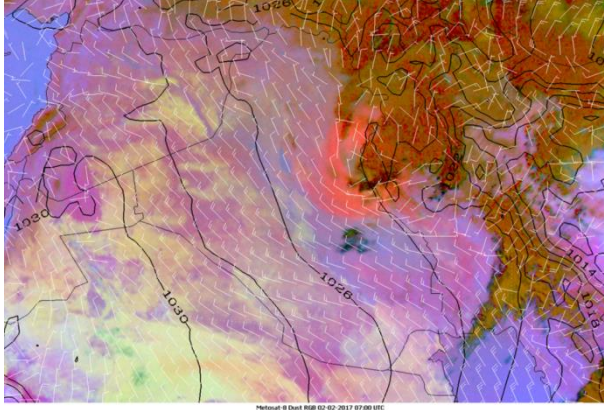


Figure 1. The wind associated with the cyclonic circulation on eastern Syria raises dust south of it, as shown in the infrared animation around 10:00 UTC on 1 February.

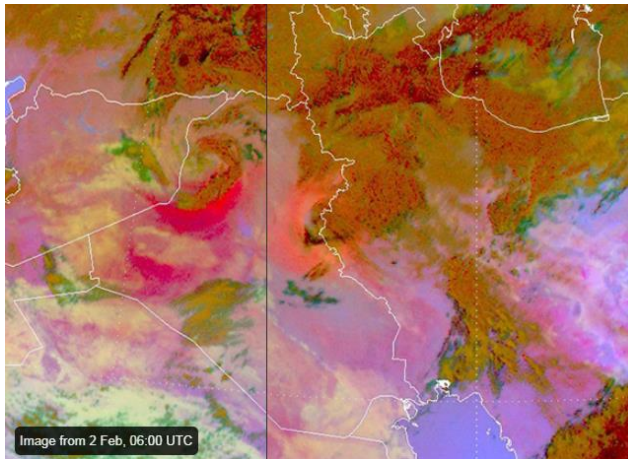


Figure 2. Comparison of two different moments in the evolution of the dust area, separated by 13 hours (1 Feb 19UTC for the left hand side, 2 Feb 06 UTC for the right hand side). The mass in magenta evolves slowly and continuously into a mass in peach colour. What is the explanation? See text.

Over the northwestern part of Iraq, the dust joins the circulation along the south flank (red and pink on the left hand side of Figure 2), but it comes out mostly from the cyclone's west flank with a peach hue near Iraq's east-

ern border. An influence of the ground in the coloration is not evident. The time of the day plays no role, since the same hues show day and night.

Both Meteosat-8 and 10 see the same colours, so the viewing angle through a thicker humidity layer is not a sufficient explanation. Differences are only around 1 K between the measurements by the two satellites, so slant effects are not impacting colour hue either.

Orange (or peach) colour results from higher green, which is a larger positive Brightness Temperature Difference (BTD) between channels at $10.8\mu\text{m}$ and $8.7\mu\text{m}$. In cloud free areas bigger BTD comes from higher water vapour, whereas in cloudy areas this BTD is affected by 1) dust height, 2) dust concentration and 3) dust properties, mainly particle size.

If the reason for peach hues in this case were dust particle size, one could imagine coalescence in the upward circulation, followed by drying up close to the circulation boundaries and by creation of dry bigger dust particles, producing the peach tone. That is suggested by the fact that volcano eruptions (made of big particles) show often in peach in the infrared window composite.

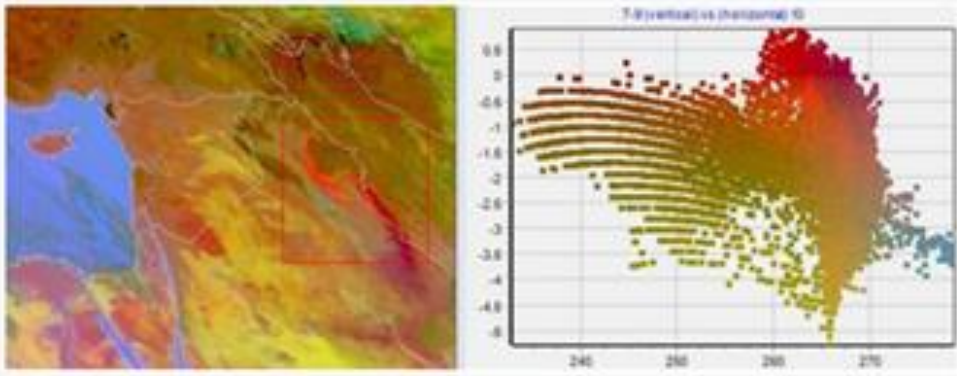


Figure 3: Meteosat-10 IR composite, 2 February 00:00 UTC and BTD graph.

Figure 3. is analysis for all pixels inside the red square on the left Meteosat-10 IR composite image. The graph on the right hand side compares $10.8\mu\text{m}-8.7\mu\text{m}$ differences (vertical axis) and values at $12\mu\text{m}$ (horizontal). The peach coloured pixels (exit of a conveyor belt) show a BTD $10.8\mu\text{m}-8.7\mu\text{m}$ which is around one kelvin higher than the magenta-red pixels at the southern part of the conveyor belt. Height or size effect?

3. The Case of a Long Distance Trip for Dust

Southern Spain Had Muddy Rain (also called Red Rain or Rain Dust) as a Result of Convection on 20 July 2016

The dust originated from one of many outbreaks in the Sahara desert a few days before. From there it travelled in the layers of the mid-atmosphere, along the western African coast, to the south-western part of the Iberian peninsula. There it became incorporated with the water and ice particles generated in updrafts, and fell to the ground as dusty rain.

The dust that travelled along the coast took in contributions from the south of Mauritania and from the Moroccan bay of Agadir. The main dust contribution reaching the Iberian peninsula originated on the South of Algeria on 16 July around 19:00 UTC and travelled, moved by different synoptic systems to the north of Morocco, through a more northern route, reaching Agadir on the early hours of 19 July, as can be seen in the [Dust RGB animation](#), 16 July 00:00 UTC–20 July 23:30 UTC (MP4, 7 MB)

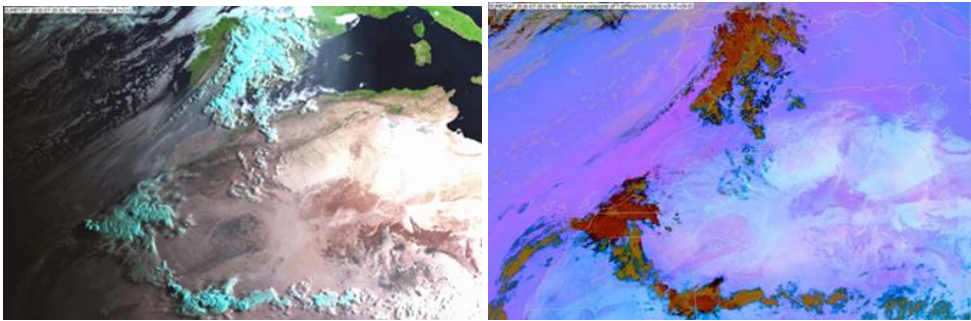


Figure 4. Met-10, 20 July 2016, 06:42–12:42 UTC Natural colour (hazy for dusty pixels) and “Dust” RGB (pink for dusty pixels)

In the infrared imagery, both the animated gif (Fig.4) and the longer [animation from 18 July 00:12 UTC to 20 July 12:42 UTC](#) (MP4, 10 MB), the dust appears in pink hues. It shows as a softer and more of a blue colour over the seas, where the thermal contrast between the surface and the dust is not so pronounced as over land; and there is more humidity in the air.

Over the ocean, dust can be confused with low-level cloud, especially in the infrared combination.

However, the more uniform areas in the infrared composite are only dust above the ocean heading towards southwestern Europe. This is confirmed in the solar imagery, animated gif (Figure 5) and the longer [animation from 18 July 06:42 UTC to 20 July 12:42 UTC](#) (MP4, 11 MB).

In the afternoon hours, the reflection conditions are perfect for showing the vertical structure of the dust front — for instance around 18 July at 18:42 UTC — or the convection generating cumulonimbus (Cb) towers along a gust line. The projection of shades allows an estimate of the Cb height above the dust level. Convection occurs at areas of high humidity in the low levels, showing in blue in the infrared animation.



Figure 5. Solar image, 20 July 06:43 UTC

Next morning, the dust seems to have disappeared, but it is there, and it becomes observable again in the afternoon. Convection then occurs in the Iberian peninsula, trapping the dust in the droplets or crystals.

Finally, on 20 July in the morning the concentration of dust is so high that it can be seen even under unfavourable conditions in the solar image (Figure 5). Frontal rain left abundant precipitation in the Iberian peninsula, putting a temporary end to a heatwave.

4. The Case of Multiple Simultaneous Events over the Middle East

A cut-off low that was travelling through this area caused a major dust event over North Africa and Arabian Peninsula. On the **Meteosat-8 Dust RGB animation** (MP4, 13 MB) thick low level dust can be observed as a swirl caused by the circulation pattern inside the cyclone (different shades of magenta).

On the second day of the animation, in the southeastern Mediterranean sea, one band of dust north of the cyclone centre was more of a peach colour — indicating dust at higher levels.

This dust was probably lifted up at the front side of the arriving cyclone (and accompanying frontal system) and incorporated into the circulation. This feature could be readily seen if we toggle between Dust RGB and strongly enhanced Natural Colour RGB in Figure 6.

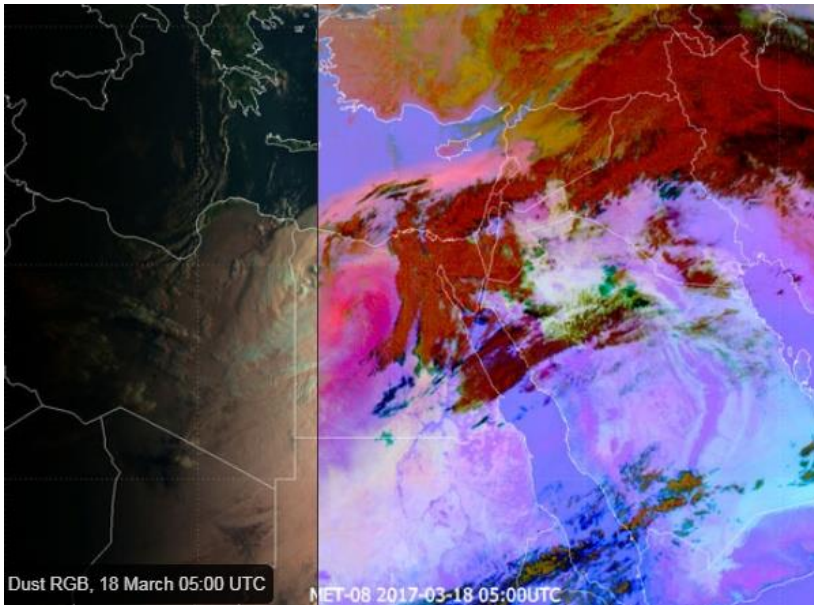


Figure 6. *Meteosat-8 Natural Colour and Dust RGB imagery showing lifting of the dust.*

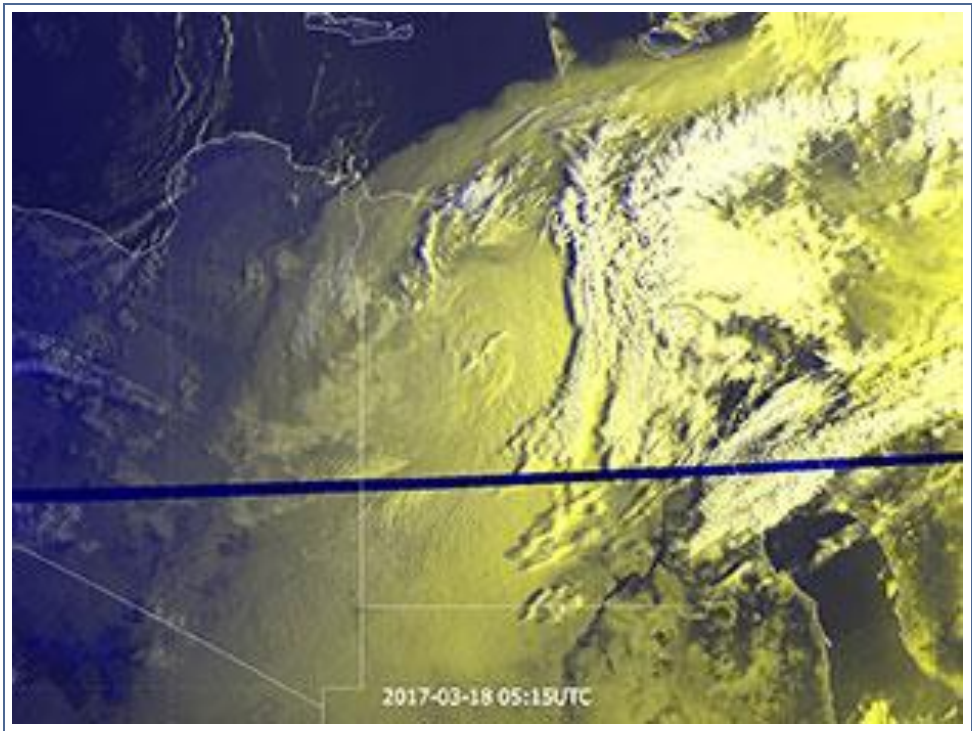


Figure 7. *Meteosat-10 HRV, 18 Feb 05:15 UTC*

Looking at the HRV image (Figure 7), on the very north side of this upper level dust band, we can notice wavy structures. This probably caused by the breaking of laminar into a turbulent flow. On the other side, south of the cyclone, there are also clearly visible gravitational waves which propagate on top of lower level dust layer.

As the system progressed over the Red Sea towards the Arabian peninsula, over Saudi Arabia and the Persian Gulf countries numerous thunderstorm events, sometimes accompanied with hail, were recorded, as seen on **Meteosat-8 infrared image taken over Saudi Arabia at 13:45 UTC.**

Also, some dust was lifted on outflow boundaries of these storms as it can be seen in second part of the Dust RGB animation.

5. Conclusion

Satellites need to be considered as a first class source of information for dust events to mitigate damage on populations. They can provide precise boundaries for events at short time intervals, namely 15 minutes for Meteosat. In addition, they supply the all-weather point of view, ensuring their operation day and night. As a limitation, the absorption of dust by humid cyclonic circulations makes the actual boundaries for dust uncertain in those cases.

Possible misleaders for dust in IR satellite images, showing also in magenta hues, are fog or stratus, cold surfaces, granite formations, thermal inversions. On the other hand, low level dust is hard to see on satellite images. For these, the thumb rule applies: “What is pink and moves? Dust”

Acknowledgement

My colleagues Vesa Nietosvaara, Jochen Kerkmann and Djordje Gencic, with whom I regularly prepare similar cases to the presented, are kindly acknowledged as co-authors of this contribution.

References

[1][HTTPS://WWW.EUMETSAT.INT/WEBSITE/HOME/IMAGES/IMAGELIBRARY/INDEX.HTML](https://www.eumetsat.int/website/home/Images/ImageLibrary/Index.html)
is EUMETSAT image library, with many cases referring to dust.

[2]https://www.eumetsat.int/website/home/Data/Training/TrainingLibrary/DAT_2042669.html?lang=EN
is a summary of resources to learn more about dust

SDS-WAS: Ensemble Prediction of Airborne Dust

G. García-Castrillo¹, A. Callado¹, E. Terradellas¹ and P. Escribà¹

¹ State Meteorological Agency of Spain (AEMET), Barcelona, Spain

Abstract

The WMO SDS-WAS Regional Center for Northern Africa, Middle East and Europe has established a protocol to routinely exchange products from dust forecast models as the basis for model inter-comparison and forecast evaluation. Currently, 12 modeling groups provide daily forecasts of dust surface concentration (DSC) and dust optical depth (DOD) at 550 nm for a reference area intended to cover the main dust source areas in the region. The action involves forecasts up to 72 h with a 3-hour frequency.

Multi-model products are daily generated after bi-linearly interpolating all forecasts to a common grid mesh of 0.5 x 0.5 degrees. Centrality products (median and mean) are aimed at improving the forecasting skill of the single-model approach and spread products (standard deviation and range of variation) indicate whether forecast fields are consistent within the models, in which case there is greater confidence in the forecast.

Evaluation scores are routinely computed using aerosol optical depth retrievals provided by the AERONET network for 45 dust-prone stations. In a pilot study, forecasts of DSC have been compared with PM₁₀ measurements performed by the Air Quality Control and Monitoring Network of the Canary Islands (Spain).

In this study, a one-month period has been selected to perform a deeper verification of the ensemble prediction system in order to evaluate its consistency and reliability. First, the ordinary deterministic verification of the different 12 models or members, as well as their median, has been carried out. Then, verification has been undertaken from a probabilistic point of view. This is a first step for the correct calibration of the system and the implementation of probabilistic forecast products as DSC and DOD EPSgrams. The study has been performed using the HARMONIE monitor deterministic and the HARP (Hirlam Aladin R-based package) probabilistic verification packages.

Keywords: Ensemble prediction system, PM₁₀, Dust optical depth, HIRLAM, HARP.

1. Introduction

Forecasting severe weather events is a key objective for National Meteorological Services around the world. Due to the large amount of processes involved in those events and their non-linearity, a probabilistic approach is required. Ensemble prediction systems are a feasible framework and the most useful tool to improve such forecasts.

Ensemble prediction aims to describe the future state of the atmosphere from a probabilistic point of view. Multiple simulations are run to account for the uncertainty of the initial state and/or for the inaccuracy of the model and the mathematical methods used to solve its equations (Palmer et al., 2005). In particular, multi-model ensembles also represent a paradigm shift in which offering the best product to the users as a collective scientific community becomes more important than competing for achieving the best forecast as individual centres (Benedetti et al., 2014).

The World Meteorological Organization's Sand and Dust Storm – Warning Advisory and Assessment System (SDS-WAS, Terradellas et al., 2015) has the mission to improve the capacity of countries to produce and distribute to end-users accurate forecasts of the mineral dust content in the atmosphere. The SDS-WAS Regional Center for Northern Africa, Middle East and Europe (NA-ME-E) daily produces a poor-man ensemble (Atger, 1999) computed from the output of different models. Centrality products (median and mean) aim at improving the forecasting skill of the single-model approach. Spread products (standard deviation and range of variation) indicate whether the forecast fields are consistent within the contributing models, in which case there is greater confidence in the forecast (Terradellas et al., 2016).

The most relevant variables provided by dust prediction models are dust load, or alternatively dust optical depth (DOD), as a measure of the total dust contents in an atmospheric column, and dust surface concentration (DSC), as a measure of the dust contents near the ground. Other variables that are relevant for specific applications are dry and wet deposition or surface extinction.

The first problem of the forecast evaluation is the scarcity of suitable in-situ measurements, especially close of the main dust sources. The first option is the use of satellite products. However, satellite measurements are integrated over the atmospheric column and also over the different aerosol species. Another option is the use of ground-based photometric retrievals,

but they present a similar problem. Initiatives to establish routine evaluation of dust predictions have been mainly focused on total-column DOD. The SDS-WAS Regional Center for NA-ME-E has set up and maintains a joint visualization and forecast evaluation (Terradellas et al., 2016), which currently involves 12 modeling systems and is based on AERONET (Holben et al., 1998; Dubovik and King, 2000) and MODIS retrievals (Kaufmann et al., 1997; Hsu et al., 2004). Other initiatives have been conducted in the framework of AeroCom (Huneeus et al., 2011), the Copernicus Atmosphere Monitoring Service (CAMS) (Eskes et al., 2015; Cuevas et al., 2015) and the International Cooperative for Aerosol Prediction (ICAP) (Sessions et al., 2015).

Many user communities are interested in the DSC (dust concentration in the air we breathe) rather than in the total column content. Therefore, evaluation of the predicted DSC is also necessary. Air quality monitoring networks are the main data providers for this purpose. They are common and with high spatial density in Europe, but very sparse and discontinuous close of the main source regions. The lack of observational data is particularly acute near the Sahara, the major dust source on Earth (Middleton and Goudie, 2001). In addition, the evaluation of dust forecasts using PM₁₀ data has some drawbacks. On the one hand, the values of PM₁₀ do not only reflect the mineral dust content in the atmosphere, but integrate the contribution of all airborne particles with aerodynamic diameter less than 10 μm , which may be of diverse origins (mineral dust, marine aerosol, anthropic pollution, etc.). On the other hand, dust prediction models provide the total content of mineral dust and, at least some of them, consider particles larger than 10 μm .

2. Observations and Forecasts

In the present study, DOD forecasts provided by different models and multi-model products are verified for April 2016 using AERONET data. Verification is performed in spring, which is known to be the dustiest season in most parts of the geographical domain. Also, DSC forecasts are verified using air-quality measurements in the Canary Islands. In this case, the verification is performed for December 2014 since Saharan dust outbreaks there occur near the ground normally in winter, but not in spring or summer. In both cases, verification is performed using the highest daily value both for observation and for prediction. This section describes the models and the observations involved in the study.

2.1. Observations

2.1.1. Aerosol Optical Depth

Direct-sun photometric measurements are a powerful tool that provides retrieval of column-integrated aerosol properties. In particular, AERONET is a comprehensive set of continental and coastal sites complemented with several sparsely distributed oceanic stations that provides large and refined data sets in near real-time (Holben et al., 1998; Dubovik and King, 2000). Retrievals from around 45 stations in Europe, Middle East and Northern Africa have been used here in the forecast verification (figure 1). A similar number of stations has been selected in each sub-region in order to prevent a part of the territory having more weight in the verification. In particular, level 1.5 of version 3 inversion products have been used. Level 1.5 data are cloud-screened, but the calibration correction has still not been applied.

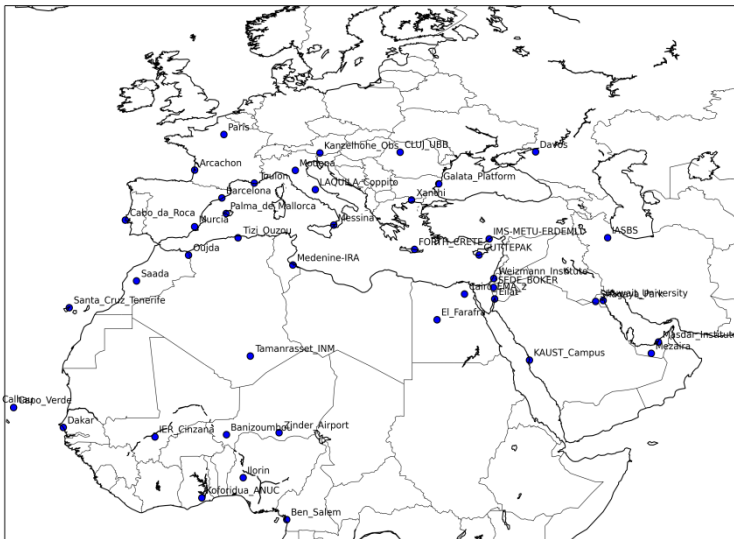


Figure 1. AERONET Stations used in this work.

To estimate the contribution of mineral dust to the total AOD, we have considered the coarse AOD yield by the spectral de-convolution algorithm described in O'Neill et al. (2003) that is part of the AERONET routine calculations. This algorithm yields fine (sub-micron) and coarse (super-micron) AODs at a standard wavelength of 500 nm.

2.1.2. Surface Concentration

The verification of DSC has been conducted for the Canary Islands. The archipelago suffers frequent intrusions of dust from the Sahara (i. e. Middleton and Goudie, 2001), with significant negative impacts, especially on air quality and health (Viana et al., 2002). Therefore, there is great interest in learning how the dust prediction models behave in the region. However, the complex orography of the islands, imperfectly represented in the models, especially in those with lower resolution, prevents a good simulation of the local variations of dust concentration and makes difficult a correct evaluation of the forecasts.

To quantify the contribution of mineral dust to PM₁₀, the most reliable method is based on the chemical analysis of filters from gravimetric samplers (Rodríguez et al., 2012). However, this is a very expensive and laborious technique, so it is difficult to apply routinely. As an alternative, the present work uses the coarse fraction of PM, defined as the difference PM₁₀-PM_{2.5}, as a proxy of the dust concentration.

We have selected five stations from the Canarian Air Quality Monitoring Network, operated by the regional government (table 1). As far as possible, the selection includes stations located away from urban centers, industrial parks and roads so that the contribution of anthropogenic particles in their records be small. Also, it has been intended that the location of the selected stations be representative of the different geographical areas of the archipelago (figure 2).

Table 1. Air quality monitoring stations used in the study

Site	Island	Measurement method
Costa Teguisse	Lanzarote	TEOM
Polideportivo Afonso - Arucas	Gran Canaria (N)	Beta attenuation
Camping Temisas - Sta Lucía de Tirajana	Gran Canaria (S)	TEOM
Granadilla	Tenerife (S)	Scattering
Vuelta Los Pájaros - Santa Cruz de Tenerife	Tenerife (N)	Beta attenuation

Different continuous particle samplers are used in the network. They measure inertial mass (Tapered Element Oscillating Microbalance, TEOM), electron attenuation (Beta attenuation) or light scattering (scattering) of fine particles at a sampling rate of 1 hour. The reference (gravimetric) method to measure PM₁₀ and PM_{2.5} consists of acquiring deposits over 24-hour periods on teflon membrane filters from air drawn at a controlled flow rate through the corresponding inlet. Then, a correction factor obtained through sampling campaigns has to be introduced to adjust the results to the reference method. The data used in the present study December 2014 had already been corrected by the network managers.

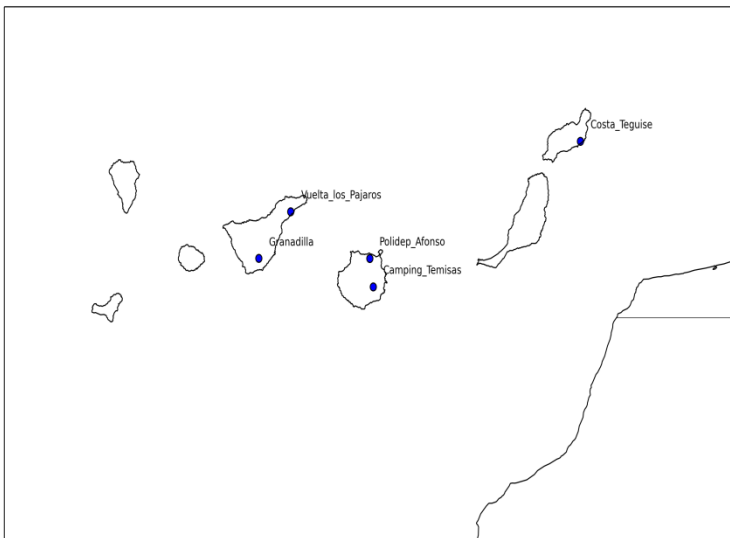


Figure 2. Location of the air-quality monitoring stations used in the present study

2.2. Forecasts

Daily predictions of DOD and DSC released by twelve dust prediction models have been considered in this work. The models have very different characteristics: there are global and limited-area models, some of them incorporate schemes of data assimilation, others do not. Their horizontal and vertical resolutions are diverse, as well as their meteorological drivers, parameterisation of the different steps of the dust cycle and physiographical databases of land use, soil texture, etc. The list of the models and their main characteristics are summarized in table 2.

Table 2. Dust models involved in the study

Model	Institution	Run time	Domain	Data assimilation
BSC-DREAM8b-v2	Barcelona Supercomputing Center	12 UTC	Regional	No
CAMS	ECMWF	00 UTC	Global	MODIS AOD
DREAM8-NMME-MACC	SEEVCCC	00 UTC	Regional	CAMS analysis
MetUM	Met Office	00 UTC	Global	MODIS AOD
NMMB/BSC-Dust	Barcelona Supercomputing Center	12 UTC	Regional	No
GEOS-5	NASA	00 UTC	Global	MODIS
NGAC	NCEP	00 UTC	Global	No
EMA REG CM4	Egyptian Meteorological Authority	00 UTC	Regional	No
DREAMABOL	ISAC	00 UTC	Regional	No
NOA WRF-CHEM	National Observatory Athens	12 UTC	Regional	No
FMI-SILAM	FMI	00 UTC	Global	No
LOTOS-EURO	TNO	00 UTC	Regional	MODIS AOD

The collected models have different run times (00 or 12 UTC, as shown in Table 2). In order to set the start time of the multi-model products at 00 UTC, we consider the previous-day runs of the models starting at 12 UTC.

A problem we have to deal with is the eventual lack of availability of models since most of them are not run in an operational mode. Daily availability of models is shown in Figure 3. We have decided not to name the models in the Figures in this study.

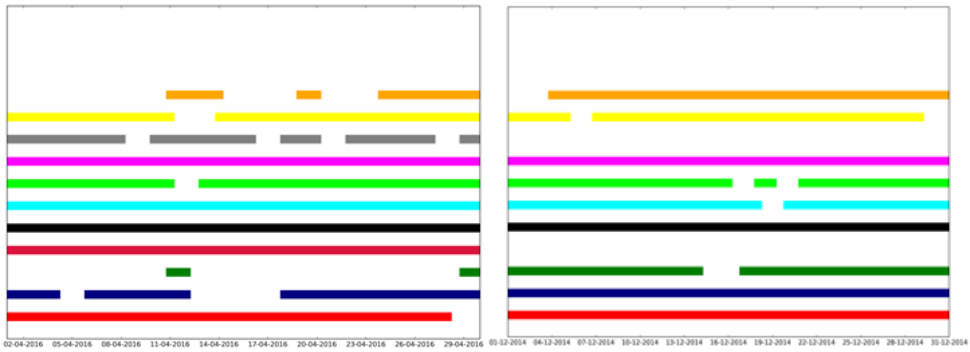


Figure 3: Model availability for April 2016 (left) and December 2014 (right).

3. Experimental Method

In this Section we describe the method followed to verify the dust forecasts. First, we proceed with a deterministic verification, which give us information about the quality of the different models. One of the objectives of this step is to determine which models will be part of the ensemble. The next step is the probabilistic verification, which gives us information about the quality and the consistency of the ensemble. Consistency means the degree to which the forecast corresponds to the forecaster's best judgement about the situation, based upon his/her knowledge base (Murphy, 1993). The consistency is related to the need for calibration and this is one key point of this work. If the ensemble has bad consistency, we will introduce a calibration to adjust the ensemble to the observation. All this process has the purpose of supplying value products for the end-users.

We have used two packages to verify DOD and DSC ensembles. As Spanish Meteorological Agency (AEMET) belongs to HARMONIE consortium for developing mesoscale Numerical Weather Prediction (NWP) modeling, we have used HARMONIE packages for deterministic and probabilistic verification. These packages are monitor and HARP (Hirlam Aladin R-based package) (HARMONIE wiki page).

4. Results

4.1 Dust optical depth

Figure 4 shows the mean bias and standard deviation of daily maximum DOD for lead times of 12 and 36 hours in April 2016. The plot only contains the eight models that will be part of our ensemble. We have removed three models for different reasons: two of them because of their sparse availability and the other because the scores were very far from those of the rest of models. The plot has been built after comparison of DOD forecasts with AERONET retrievals from 35 stations.

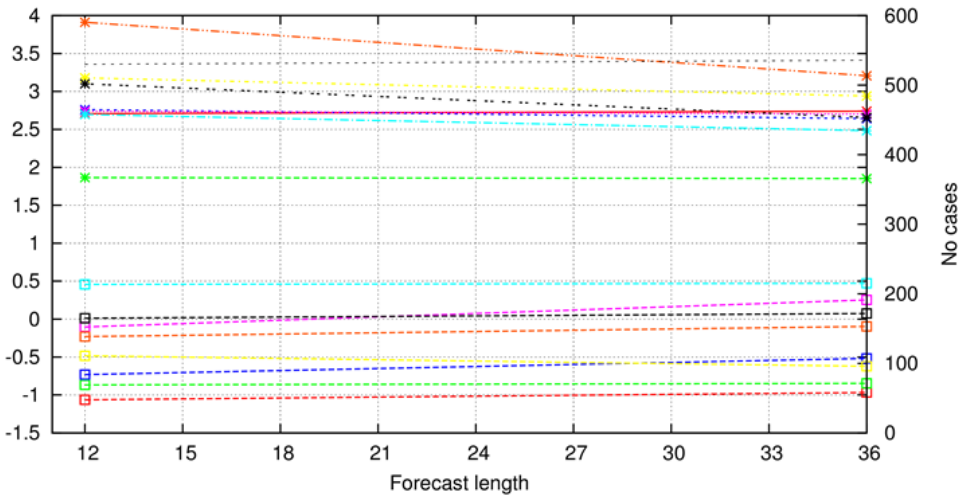


Figure 4. Deterministic verification of daily maximum DOD for lead times of 12 and 36 hours in April 2016 (* represents standard deviation and \square bias Each color corresponds to a different model.)

We present two of the most common methods to determine the consistency of an ensemble. The first one is based on the Rank Histogram or Talagrand diagram (Talagrand et al, 1997; Hamill, 2001). If the ensemble forecast is consistent, the Rank Histogram will be flat. Deviations from a uniform distribution denote lack of consistency. Figure 5 shows the Rank Histogram of our ensemble for forecast times of 12 and 36 hours. Both plots show a slightly descending tendency, indicating that there is a small positive bias, which means over-prediction of the ensemble.

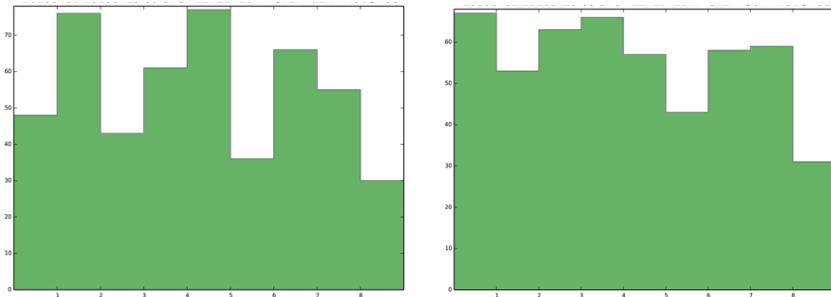


Figure 5: Rank Histogram of daily maximum DOD in April 2016 for 35 stations. The left plot corresponds to a lead time of 12h and the right one to 36h

A second method to assess the quality of an ensemble is based on the reliability and sharpness diagrams. The reliability diagram groups the forecasts into bins according to the issued probability of exceeding a specific threshold (horizontal axis). The frequency with which the event was observed to occur for this sub-group of forecasts is then plotted against the vertical axis. For perfect reliability the forecast probability and the frequency of occurrence should be equal, and the plotted points should lie on the diagonal

The sharpness diagrams show the frequency with which the event has been predicted with different levels of probability. Forecast systems that are capable of predicting events with probabilities different from the observed event frequency are said to have 'sharpness'. Diagrams for forecast systems with little sharpness would exhibit a frequency peak near the climatological frequency. So the ideal ensembles would present a U-shape, in which case the ensemble perfectly predicts an event or discards it (Hamill, 1997).

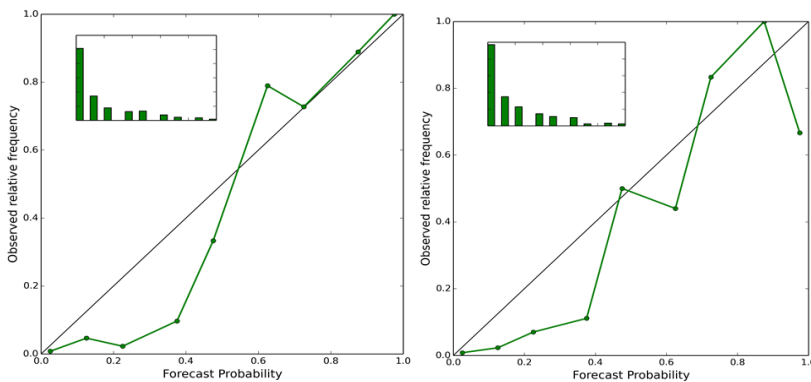


Figure 6. Reliability (large plot) and sharpness (small plot) diagrams of daily maximum DOD in April 2016 and a threshold of 0,5. The left plot corresponds with a leadtime of 12h and the right one of 36h

Figure 6 shows the reliability (large plot) and sharpness (small plot) diagrams for a threshold value of 0,5 and forecast times of 12 and 36 hours. The sharpness diagrams present a normal shape, as most of the ensembles. Regarding the reliability diagrams, the plots are not far from the diagonal. However, it can be mentioned that when the ensemble predicts a low probability of occurrence, the observed frequency is smaller than expected. This means that our ensemble is over-predictive for some models (left region of the diagram).

4.2 Dust Surface Concentration

Figure 7 shows the mean bias and standard deviation of daily maximum DSC for lead times of 12 and 36 hours in December 2014. The plot contains the nine available models in this period; in this case any of the models has been removed. The plot has been built after comparison of DSC forecasts with PM data from 5 stations.

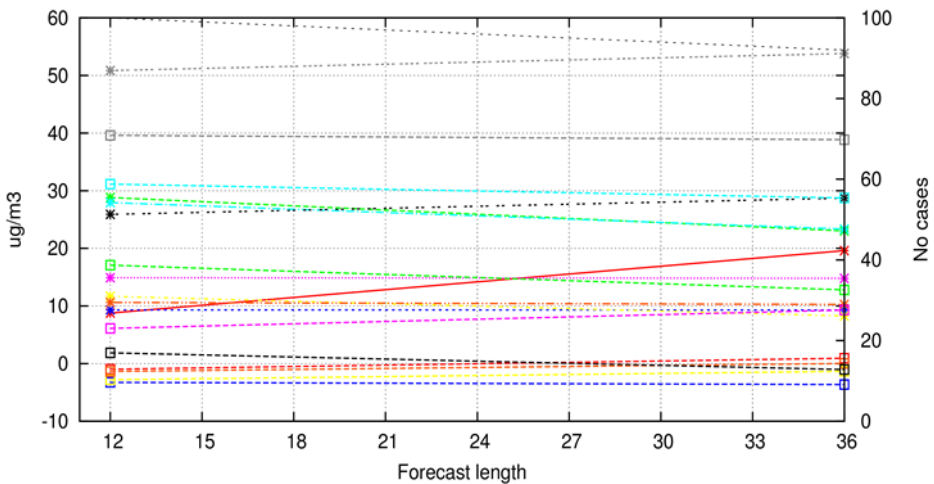


Figure 7. Deterministic verification of daily maximum DSC for lead times of 12 and 36 hours in December 2014 (* represents standard deviation and □ bias. Each color corresponds to a different model.)

The Rank Histogram for DSC (see Figure 8) has a different shape in comparison with that for DOD. In this case, most observations fall in the central bins of the ensemble and the plot shows a dome shape. It means that the ensemble spread too large and the reason is that the models yield too scattered results.

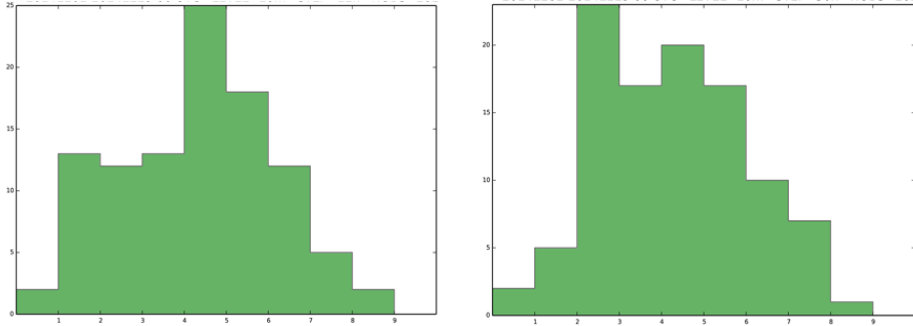


Figure 8. Rank Histogram of daily maximum DSC in December 2014 for 5 stations. The left plot corresponds to a lead time of 12h and the right one to 36h

Figure 9 shows the reliability and the sharpness diagrams for a threshold of $50 \mu\text{g}/\text{m}^3$. In this case, results are not satisfactory. On the one hand, sharpness is scarce. On the other hand, most points in the reliability diagram lie far from the diagonal, with important over-forecast in the left half of the plot.

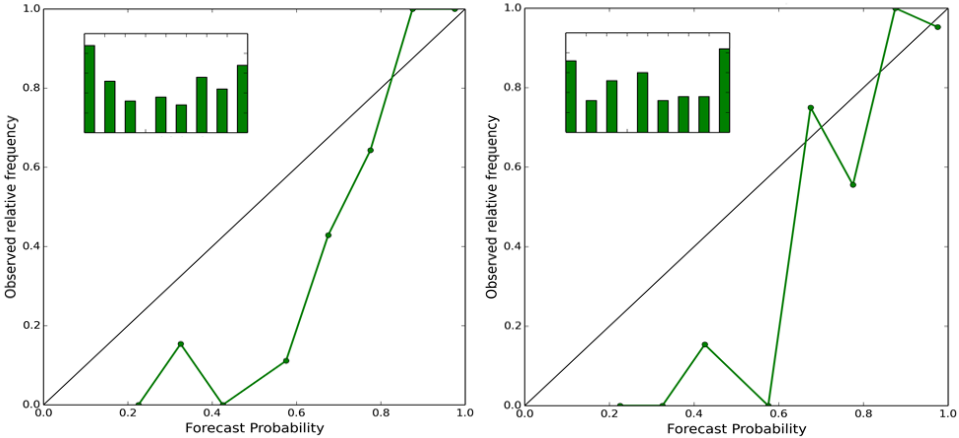


Figure 9. Reliability diagram of daily maximum DSC in December 2017 and a threshold of $50 \mu\text{g}/\text{m}^3$. The left plot corresponds with a leadtime of 12h and the right one of 36h .

5. Conclusions and open issues

In the present work, we assess the skill of an ensemble prediction system to forecast DOD and DSC using probabilistic and deterministic verification.

For DOD, our ensemble is built from seven models. The Rank Histogram presents a slightly descending tendency, denoting a small over-prediction. The sharpness diagram presents a typical shape for this parameter. Finally, the reliability diagram denotes over-forecasting in the region of low probabilities. So, we have a relatively good ensemble in terms of consistency, sharpness and reliability.

For DSC, it is important to bear in mind that conclusions have limited significance, since evaluation has been performed with only five stations from the Canary Islands. In this case our ensemble has been built from nine dust models. In the probabilistic verification we find a too large spread, over-forecasting in low-medium probabilities and poor sharpness. In short, we have a worse ensemble than for DOD.

From these results we can conclude that DOD is much more predictable from a probabilistic point of view than DSC with our system. Finally, bias correction and other post-processing tools like statistical calibration could potentially increase the quality of these ensembles.

References

- Atger, F. (1999). The skill of ensemble prediction systems. *Monthly Weather Review*, 127(9), 1941-1953.
- Benedetti, A., Baldasano, J. M., Basart, S., Benincasa, F., Boucher, O., Brooks, M. E., ... & Jones, L. (2014). Operational dust prediction. In *Mineral Dust* (pp. 223-265). Springer Netherlands.
- Callado, A., Escribà, P., García-Moya, J. A., Montero, J., Santos, C., Santos-Muñoz, D., & Simarro, J. (2013). Ensemble forecasting. In *Climate change and regional/local responses*. InTech.
- Cuevas, E., Camino, C., Benedetti, A., Basart, S., Terradellas, E., Baldasano, J. M., ... & Berjón, A. (2015). The MACC-II 2007–2008 reanalysis: atmospheric dust evaluation and characterization over northern Africa and the Middle East. *Atmos. Chem. Phys*, 15(8), 3991-4024.
- Dubovik, O., & King, M. D. (2000). A flexible inversion algorithm for retrieval of aerosol optical properties from Sun and sky radiance measurements. *Journal of*

Geophysical Research, 105(D16), 20673-20696.

Eskes, H., Huijnen, V., Arola, A., Benedictow, A., Blechschmidt, A. M., Botek, E., ... & Engelen, R. (2015). Validation of reactive gases and aerosols in the MACC global analysis and forecast system. *Geoscientific model development*, 8(11), 3523-3543.

Hamill, T. M. (2001). Interpretation of rank histograms for verifying ensemble forecasts. *Monthly Weather Review*, 129(3), 550-560.

Hamill, T. M. (1997). Reliability diagrams for multicategory probabilistic forecasts. *Weather and forecasting*, 12(4), 736-741.

HARMONIE wiki page. <https://hirlam.org/trac/wiki/HarmonieSystemDocumentation>

Holben, B. N., Eck, T. F., Slutsker, I., Tanre, D., Buis, J. P., Setzer, A., ... & Lavenu, F. (1998). AERONET—A federated instrument network and data archive for aerosol characterization. *Remote sensing of environment*, 66(1), 1-16.

Hsu, N. C., Tsay, S. C., King, M. D., & Herman, J. R. (2004). Aerosol properties over bright-reflecting source regions. *IEEE Transactions on Geoscience and Remote Sensing*, 42(3), 557-569.

Huneus, N., Schulz, M., Balkanski, Y., Griesfeller, J., Prospero, J., Kinne, S., ... & Diehl, T. (2011). Global dust model intercomparison in AeroCom phase I. *Atmospheric Chemistry and Physics*, 11(15).

Murphy, A.H., 1993: What is a good forecast? An essay on the nature of goodness in weather forecasting. *Wea. Forecasting*, 8, 281-293.

Kaufman, Y. J., Tanré, D., Remer, L. A., Vermote, E. F., Chu, A., & Holben, B. N. (1997). Operational remote sensing of tropospheric aerosol over land from EOS moderate resolution imaging spectroradiometer. *Journal of Geophysical Research: Atmospheres*, 102(D14), 17051-17067.

Middleton, N. J., & Goudie, A. S. (2001). Saharan dust: sources and trajectories. *Transactions of the Institute of British Geographers*, 26(2), 165-181.

Palmer, T. N., Shutts, G. J., Hagedorn, R., Doblas-Reyes, F. J., Jung, T., & Leutbecher, M. (2005). Representing model uncertainty in weather and climate prediction. *Annu. Rev. Earth Planet. Sci.*, 33, 163-193.

Pérez, C., Nickovic, S., Baldasano, J. M., Sicard, M., Rocadenbosch, F., & Cachorro, V. E. (2006). A long Saharan dust event over the western Mediterranean: Lidar, Sun photometer observations, and regional dust modeling. *Journal of Geophysical Research: Atmospheres*, 111(D15).

O'Neill, N. T., Eck, T. F., Smirnov, A., Holben, B. N., & Thulasiraman, S. (2003). Spectral discrimination of coarse and fine mode optical depth. *Journal of Geophysical Research: Atmospheres*, 108(D17).

Rodríguez, S., Alastuey, A., & Querol, X. (2012). A review of methods for long term



in situ characterization of aerosol dust. *Aeolian Research*, 6, 55-74.

Sessions, W. R., Reid, J. S., Benedetti, A., Colarco, P. R., da Silva, A., Lu, S., ... & Brooks, M. E. (2015). Development towards a global operational aerosol consensus: basic climatological characteristics of the International Cooperative for Aerosol Prediction Multi-Model Ensemble (ICAP-MME). *Atmos. Chem. Phys*, 15, 335-362.

Talagrand, O. (1999). Evaluation of probabilistic prediction systems. In *Workshop proceedings "Workshop on predictability"*, 20-22 Oc. 1997, ECMWF, Reading, UK.

Terradellas, E., Nickovic, S., and Zhang, X. (2015): Airborne dust: a hazard to human health, environment and society, *WMO Bulletin*, 64, 42–46.

Terradellas, E., Basart, S., & Cuevas, E. (2016). Airborne dust: From R&D to Operational forecast. AEMET, Madrid, NIPO: 281-16-007-3; WMO, Geneva, WMO/GAW Report No. 230; WMO/WWRP No. 2016-2.

Viana, M., Querol, X., Alastuey, A., Cuevas, E., & Rodriguez, S. (2002). Influence of African dust on the levels of atmospheric particulates in the Canary Islands air quality network. *Atmospheric Environment*, 36(38), 5861-5875.

Spatial and Temporal Analysis of Sand and Dust Storms between the years 2003 and 2016 in the Middle East

Cihan DUNDAR¹, Ayse Gokcen ISIK¹, Kahraman OGUZ¹, Gulen GULLU²

¹Turkish State Meteorological Service, Research Department, Ankara, TURKEY,
cdundar@mgm.gov.tr, agisik@mgm.gov.tr, koguz@mgm.gov.tr

²Hacettepe University, Department of Environmental Engineering, Ankara, TURKEY,
ggullu@hacettepe.edu.tr

ABSTRACT

Mineral dust particles, aerosols suspended in the atmosphere, play a key role in the atmospheric radiation budget and hydrological cycle through their radiative and microphysics effects. Moreover, mineral dust aerosols influence the climate system in multiple ways. The most important sources of dust aerosols are located in the Northern Hemisphere, primarily over the Sahara in North Africa, the Middle East, Central and South Asia respectively. The objective of this study to carry out intensity and frequency analysis of sand and dust storm in the Middle East for the period 2003-2016. To identify aerosol episodes, the method, at which Gkikas et al (2009) investigated the aerosol events based on their frequency and intensity in the Mediterranean Basin by using AOD (Aerosol Optical Depth) data from MODIS, is applied. The AOD and AE parameters can be used to differentiate between coarse and fine particles of aerosols. To investigate average annual and monthly AOD and AE for the period 2003-2016, AOD and AE data of MODIS Aqua is obtained from Giovanni website. Spatial and temporal analyses of the Middle East (extending from 20° to 38° North and 36° to 64° East) between the years 2003 and 2016 are performed with three sub-regions: Middle East North (ME-N), Middle East Centre (ME-C), and Middle East South (ME-S). In summary, for the last years (2013-2016), annual mean AOD and the number of SDS are comparably lower than the other periods while the values are the highest between 2008 and 2012.

Keywords: AOD, dust, Middle East, trend

1. Introduction

Mineral dust aerosols, the tiny soil particles suspended in the atmosphere, have a key role in the atmospheric radiation budget and hydrological cycle through their radiative and cloud condensation nucleus effects. Mineral dust aerosols are blown into the atmosphere mainly from arid and semi-arid regions where annual rainfall is extremely low and substantial amounts of alluvial sediment have been accumulated over long periods. They are subject to long-range transport of an intercontinental scale, including North African dust plumes over the Atlantic Ocean, summer dust plumes from the Arabian Peninsula over the Arabian Sea and Indian Ocean and spring dust plumes from East Asia over the Pacific Ocean. Mineral dust aerosols influence the climate system and cloud microphysics in multiple ways [1].

Furthermore, the Intergovernmental Panel on Climate Change (IPCC) accepts mineral dust as a very important component of atmospheric aerosols, one of the main climate variables. According to the IPCC's latest climate predictions, it is expected that sand and dust storms will be more intense as the frequency and severity of the drought has increased [5].

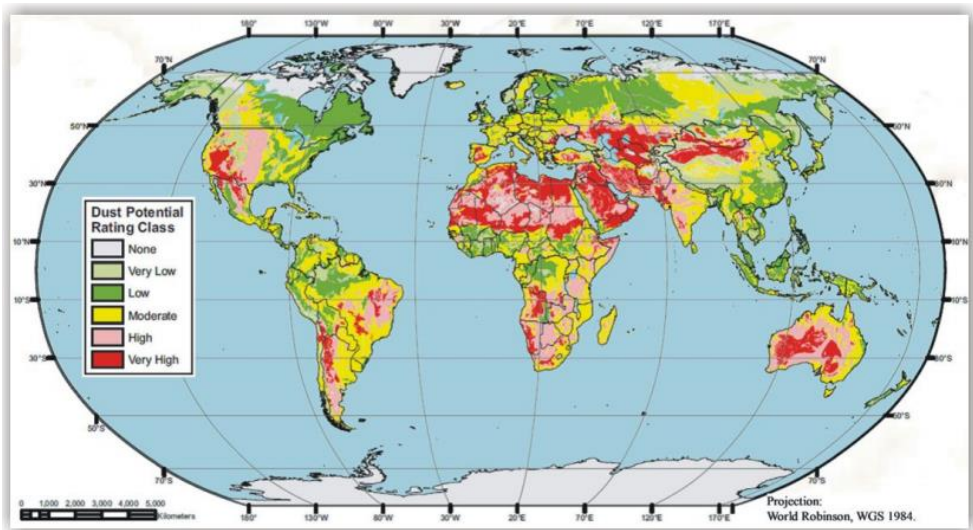


Figure 1. Global Dust Potential Map. Source: DTF (2013) [9]

Approximately 1,000 Tg to 2,000 Tg (1-2 billion tons) of dust is emitted to the atmosphere from the deserts every year [8]. The most important sources of dust aerosols are located in the Northern Hemisphere, primarily over the Sahara and Sahel in North Africa, the Middle East, Central and South Asia respectively [1]. Potential areas for dust storms are illustrated

on Figure 1. The annual amount of dust released from the Sahara into the atmosphere is about the half of dust released from all sources on Earth, while the dust released from the Sahara and Middle East regions is about 70% of global annual dust emissions. The annual amount of dust emitted from Arabian Peninsula (Middle East) to the atmosphere was estimated to 221 million tons [8].

Transport from North Africa to the Eastern Mediterranean occurs predominantly during spring and is commonly associated with the eastward passage of frontal low-pressure systems. Dust from sources in the Middle East is more typically transported to the Mediterranean in the fall [2].

2. Material and Methodology

2.1. Aerosol Optical Depth (AOD)

Aerosol Optical Depth (AOD) provides important information about the concentration, size distribution, and variability of aerosols (desert dust, sea salt, haze, and smoke particles) in the atmosphere. It is a dimensionless number related to the amount of aerosol distributed within the vertical column of atmosphere over the observation location. AOD provides a quantitative measure of the extinction of solar radiation due to aerosol scattering and absorption [4]. Heavy dust regions are defined by AOD higher than 0.3. Around deserts, AOD values are above 1.0 and usually below 3.0 [7].

Giovanni website provides a simple way to visualize, analyze, and access Earth science remote sensing data, particularly from satellites, without having to download the data. It includes data for aerosols, atmospheric chemistry, atmospheric temperature and moisture, and rainfall. It was developed by the Goddard Earth Sciences Data and Information Services Center (GES DISC).

2.2. Angstrom Exponent (AE)

The Angstrom Exponent (AE) is an exponent that expresses the spectral dependence of aerosol optical thickness (τ) with the wavelength of incident light (λ). It provides additional information on the particle size, aerosol phase function and the relative magnitude of aerosol radiances at different wavelengths. AE (computed from τ measurements on two different wavelengths) can be used to find τ on another wavelength using the relation below:

$$\tau_{\lambda} = \tau_{\lambda_0} \left(\frac{\lambda}{\lambda_0} \right)^{-\alpha}$$

$\alpha = \text{Angstrom exponent}$

The Angstrom Exponent is a useful quantity to evaluate the particle size of atmospheric aerosols or clouds, and the wavelength dependence of the aerosol/cloud optical properties. It is inversely related to the average size of the particles in the aerosol: the smaller the particle size, the larger the Angstrom Exponent is. Therefore, low AE values indicate strong presence of coarse aerosols relating to the dust events.

2.3. Sand and Dust Storms (SDS) Analysis

In literature, a well-defined methodology to investigate aerosol events does not exist. By using threshold values of AOD, several researchers tried to identify aerosol episodes. Gkikas et al (2009) investigated the aerosol events based on their frequency and intensity in the Mediterranean Basin for 7-year period (2000-2007) by using AOD data from MODIS (Moderate Resolution Imaging Spectroradiometer) [4].

Strong aerosol events were observed frequently (14 aerosol events/year) in the western and central Mediterranean Basin while extreme events (AOD up to 5.0) occurred throughout the years systematically in the eastern Mediterranean Basin. Seasonally, while strong aerosol events in the western Mediterranean Basin occurred in summer and extreme events in the eastern part of the basin were observed in the spring season [4].

$$AOD_{Threshold} = \overline{AOD} + i \times \sigma_{AOD} \text{ with } i = 1, 2, 3, 4 \quad (1)$$

$$\overline{AOD} + 2 \times \sigma_{AOD} \leq AOD < \overline{AOD} + 4 \times \sigma_{AOD} \quad \text{strong aerosol case} \quad (2)$$

$$AOD \geq \overline{AOD} + 4 \times \sigma_{AOD} \quad \text{extreme aerosol case} \quad (3)$$

Methodology is based on calculating mean average AOD (\overline{AOD}) and standard deviation values (σ_{AOD}). Equation 1 above shows the calculation of threshold: adding 1, 2, 3 and 4 standard deviation (σ_{AOD}) to the mean

AOD value. Equation 2 and equation 3 define the limit values for strong and extreme aerosol events [4].

Extreme aerosol events point out dust storms while strong aerosol events are linked to sea salt, biomass burning (forest fires), and anthropogenic activities [4].

2.4. Study Area and Period

For the analysis between the years 2003 and 2016, domain covering Middle East (extending from 20° to 38° North and 36° to 64° East) is selected. Domain is divided into three subregions as Middle East North (ME-N), Middle East Centre (ME-C), and Middle East South (ME-S) for further analysis (Figure 2). To investigate average annual and monthly AOD and AE for the period 2003-2016, MODIS Aqua data is obtained from Giovanni website. (<http://disc.sci.gsfc.nasa.gov/giovanni>).



Figure 2. Study domain for the Middle East

3. Results

In general, the AOD and AE parameters can be used to differentiate between coarse and fine particles of aerosols. Mean AOD of the period 2003-2016 (Figure 3) illustrates high AOD values reaching up to 0.5 over east of Saudi Arabia, Kuwait, Bahrain, Qatar, Iraq and Persian Gulf. Furthermore, to identify dust particles, low AE values are tracked on the plot of mean AOD of the period 2003-2016 (Figure 4). Low values are observed over Saudi Arabia, Iraq, Syria and lowest ones over Persian Gulf. Those areas with low AE and high AOD point out dust storms.

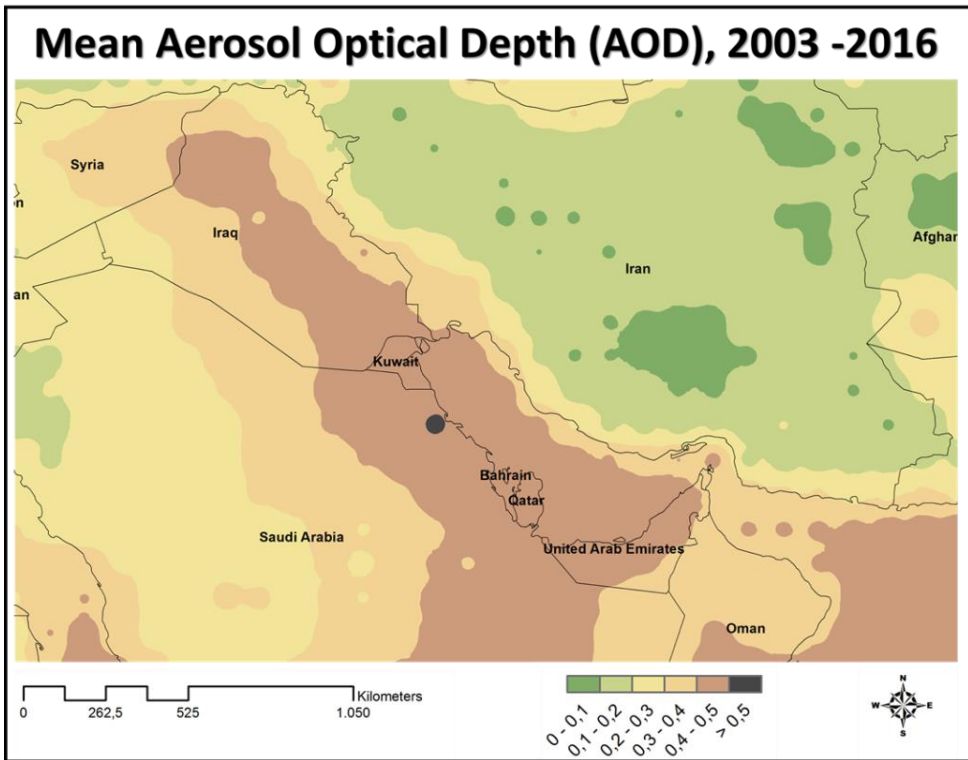


Figure 3. Mean AOD of the period 2003-2016 in the Middle East

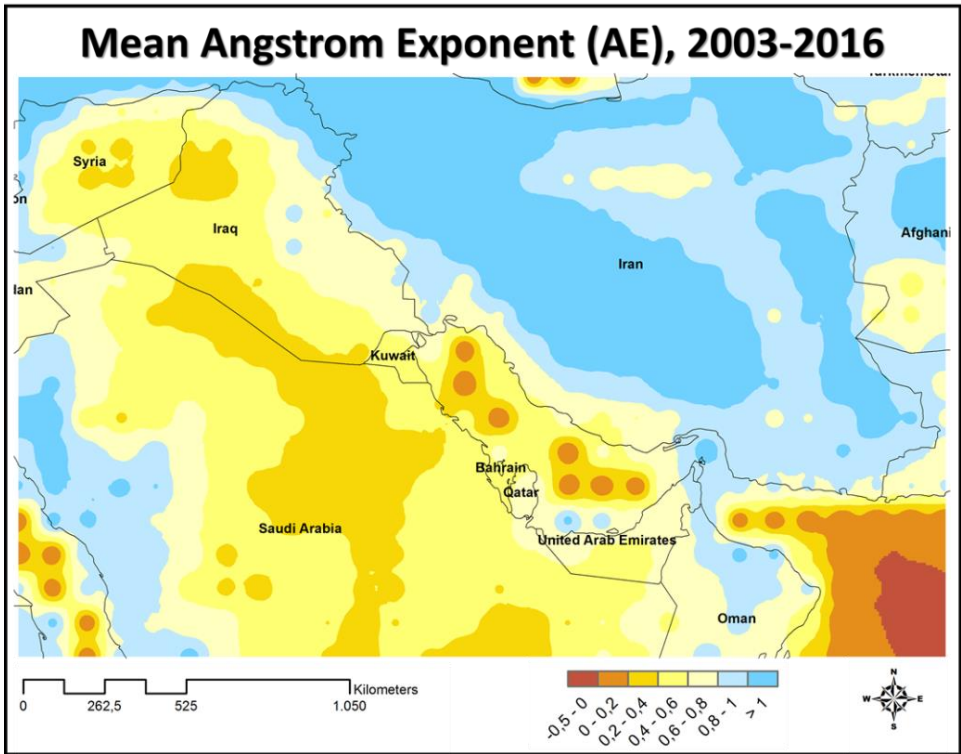


Figure 4. Mean AE of the period 2003-2016 in the Middle East

Plots for latitude cross-section of AOD and AE averaged over Middle East region are prepared (Figure 5). Moving northward along 20-38°N, AOD values decrease while AE values show an increase. In the southern part of the Middle East, this behavior can be closely related to more strong and frequent dust storms characterized by high AOD and low AE.

Average annual and monthly AOD graphs are plotted for three regions (Figure 5) to investigate the trends. Annual AOD values of the Central Middle East almost follow the averaged values of the Middle East Region as expected, while higher values of AOD are observed in the Southern ME.

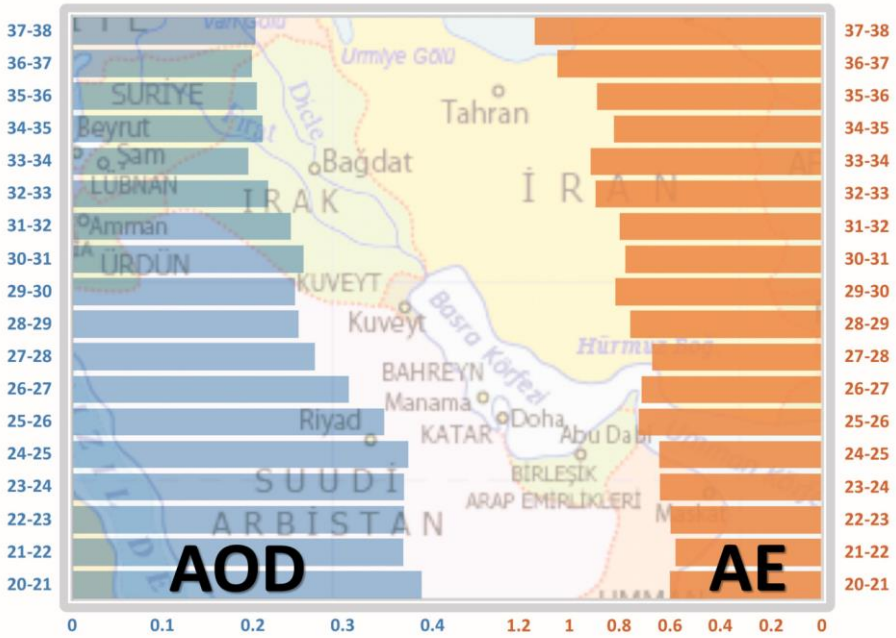


Figure 5. Latitude cross-section of AOD and AE averaged between 36°E and 64°E along 20–38°N

Seasonal variation of AOD in the Central Middle East is similar to averaged AOD values of the Middle East which has a maximum in April. On the other hand, the Southern Middle East exhibits a different seasonal pattern with a maximum AOD value in July (Figure 6b). AOD values have a maximum in spring and low AOD values are observed during winter season for both Northern and Central ME.

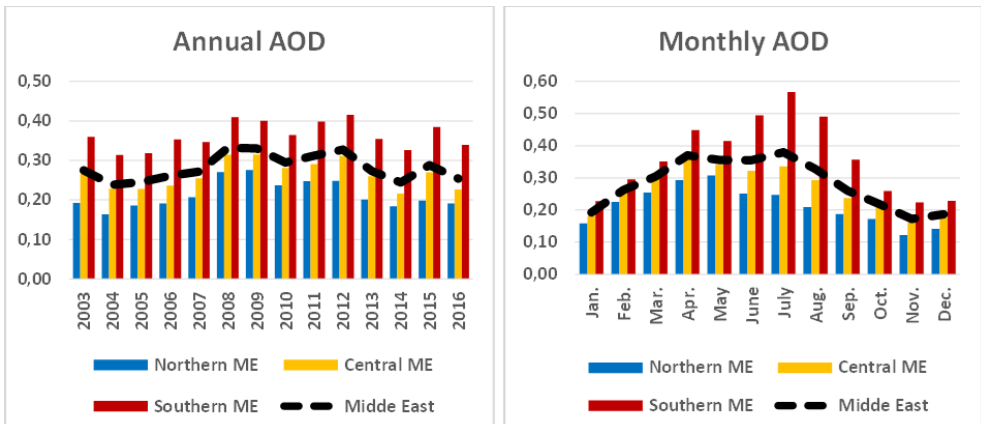


Figure 6. Average (a.) annual and (b.) monthly AOD

SDS analysis of 2003-2016 has been carried out to estimate SDS number for each year for three regions and points out the 14 years trend of SDS. The number of strong and extreme aerosol events is calculated by the method explained in the methodology section. Extreme aerosol events indicate SDS [4].

In the southern region, high number of SDS occurs compared to the northern region throughout 14 years (Figure 7a). Between 2008 and 2012, annual average SDS number reaches values above 15 up to 40 in the southern region which has a peak value in 2011. Figure 7b illustrates the seasonal variability of SDS for those three subregions. High values of monthly dust events shift to summer when we move southward in the Middle East. Southern ME is affected by high number of dust events in July while Northern and Central ME have their peak values in spring.

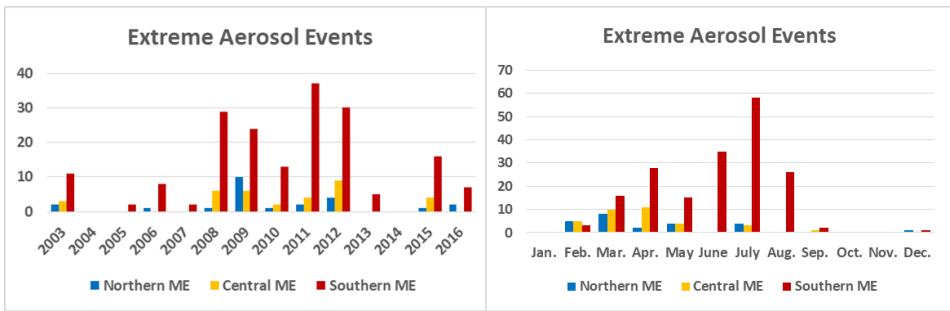


Figure 7. (a.) annual and (b.) monthly extreme events

4. Conclusion

Spatial and temporal analyses of the Middle East (extending from 20° to 38° North and 36° to 64° East) between the years 2003 and 2016 are performed with three subregions: Northern Middle East, Central Middle East and Southern Middle East. Moving southward along 20-38N latitudes, there is a significant increase in AOD values, accompanied by a decrease in AE values (coarse particles) in the same direction. It concludes that throughout 14 years, more strong and frequent dust storms are observed in the Southern Middle East which also shows different seasonal SDS characteristics.

To sum up, for the last years (2013-2016), annual mean AOD and the number of SDS are comparably lower than the other periods while the values are the highest between 2008 and 2012.

References

- [1] O. Alizadeh Choobari, P. Zawar-Reza, A. Sturman, The global distribution of mineral dust and its impacts on the climate system: A review, *Atmospheric Research* 138 (2014) 152–165.
- [2] N. J. Middleton and A. S. Goudie, Saharan Dust: Sources and Trajectories, *Transactions of the Institute of British Geographers* Vol. 26, No. 2 (2001), pp. 165-181.
- [3] Dündar C., Oğuz K., Öz N., Güllü G., Aerosol Optik Derinliği Verilerinin Türkiye İçin Alansal ve Zamansal Değişimlerinin İncelenmesi, VII. Atmosfer Bilimleri Sempozyumu, 28-30 Nisan 2015, İstanbul Teknik Üniversitesi, İstanbul (in Turkish).
- [4] Gkikas, A., Hatzianastassiou, N., and Mihalopoulos, N.: Aerosol events in the broader Mediterranean basin based on 7-year (2000–2007) MODIS C005 data, *Ann. Geophys.*, 27, 3509– 3522, doi:10.5194/angeo-27-3509-2009, 2009.
- [5] IPCC: Climate Change 2013: The Physical Science Basis; 5th Assessment Report, Cambridge University Press, Cambridge and New York, 2014.
- [6] Martínez Avellaneda N., Serra N., Stammer D., Minnett P.J. (2010) Response of the eastern subtropical Atlantic SST to Saharan dust: a modeling and observational study. *J Geophys Res* 115:C08015. doi:10.1029/2009 Jc005692
- [7] NASA, National Aeronautics and Space Administration, Science Mission Directorate. NP- 2005-8-709-GSFC.
- [8] Tanaka, T. Y., & Chiba, M. (2006). A numerical study of the contributions of dust source regions to the global dust budget. *Global and Planetary Change*, 52(1), 88-104.
- [9] UNEP, WMO, UNCCD (2016). Global Assessment of Sand and Dust Storms. United Nations Environment Programme, Nairobi.

Dust variability in the Middle East recorded in the Elbrus Mt. ice core

Stanislav Kutuzov¹, Patrick Ginot², Vladimir Mikhaleiko¹, Michel Legrand²,
Suzanne Preunkert², Alexey Poliukhov³, Alexandra Khairedinova³

¹ Institute of Geography Russian Academy of Sciences, Moscow, Russia,

² Laboratoire de Glaciologie et Géophysique de l'Environnement, -, St Martin d'Hères, France,

³ Faculty of Geography, Moscow State University

Abstract

Dust plays an important role in Earth's system. Airborne dust, mostly emitted from soils in arid and semi-arid regions, is a key atmospheric constituent and represents an important natural source of atmospheric particulate matter. Ice cores can be considered as natural archives of data on dust in the atmosphere, they can provide information not only on amount of dust particles in the atmosphere but also give insights on strengths of the dust sources and its changes in the past.

A 182 meter ice core has been recovered from a borehole drilled through the glacier to the bedrock at the Western Plateau of Mt. Elbrus (5115 m a.s.l.) in 2009. This is the first ice core in the region which represents a paleoclimate record practically undisturbed by seasonal melting. Ice samples were analysed for chemistry, concentrations of dust and black carbon, and particle size distributions. Dust mineralogy was assessed by XRD. Individual dust particles were analysed using SEM. Dust particle number concentration was measured using the Markus Klotz GmbH (Abakus) implemented into the CFA system. It was shown that desert dust deposition events occur on Mt. Elbrus 5-6 times a year. Dust originates most frequently from the Middle East, more specifically from the northern Mesopotamia and the Syrian desert. Dust from Sahara is transported to the Caucasus once or twice per year, although these events are less frequent, they result in higher dust load. The Elbrus ice core dust record correlates with the droughts indexes in the Levant region and can be used for the droughts reconstruction in this region. A prominent increase of dust and Ca²⁺ concentration was registered since the beginning of XX century with a highest dust concentration recorded in 1990-2009. Study was supported by the President Grants for Government Support of Young Russian Scientists and the Leading Scientific Schools of the Russian Federation grant № MK-2508.2017.5.

Keywords: Dust, ice core, Middle East, calcium, droughts

1. Introduction

Dust is the most important aerosol by mass (Knippertz and Stuut, 2014). It affects planetary radiation balance, atmosphere, biosphere and humans health. Despite the significance of atmospheric dust our knowledge on this parameter is still weak. To improve climate models and our general understanding of dust particles impacts it is very important to reconstruct the dust variability in the past.

In this respect proxy data becomes of great importance. Ice cores can be considered as natural archives of data on dust in the atmosphere. Ice cores can provide information not only on amount of dust particles in the atmosphere in the past but also give insights on strengths of the dust sources and its changes through the time. Number and mass particles concentrations were used as a proxy for dust flux variability. The long range dust transport patterns can be used to evaluate the atmospheric circulation change in the past. Polar ice cores from Greenland and Antarctica have been used to reconstruct the changes of dust content in the atmosphere over the hundreds thousands of years on a global scale e.g. (Delmonte et al., 2002; Petit et al., 1999; Ruth et al., 2003). However it was shown by the study of (Mahowald et al., 2010) there are only few data exist on dust variability over the recent hundreds years in different regions of the world. Therefore data from ice cores drilled at mountain glaciers located at the proximity of the arid areas and close to the densely populated areas becoming essential. Moreover despite the effort put into development of the observational network there is no confidence in dust changes even over the recent decades. The existing climate models need to be properly evaluated and validated in terms of reproducibility of the dust content in the atmosphere. There are still debates what is a trend in dust amount in the atmosphere over the past centuries (Mahowald et al. 2010).

Analyses of ice cores have shown that mineral dust originating in deserts is deposited on glaciers in Antarctica (Delmonte et al., 2002; Petit et al., 1999; Ruth et al., 2003), Greenland (Steffensen, 1997), Tibet and Himalayas (e.g. Xu et al., 2010), Central Asia (Dong et al., 2009; Kreutz et al., 2001; Thompson et al., 1989; Wake et al., 1994; Yang et al., 2006), Altai (Olivier, 2003; Olivier et al., 2006), and the European Alps (De Angelis and Gaudichet, 1991; Collaud Coen et al., 2004; Schwikowski et al., 1999, 1995; Sodemann et al., 2006; Thevenon et al., 2009, 2012; Wagenbach and Geis, 1989).

One glaciated region with the influx of mineral dust from the Sahara and

deserts of the Middle East is the Caucasus Mountains. Conditions near the top of Mt. Elbrus suggest the possibility of a reasonably long climatic record in an ice core not affected by meltwater infiltration and relatively high accumulation on the western plateau assures high temporal resolution of the ice-core data (Mikhaleenko et al., 2015).

Here we present an overview of the mineral dust analysis in Elbrus ice cores published previously together with the results from dust sources identification using satellite imagery and backtrajectory analysis. New data on relation of the dust concentration in Elbrus glaciers to droughts frequency in the Middle East are discussed.

2. Geographical Settings and Methods

The Caucasus Mountains are situated between the Black and the Caspian seas, and are generally trending east-southeast, with the Greater Caucasus range often considered as the divide between Europe and Asia. The glaciers in the Caucasus cover an area of around 1121 ± 30 km² (Kutuzov et al., 2015). Due to its elevation (over 5000 m a.s.l.), proximity to the deserts of the Middle East, Central Asia and location on the track of Saharan depressions, the Caucasus is a perfect long-travelled desert dust trap (Fig. 1). Atmospheric dust particles are preserved in snow and ice at elevations above ~ 4800 m a.s.l. where seasonal melt is negligible.

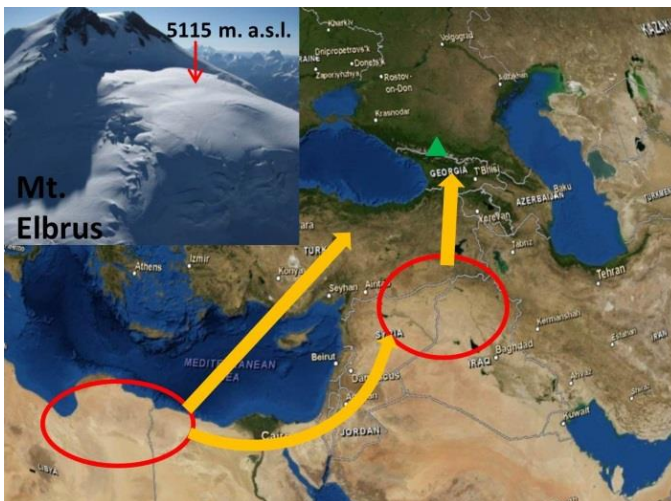


Figure 1. Study area. Location of Mt. Elbrus is marked by green triangle and the major dust sources are circled. The orange arrows indicate the main pathways of dust to the Caucasus.

Elbrus Mountain with the elevation of 5642 m a.s.l. is the highest peak in Russia. It's a dormant volcano covered by glaciers with total surface area of

120 km². Western Elbrus plateau proved to be a place of special interest with respect to ice core drilling. Flat plateau with surface area 0.5 km² is located at the accumulation zone of Bolshoy Azau and Kukurtlu glaciers to the west of Elbrus highest summit at the elevation range of 5000-5150 m a.s.l. (Fig 1). In 2004-2007 several snow pits and shallow ice cores together with radio-echo sounding surveys revealed absence of the seasonal melt. In 2009 deep ice core was drilled to the bedrock (Mikhalenko et al. 2015). In June 2012 shallow ice core was drilled at the same location at mnt Elbrus. The core was sampled on site for oxygen isotopes analysis and 13 sections on the core with visually distinctive dust layers were cut off.

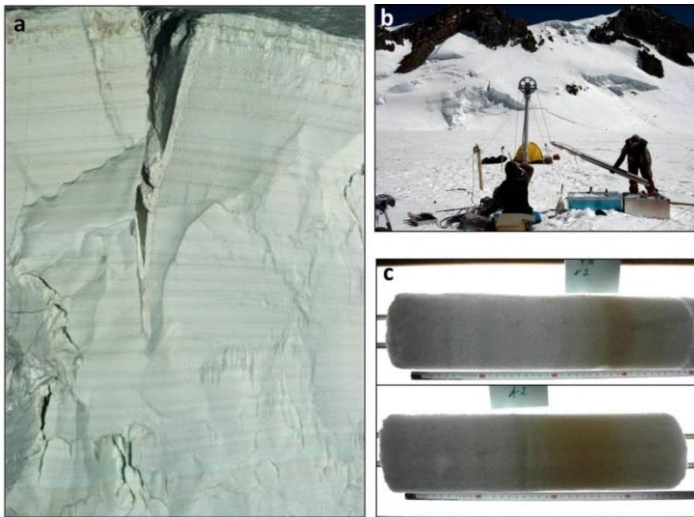


Figure 2. Sidewall of Elbrus glacier with visible dust layers (a) (photo by Mikhalenko V.N.), ice core drilling of 2009 (b), ice cores from Elbrus glacier with visible dust layers (c).

The ice cores has been analyzed for stable isotopes ($\delta^{18}\text{O}$ and δD), major ions (K^+ , Na^+ , Ca^{2+} , Mg^{2+} , NH_4^+ , SO_4^{2-} , NO_3^- , Cl^- , F^-), succinic acid ($\text{HOOCCH}_2\text{COOH}$), and tritium content. The mean annual net accumulation rate was estimated from distinct annual oscillations of $\delta^{18}\text{O}$, δD , succinic acid, and NH_4^+ and is 1455 mm w.e. for the last 140 years. Using annual layer counting also for the dating of the ice core, a good agreement with the absolute markers of the tritium 1963 bomb test time horizon located at the core depth of 50.7 m w.e. and the sulfate peak of the Katmai eruption (1912) at 87.7 m w.e. was obtained (Mikhalenko et al., 2015).

Data from the Spinning Enhanced Visible and Infra-Red Imager (SEVIRI) on board the Meteosat Second Generation (MSG) satellite were used to detect possible dust deposition events in 2009-2012 period covered by the

shallow ice core of 2012. MSG is located in a geostationary orbit at 0°W over the equator and provides images with 15 min temporal resolution and 3 km spatial resolution at nadir. The SEVIRI dust red-green-blue (RGB) images were produced from three thermal infrared channels: 10 (12.0 μm), 9 (10.8 μm), and 7 (8.7 μm). The RGB composites were created by displaying the differences between channels 10 and 9 as red, 9 and 7 as green and channel 9 as blue (Schepanski et al., 2007). On these images, dust appears bright pink or magenta and clouds appear as dark red. The dust effect on brightness temperature depends on the underlying surface, time of day, moisture content of the atmosphere, and altitude of dust cloud and composite images may favour elevated layers of dust (Brindley et al., 2012). 3 km spatial resolution may be expected mainly over the African continent due to satellite positioning. However, Middle East sector is also presented on images with a coarser resolution but enough to perform back tracking procedure similar to (Schepanski et al., 2007, 2012). After days with possible dust deposition events over the Caucasus were detected SEVIRI images were downloaded with 15 min resolution to reconstruct the dust plumes transportation history.

Twenty-seven member ensembles of three-dimensional trajectories were calculated using HYSPLIT model run with the Global Data Assimilation System (GDAS) meteorological input (Draxler and Rolph, 2013; <http://ready.arl.noaa.gov/HYSPLIT.php>). In HYSPLIT, each member of the trajectory ensemble is calculated by offsetting meteorological data by a fixed grid factor (one meteorological grid point in the horizontal and 0.01 sigma unit in the vertical). HYSPLIT was run in the backward mode for the Elbrus mnt. for each date of possible dust deposition event derived using SEVIRI images.

Three-dimensional 3-day backward trajectories arriving at Elbrus (5000 m above sea level) were calculated every 1 h using the National Oceanic and Atmospheric Administration (NOAA) HYSPLIT-4 (Hybrid Single-Particle Lagrangian Integrated Trajectory) model, (Draxler and Rolph, 2013), for the 2007 to 2013. The final model outputs were hourly backward trajectory endpoints indicating the geographical location and the height of the air parcel. Cluster analysis was performed for the back trajectories and a potential source contribution function values for the grid cells in the study domain were calculated by counting the trajectory segment endpoints terminating within each cell.

3. Results

3.1. Shallow ice core analysis

As a result of combined use of the satellite imagery, back trajectories and ice-core analysis the chronology of dust deposition events on Elbrus was reconstructed since March 2009 until June 2012. Seventeen dust layers in the snow pack correspond to dust outbreaks from distant deserts of Middle East (12 events) and Northern Sahara (4 events). However in all four cases dust was probably originated from the multiple sources. Most of the dust events attribute to the March-June season with two events occurred in October (Kutuzov et al., 2013).

Dust transport from Sahara occurred in March and May. Three times dust originated from the foothills of Akhdar Mountains. It's a well-known dust source in the northeast of Libya with a maximum of activity in spring-early summer (Schepanski et al., 2009). In March 2010 mineral dust was initially uplifted from the foothills of the Hoggar Mountains in Algeria then an additional input of dust occurred in northern Lybia, Egypt and Middle East.

The majority of dust events originated from the Middle East was caused by prefrontal and post frontal winds. E.g. on 20 May 2009 a low was centred over the Iraq and northern Syria, with a strong pressure gradient to the north. As a result the flow to the north was established and a postfrontal dust storm occurred over the eastern Syria and western Iraq (Fig 2). Dust plume extended over the eastern Turkey on 21 of May following the warm front and reaching the Caucasus region on 21-22 UTC the same day (Fig. 3).

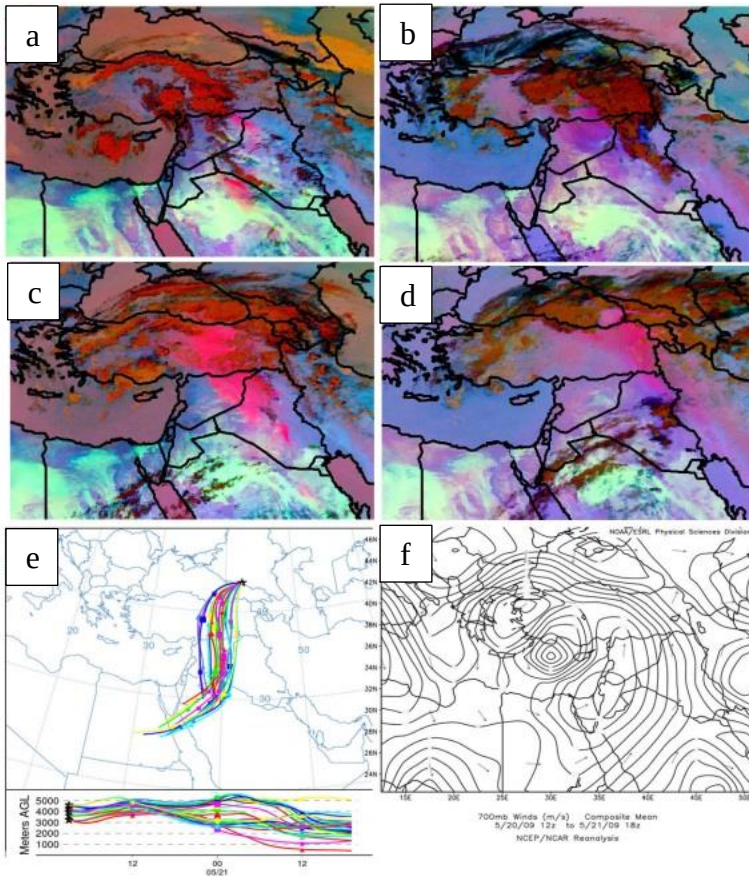


Figure 3. (a-d) SEVIRI-derived RGB false color composite images for 16-19 May 2011. (e) Two-day three-dimensional back trajectories from HYSPLIT model starting at 43.348°N; 42.427°E; 5000 m a.s.l. at 03 UTC on 19 May 2011. (f) Four-day (16-19 May 2009) average wind speed (m s⁻¹) and direction at 700 hPa.

General information on the dust sources in Middle East can be found in (Edgell, 2006). A number of studies focused of dust storm activity in region (Barkan et al., 2005; Middleton, 1986). It was shown that nearly the whole Middle East is influenced by the dust storms with the maximum frequency of dust events in spring-summer season (Middleton 1986; (Furman, 2003). Mapping of the Middle East dust sources has been accomplished in Naval Research Laboratory where a high-resolution (1-km) dust source database was developed using satellite derived Dust Enhancement Product imagery identifying and mapping point sources (Walker et al., 2009).

The back tracking technique has enabled location of dust sources for dust deposition events. Dust sources were mapped as a square of 20x20 km on

the georeferenced SEVIRI image centred over the clearly distinguishable dust plume at the very beginning of dust event. Our results well correspond to the dust sources map for NW Asia (Fig. 4, Walker et al, 2009). The main sources of dust storm events for the described period where the Jazirah region of eastern Syria, the widyan area of western Syrian desert in northern Saudi Arabia and western Iraq and the plateau of eastern Jordan. Dust was mainly originated from the small scale sources such as wadi networks, dry lakes and agricultural lands.

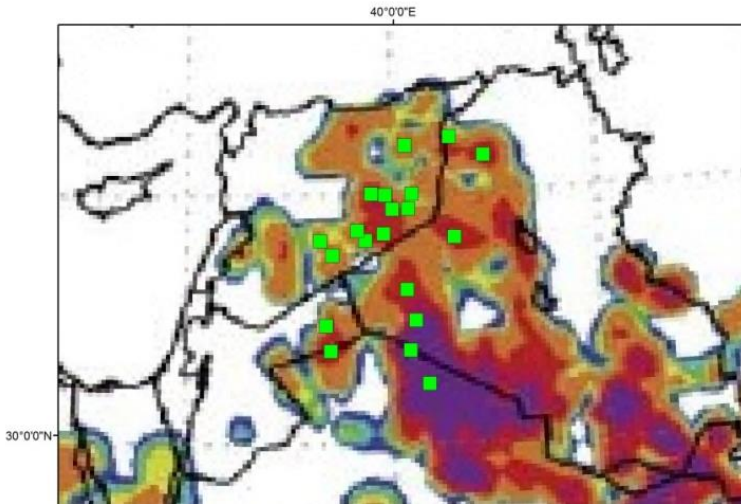


Figure 4. Middle East sources for mineral dust in Caucasus (green squares) shown over the NRL DSD dust source distribution map for the 27-km grid domain expressed as grid erodible fraction (0.0–1.0) (Walker et al, 2009).

3.2. Back trajectory analysis

Cluster analysis was performed for the 1-h back trajectories for the March-October periods of 2007-2013. 5 clusters were identified for each year. On Figure 5 we show an example of cluster analysis for the 2007. The majority of the trajectories show a south-west origin (246) and specifically the Middle East region. The next important aerosol source is the Western and Eastern Europe due to prevailing of the westerlies. Lowest share of summer trajectories is attributed to regions located to the north and east from Caucasus. In total during 2007-2013 the Middle East region was a dominant source of air masses arriving at Elbrus (32%). 20-25% of air masses were originating in Europe, 15% - in North Africa and 20% from the nearby regions. Sources located to the north from Elbrus contribute only about 10 % of the air masses arriving at Elbrus in summer.

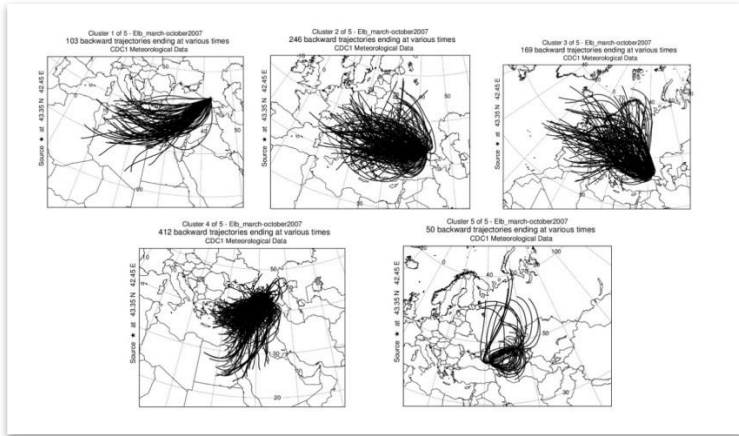


Figure 5. Back trajectories arriving at Elbrus mt. cluster analysis for 2007.

3.3. Deep ice core

Ca²⁺ is a common dust tracer used for ice core records interpretation (e.g. (Grigholm et al., 2017). Here we present analysis of the annual average Ca²⁺ concentrations recorded in Elbrus ice core over the period 1920-2013. More detailed analysis will be presented in follow up designated publications.

The Elbrus Ca²⁺ record reveals a quasi decadal variability with a general increasing trend. The maximum annual concentrations were preserved in 1999 and 2000 annual layers. We compared ice core record to various parameters in the potential source regions for natural dust. We found a statistically significant spatial correlation of the Elbrus Ca²⁺ annual concentrations and precipitation and soil moisture content in Levant region (specifically Syria and Iraq). On figure 6 the Ca²⁺ record is shown together with Standardised Precipitation-Evapotranspiration Index for the region of Fertile Crescent ($r=0.62$ $p<0.001$). Therefore we can conclude that Elbrus ice cores can be used to reconstruct the dust variations over the Middle East region and more specifically to reconstruct droughts variability in Fertile Crescent.

Description of dust pathways from the Middle East to the Caucasus leads to better understanding of atmospheric circulation patterns in the region. Arid and semi-arid regions in Syria and Iraq are highly instable under the climatic changes. Temperature and hydrological anomalies during the last millennium have led to large variations in human occupation and agricultural production (Kaniewski, 2012). Ice core record from Elbrus

independently confirms previous findings (Cook et al., 2016; Kelley et al., 2015) that the recent droughts in 1998-2012 period were most severe at least over the past century. This is the only record also to suggest that the droughts in the Levant region lead to the elevated atmospheric dust concentration over the Middle East and Caucasus region.

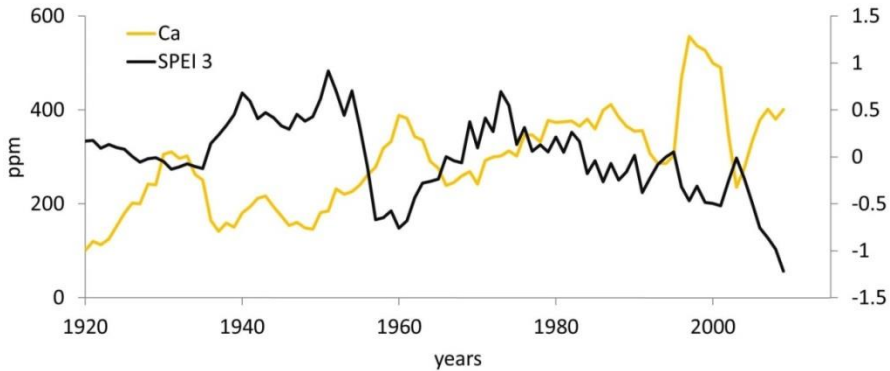


Figure 6. 3-yr moving average of the Ca^{2+} concentration record from the Elbrus ice core and Standardised Precipitation-Evapotranspiration Index for the region of Fertile Crescent.

Attribution of mechanisms responsible for dust variations within the Elbrus ice core to natural and anthropogenic drivers requires further investigation. Which will include: more strict separation of individual dust events, frequency analysis and comparison to background concentrations; mineralogical analysis; comparison to observations and proxy data; better understanding of changes in atmospheric circulation; combined analysis of ammonia, sulphate and dust records.

4. Conclusion

- Elbrus ice core is the first ice core to represent environmental changes in the Middle East region.
- Frequent dust events affect Caucasus glaciers in Spring-Summer
- Variations in Ca^{2+} concentration are related to the drought conditions in Syria-Iraq region
- There is a prominent increase in distant dust concentration in the ice core over the past 100 years which is likely confirms that the recent droughts in Fertile Crescent 1998-2012 period were most severe at least for the past century.

Acknowledgements

Study was supported by the President Grants for Government Support of Young Russian Scientists and the Leading Scientific Schools of the Russian Federation grant № MK-2508.2017.5.

References

1. De Angelis, M. and Gaudichet, A.: Saharan dust deposition over Mont Blanc (French Alps) during the last 30 years, *Tellus B*, 43(1), 61–75, doi:10.1034/j.1600-0889.1991.00005.x, 1991.
2. Barkan, J., Alpert, P., Kutiel, H. and Kishcha, P.: Synoptics of dust transportation days from Africa toward Italy and central Europe, *J. Geophys. Res.*, 110(D7), D07208, doi:10.1029/2004JD005222, 2005.
3. Brindley, H., Knippertz, P., Ryder, C. and Ashpole, I.: A critical evaluation of the ability of the Spinning Enhanced Visible and Infrared Imager (SEVIRI) thermal infrared red-green-blue rendering to identify dust events: Theoretical analysis, *J. Geophys. Res.*, 117(D7), D07201, doi:10.1029/2011JD017326, 2012.
4. Collaud Coen, M., Weingartner, E., Schaub, D., Hueglin, C., Corrigan, C., Henning, S., Schwikowski, M. and Baltensperger, U.: Saharan dust events at the Jungfraujoch: detection by wavelength dependence of the single scattering albedo and first climatology analysis, *Atmos. Chem. Phys.*, 4(11/12), 2465–2480, doi:10.5194/acp-4-2465-2004, 2004.
5. Cook, B. I., Anchukaitis, K. J., Touchan, R., Meko, D. M. and Cook, E. R.: Spatiotemporal drought variability in the mediterranean over the last 900 years, *J. Geophys. Res.*, 121(5), 2060–2074, doi:10.1002/2015JD023929, 2016.
6. Delmonte, B., Petit, J.-R. and Maggi, V.: Glacial to Holocene implications of the new 27000-year dust record from the EPICA Dome C (East Antarctica) ice core, *Clim. Dyn.*, 18(8), 647–660, doi:10.1007/s00382-001-0193-9, 2002.
7. Dong, Z., Li, Z., Wang, F. and Zhang, M.: Characteristics of atmospheric dust deposition in snow on the glaciers of the eastern Tien Shan, China, *J. Glaciol.*, 55(193), 797–804, doi:10.3189/002214309790152393, 2009.
8. Draxler, R. R. and Rolph, G. D.: HYSPLIT (HYbrid Single-Particle Lagrangian Integrated Trajectory) Model access via NOAA ARL READY Website (<http://ready.arl.noaa.gov/HYSPLIT.php>). NOAA Air Resources Laboratory, Silver Spring, MD., 2013.
9. Edgell, H. S.: *Arabian Deserts*, Springer Netherlands, Dordrecht., 2006.
10. Furman, H. K. H.: Dust Storms in the Middle East: Sources of Origin and Their Temporal Characteristics, *Indoor Built Environ.*, 12(6), 419–426, doi:10.1177/1420326X03037110, 2003.
11. Grigholm, B., Mayewski, P. A., Aizen, V., Kreutz, K., Aizen, E., Kang, S., Maasch, K. A. and Sneed, S. B.: A twentieth century major soluble ion record of dust



- and anthropogenic pollutants from Inilchek Glacier, Tien Shan, *J. Geophys. Res.*, 122(3), 1884–1900, doi:10.1002/2016JD025407, 2017.
12. Kaniewski, D.: Drought is a recurring challenge in the Middle East, *Proc. ...*, doi:10.1073/pnas.1116304109/- /DCSupplemental.www.pnas.org/cgi/doi/10.1073/pnas.1116304109, 2012.
 13. Kelley, C. P., Mohtadi, S., Cane, M. A., Seager, R. and Kushnir, Y.: Climate change in the Fertile Crescent and implications of the recent Syrian drought, *Proc. Natl. Acad. Sci.*, 112(11), 3241–3246, doi:10.1073/pnas.1421533112, 2015.
 14. Knippertz, P. and Stuut, J. B. W.: Mineral dust: A key player in the earth system, *Miner. Dust A Key Play. Earth Syst.*, (June), 1–509, doi:10.1007/978-94-017-8978-3, 2014.
 15. Kreutz, K. J., Aizen, V. B., Cecil, L. D. and Wake, C. P.: Oxygen isotopic and soluble ionic composition of a shallow firn core, Inilchek glacier, central Tien Shan, *J. Glaciol.*, 47(159), 548–554, doi:10.3189/172756501781831819, 2001.
 16. Kutuzov, S., Shahgedanova, M., Mikhaleiko, V., Ginot, P., Lavrentiev, I. and Kemp, S.: High-resolution provenance of desert dust deposited on Mt. Elbrus, Caucasus in 2009–2012 using snow pit and firn core records, *Cryosphere*, 7(5), 1481–1498, doi:10.5194/tc-7-1481-2013, 2013.
 17. Kutuzov, S. S., Lavrentiev, I. I., Vasilenko, E. V., Macheret, Y. Y., Petrakov, D. A. and Popov, G. V.: Estimation of the greater caucasus glaciers volume, using radio-echo sounding data and modelling, *Earth's Cryosph.*, 19(1), 78–88, 2015.
 18. Mahowald, N. M., Kloster, S., Engelstaedter, S., Moore, J. K., Mukhopadhyay, S., McConnell, J. R., Albani, S., Doney, S. C., Bhattacharya, A., Curran, M. A. J., Flanner, M. G., Hoffman, F. M., Lawrence, D. M., Lindsay, K., Mayewski, P. A., Neff, J., Rothenberg, D., Thomas, E., Thornton, P. E. and Zender, C. S.: Observed 20th century desert dust variability: Impact on climate and biogeochemistry, *Atmos. Chem. Phys.*, 10(22), 10875–10893, doi:10.5194/acp-10-10875-2010, 2010.
 19. Middleton, N. J.: Dust storms in the Middle East, *J. Arid Environ.* Arid Env., (10), 83–96 [online] Available from: <http://ukpmc.ac.uk/abstract/AGR/ADL86048831> (Accessed 14 November 2012), 1986.
 20. Mikhaleiko, V., Sokratov, S., Kutuzov, S., Ginot, P., Legrand, M., Preunkert, S., Lavrentiev, I., Kozachek, A., Ekaykin, A., Fain, X., Lim, S., Schotterer, U., Lipenkov, V. and Toropov, P.: Investigation of a deep ice core from the Elbrus western plateau, the Caucasus, Russia, *Cryosphere*, 9(6), 2253–2270, doi:10.5194/tc-9-2253-2015, 2015.
 21. Olivier, S.: Glaciochemical investigation of an ice core from Belukha glacier, Siberian Altai, *Geophys. Res. Lett.*, 30(19), 2019, doi:10.1029/2003GL018290, 2003.
 22. Olivier, S., Blaser, C., Brütsch, S., Frolova, N., Gäggeler, H. W., Henderson, K. a., Palmer, a. S., Papina, T. and Schwikowski, M.: Temporal variations of mineral dust, biogenic tracers, and anthropogenic species during the past two



- centuries from Belukha ice core, Siberian Altai, *J. Geophys. Res.*, 111(D5), D05309, doi:10.1029/2005JD005830, 2006.
23. Petit, J. R., Jouzel, J., Raynaud, D., Barkov, N. I., Barnola, J. M., Basile, I., Bender, M., Chappellaz, J., Davis, M., Delaygue, G., Delmotte, M., Kotlyakov, V. M., Legrand, M., Lipenkov, V. Y., Lorius, C., Pépin, L., Ritz, C., Saltzman, E. and Stievenard, M.: Climate and atmospheric history of the past 420,000 years from the Vostok ice core, Antarctica, *Nature*, 399, 429–436, doi:10.1038/20859, 1999.
 24. Ruth, U., Wagenbach, D., Steffensen, J. P. and Bigler, M.: Continuous record of microparticle concentration and size distribution in the central Greenland NGRIP ice core during the last glacial period, *J. Geophys. Res.*, 108(D3), 4098, doi:10.1029/2002JD002376, 2003.
 25. Schepanski, K., Tegen, I., Laurent, B., Heinold, B. and Macke, A.: A new Saharan dust source activation frequency map derived from MSG-SEVIRI IR-channels, *Geophys. Res. Lett.*, 34(18), L18803, doi:10.1029/2007GL030168, 2007.
 26. Schepanski, K., Tegen, I., Todd, M. C., Heinold, B., Bönisch, G., Laurent, B. and Macke, A.: Meteorological processes forcing Saharan dust emission inferred from MSG-SEVIRI observations of subdaily dust source activation and numerical models, *J. Geophys. Res.*, 114(D10), D10201, doi:10.1029/2008JD010325, 2009.
 27. Schepanski, K., Tegen, I. and Macke, a.: Comparison of satellite based observations of Saharan dust source areas, *Remote Sens. Environ.*, 123, 90–97, doi:10.1016/j.rse.2012.03.019, 2012.
 28. Schwikowski, B. M., Doscher, a., Gaggeler, H. W. and Schotterer, U.: Anthropogenic versus natural sources of atmospheric sulphate from an Alpine ice core, *Tellus B*, 51(5), 938–951, doi:10.1034/j.1600-0889.1999.t01-4-00006.x, 1999.
 29. Schwikowski, M., Seibert, P., Baltensperger, U. and Gaggeler, H. W.: A study of an outstanding Saharan dust event at the high-alpine site Jungfrauoch, Switzerland, *Atmos. Environ.*, 29(15), 1829–1842, doi:10.1016/1352-2310(95)00060-C, 1995.
 30. Sodemann, H., Palmer, A. S., Schwierz, C., Schwikowski, M. and Wernli, H.: The transport history of two Saharan dust events archived in an Alpine ice core, *Atmos. Chem. Phys.*, 6(3), 667–688, doi:10.5194/acp-6-667-2006, 2006.
 31. Steffensen, J. P.: The size distribution of microparticles from selected segments of the Greenland Ice Core Project ice core representing different climatic periods, *J. Geophys. Res.*, 102(C12), 26755, doi:10.1029/97JC01490, 1997.
 32. Thevenon, F., Anselmetti, F. S., Bernasconi, S. M. and Schwikowski, M.: Mineral dust and elemental black carbon records from an Alpine ice core (Colle Gnifetti glacier) over the last millennium, *J. Geophys. Res.*, 114(D17), D17102, doi:10.1029/2008JD011490, 2009.
 33. Thevenon, F., Chiaradia, M., Adatte, T., Hueglin, C. and Poté, J.:

Characterization of Modern and Fossil Mineral Dust Transported to High Altitude in the Western Alps: Saharan Sources and Transport Patterns, *Adv. Meteorol.*, 2012, 1–14, doi:10.1155/2012/674385, 2012.

34. Thompson, L. G., Mosley-Thompson, E., Davis, M. E., Bolzan, J. F., Dai, J., Klein, L., Yao, T., Wu, X., Xie, Z. and Gundestrup, N.: Holocene–late pleistocene climatic ice core records from qinghai-tibetan plateau., *Science*, 246(4929), 474–7, doi:10.1126/science.246.4929.474, 1989.
35. Wagenbach, D. and Geis, K.: The mineral dust concentrations and depositions of sulphur in Europe record in a high altitude glacier (Colle Gnifetti, Swiss Alps), in *Paleoclimatology and paleometeorology: modern and past patterns of global atmospheric transport*, edited by M. Leinen and M. Sarnthein, pp. 543–564, Kluwer Academic Publishers, Dordrecht., 1989.
36. Wake, C. P., Mayewski, P. a., Li, Z., Han, J. and Qin, D.: Modern eolian dust deposition in central Asia, *Tellus B*, 46(3), 220–233, doi:10.1034/j.1600-0889.1994.t01-2-00005.x, 1994.
37. Walker, A. L., Liu, M., Miller, S. D., Richardson, K. a. and Westphal, D. L.: Development of a dust source database for mesoscale forecasting in southwest Asia, *J. Geophys. Res.*, 114(D18), D18207, doi:10.1029/2008JD011541, 2009.
38. Xu, J., Hou, S., Qin, D., Kaspari, S., Mayewski, P. A., Petit, J. R., Delmonte, B., Kang, S., Ren, J., Chappellaz, J. and Hong, S.: A 108.83-m ice-core record of atmospheric dust deposition at Mt. Qomolangma (Everest), Central Himalaya, *Quat. Res.*, 73(1), 33–38, doi:10.1016/j.yqres.2009.09.005, 2010.
39. Yang, M., Yao, T. and Wang, H.: Microparticle content records of the Dunde ice core and dust storms in northwestern China, *J. Asian Earth Sci.*, 27(2), 223–229, doi:10.1016/j.jseaes.2005.03.007, 2006.

Contribution of Desert Dust Transport to Daily PM₁₀ Concentrations in Aksaray, Istanbul: A Long-Term Study

Rosa M Flores, Nefel Kaya, Övgü Eşer, Şehnaz Saltan

Environmental Engineering Department, Marmara University, Istanbul, Turkey
(rflores@marmara.edu.tr)

Abstract

The Megacity of Istanbul is a sensitive area due to various local and regional air pollution sources. Its large population is frequently exposed to high concentrations of particulate matter (PM) emitted by domestic heating, industrial activities, road traffic, and ship emissions. PM concentrations due to local anthropogenic emissions are worsened by certain meteorological conditions such as daily and seasonal temperature inversions that cause air stagnation, long-range transport of air pollutants from Mediterranean, Balkan region, and Eastern Europe, and natural contribution from Sahara desert, Asian deserts, and the Arabian Peninsula. In this work, the effect of desert dust transport on PM₁₀ concentrations in Aksaray, Istanbul during 2007-2014 was investigated. Desert dust loadings in Istanbul were obtained from the BSC-DREAM8b forecast model and used to select desert dust outbreaks. The reference EU method (2008/50/EC) was used to quantify the impact of desert dust transport on daily PM₁₀ concentrations. The HYSPLIT model was used to study frequency and magnitude of PM₁₀ concentrations associated to mean air mass backward trajectories. Daily-averaged PM₁₀ concentrations exceeded the EU air quality standard of 50 $\mu\text{g m}^{-3}$ 50% of the time during the study period. The largest air quality standard exceedances established by the EU occurred during the spring and winter seasons with factors of 1-10. The total number of dust transport events ranged between 49 and 137 per year, with approximately 40–60% of the dust loading during the spring season. Desert dust contributed to 14-33 $\mu\text{g m}^{-3}$ in 2014 and 2009, representing 22% and 72% of the yearly-averaged surface PM₁₀ concentration, respectively. The work presented here provides the first integrated assessment for evaluation of occurrence and quantification of the effect of dust transport to ground-level PM₁₀ concentrations in Istanbul, which is helpful for human health prevention and implementation of air quality control measures.

Keywords: Mineral Dust, PM₁₀, DREAM8b, HYSPLIT.

1. Introduction

The study of temporal variation of atmospheric aerosols is essential for a better understanding of sources, transport, and accumulation in the atmosphere. In addition, the study of aerosol properties is important for the understanding of their formation and potential impacts in ecosystems and climate change. Istanbul is a Megacity that often shows exceedance in particulate matter (PM) standard values, especially during the winter season due to the use of low quality fuel for residential heating and temperature inversion that hinders the dispersion of pollutants (Tayanç, 2000). In addition to local anthropogenic pollution by domestic heating, industrial emissions, road traffic activities, and ship emissions (Deniz and Durmuşoğlu, 2008; Im et al., 2010; Tayanç, 2000), important contributions from natural sources have been found in Istanbul. According to (Theodosi et al., 2010), PM₁₀ concentrations were apportioned to natural sources (27%), traffic and industrial activities (22%), fuel oil combustion (16%), secondary (10%), and ammonium sulfate (7%). Kabatas et al. (2014) estimated that 96.6% of PM₁₀ concentrations were due to desert dust during an episodic event in April 2008. Agacayak et al. (2015) quantitatively used the BSC-DREAM8b model to select a desert dust transport episode occurring in Istanbul in March 2008. During this episode, the RegCM4 regional model estimated an aerosol optical depth of 0.87, a negative radiative effect (-61.9 W m⁻² shortwave radiation at the surface), and dust load greater than 700 mg m⁻² (Agacayak et al., 2015). In addition, High PM₁₀ concentrations have been also attributed to long-range transport from Sahara desert, Arabian Peninsula, and southwestern Mediterranean region during the spring, Balkan region during the winter, and Eastern Europe (Karaca et al., 2009; Karaca and Camci, 2010; Kuzu et al., 2013). In this work, an integrated assessment of the contributions of long range transport of desert dust to surface PM₁₀ concentrations was performed. Temporal variations of hourly ground-level PM₁₀ concentrations, aerosol optical depth (AOD), aerosol index (AI), vertical distribution, and mineral dust loadings were investigated according to air mass trajectory clusters in Istanbul during 2007-2015. Aerosol properties (i.e., AOD, AI, and vertical distribution) and mineral dust loadings were retrieved from satellite observations and the BSC-DREAM8b model, respectively. Air mass backward trajectories and clustering were supplied by NOAA-HYSPLIT model. Mineral dust transport events were characterized according to the exceedance of a dust loading threshold value. A detailed explanation of methods and discussion of results has been reported by (Flores et al., 2017)

area that corresponds to North Africa, Middle East, and Europe. The model was used quantitatively to evaluate the occurrence of desert dust transport advection and dust loadings (g m^{-2}) in Istanbul. The occurrence of desert dust transport was identified when dust loading exceeded a threshold value of 0.25 g m^{-2} over Istanbul, which in the model output is characterized by a light green color.

2.4. Contribution of desert dust transport to daily PM_{10} concentrations

The reference method under the directive 2008/50/EC on ambient air quality and cleaner air for Europe (EC, 2011; Stafoggia et al., 2016) was used to quantify the contribution of desert dust to daily surface PM_{10} concentrations during the 2007-2014 period as follows: (1) background PM_{10} concentrations at the closest urban background station were obtained as the 30-day moving percentile of PM_{10} concentrations for days that did not have the influence of desert dust transport and (2) PM_{10} concentrations due to desert dust advectations were calculated by subtracting the PM_{10} background concentration obtained in (1) from PM_{10} concentrations observed during dust transport events at the urban background station (Aleksandropoulou and Lazaridis, 2013; EC, 2011; Querol et al., 2009; Salvador et al., 2013; Stafoggia et al., 2016; Viana et al., 2010). This method has been developed for the Mediterranean region and validated with chemical speciation analysis in the presence and absence of dust advection (Escudero et al., 2007). The urban traffic and urban background stations are Aksaray and Sariyer, respectively.

2.5. Satellite observations

Monthly-averaged and daily aerosol optical depth (AOD) and aerosol index (AI) were used to evaluate aerosol extinction properties and aerosol layer height and thickness during dust transport events in Istanbul from 2007 to 2014. Combined dark target and deep blue AOD at $0.55 \mu\text{m}$ for lands and ocean $1^\circ \times 1^\circ$ ($\sim 140 \text{ km}$) were obtained with MODIS Terra v 6.0 over the region enclosed in the matrix 15.82E, 27.45N, 54.31E, 50.30N. AOD and AI were acquired using the National Aeronautics and Space Administration (NASA) Goddard Earth Sciences Data and Information Services Center (GES DISC) Interactive Online Visualization and Analysis Infrastructure (GIOVANNI)(Lloyd et al., 2008).

2.6. Cluster analysis

Three day backward trajectories were obtained with NOAA-HYSPLIT4 model at three heights 10, 500 and 3000 m above ground level. Additionally, three-day backward trajectories were obtained at 500 m to for cluster analysis, which was performed with the clustering algorithm included in the HYSPLIT4 model. The total number of clusters was chosen as 5 and represents more than 75% of the total variance.

3. Results

3.1. PM₁₀ concentrations

The yearly distribution of PM₁₀ concentrations between 2007 and 2015 in Aksaray, Istanbul can be observed in the box plot in Fig. 3. Overall, PM₁₀ concentrations have been variable during the study period, with average concentrations exceeding the yearly air quality standard of 40 µg/m³ all the years. The lowest yearly-averaged PM₁₀ concentrations were observed in 2009-2011 with average concentrations ranging 46-48 µg/m³ and 29-38% of the data exceeding the daily air quality standard of 50 µg/m³. The daily averaged PM₁₀ concentrations were exceeded 54-79% of the time between 2007-2008 and 2012-2015 (Fig. 3).

High concentrations are observed in winter season followed by spring, autumn and summer (Fig. 4). High concentrations in winter have been attributed to the use of low quality fuels for residential heating augmented by temperature inversions and stagnation conditions in the atmosphere. In the spring, winds from African desert contribute to PM₁₀ concentrations. During the summer, low traffic density contributes to decrease in PM₁₀ conc. however, dust transport is also observed during the summer.

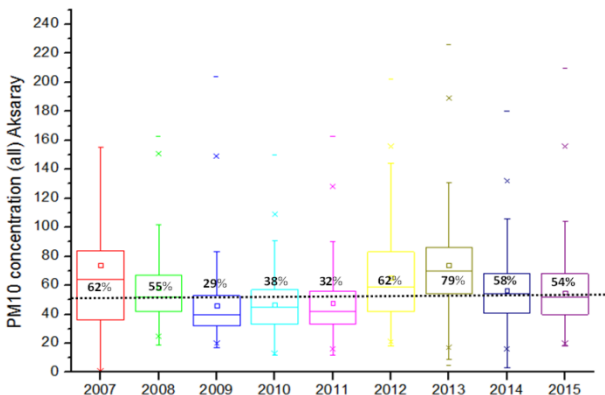


Figure 3. PM₁₀ concentrations (µg/m³) in Aksaray 2007-2015

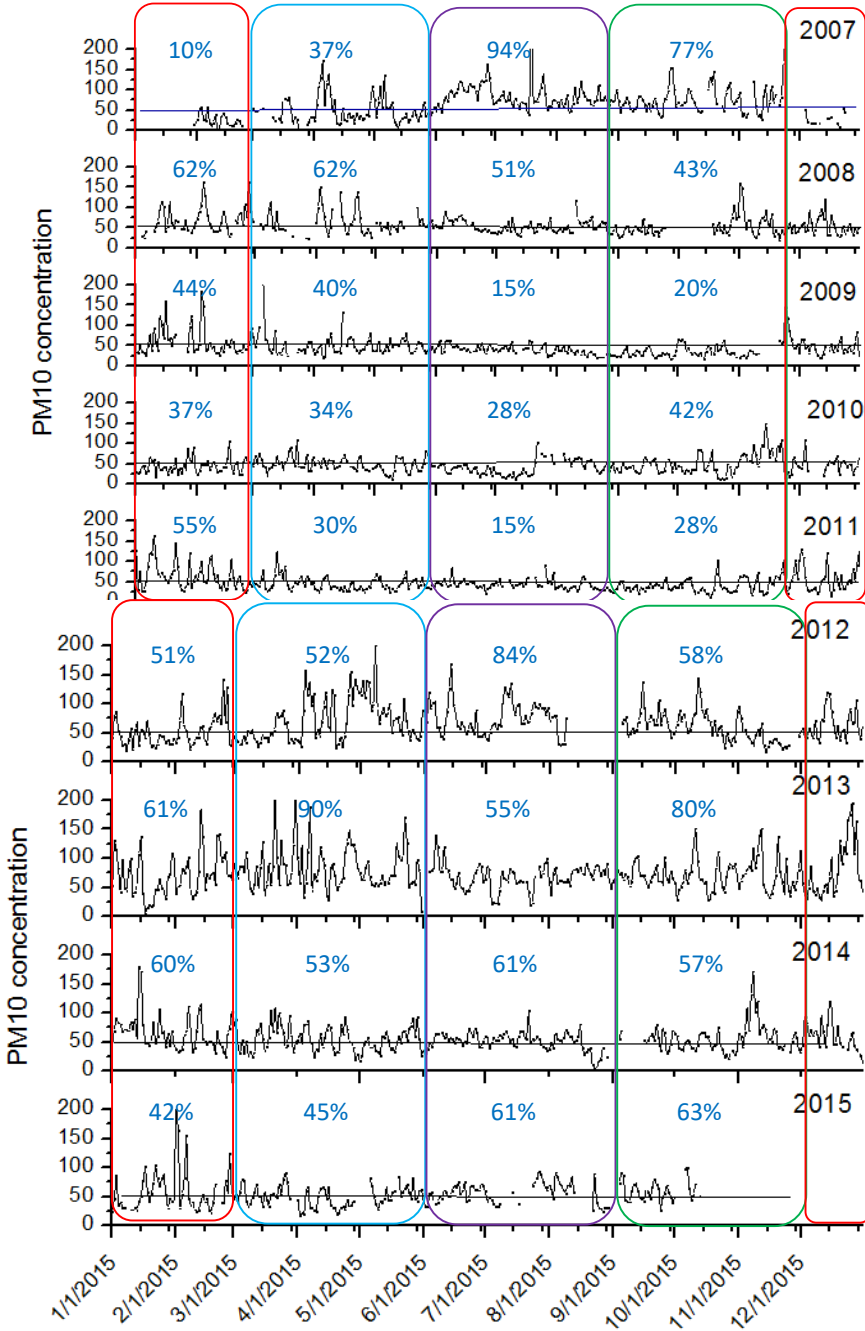


Figure 4. PM₁₀ concentrations in Aksaray. The numbers indicate percent exceedance of the PM₁₀ air quality standard (50 µg/m³) per season. red-winter, blue-spring, purple-summer, green-autumn

3.2. Identification of dust transport events

The BSC-DREAM v8 model was used to identify dust transport events over Istanbul. Figure 5 shows an example of a desert dust transport event that lasted 6 days in April 2012. The duration of the transport events and dust load signature depend on local surface wind at origin, large scale pressure systems and stability of the atmosphere that determine transport, and local topography and meteorological conditions that determine dry or wet precipitation (Flores et al., 2017). In this specific event, dust load was 0.05 g m^{-2} for three days, increased to 0.25 g m^{-2} on fourth day, and increased to 1.0 g m^{-2} on the sixth day (Fig. 5). Surface PM_{10} concentrations varied $88\text{--}158 \text{ }\mu\text{g/m}^3$ and did not show a direct correlation with dust loading. The lack of strong correlations between PM_{10} concentrations and dust loading may be related to local meteorological conditions in Istanbul that determine precipitation and deposition. Figure 6 shows PM_{10} concentrations observed only during identified dust transport events (left) and the number of dust transport events for each year (right). The number of dust transport events shows a general decreasing trend and ranges between 49 (2015) and 137 (2007) during the study period. A correlation between number of dust transport events PM_{10} concentrations can be observed in 2007-2011. High occurrence of dust transport events and high PM_{10} concentrations are observed in 2007 (Fig. 6). Similarly, decreased occurrence of dust transport events and PM_{10} concentrations are observed in 2008-2011. However, correlation between dust transport events and PM_{10} concentrations can't be observed in 2012-2015 where lower dust transport events and high PM_{10} concentrations are observed. This is possibly due to high dust intensity (g m^{-2}) specially during spring, and a combination of increased local and regional natural and anthropogenic sources of PM_{10} (Flores et al., 2017).

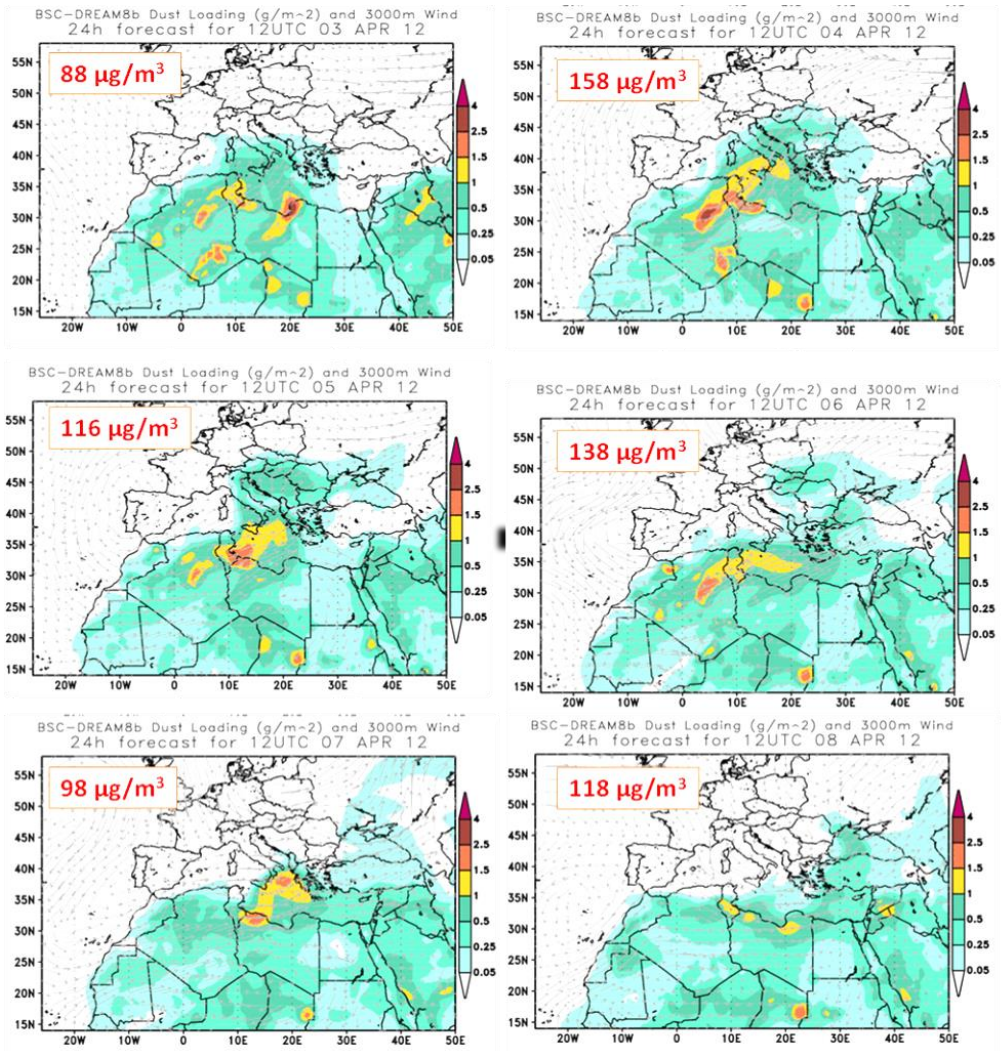


Figure 5. Identification of dust transport events with BSC-DREAM model

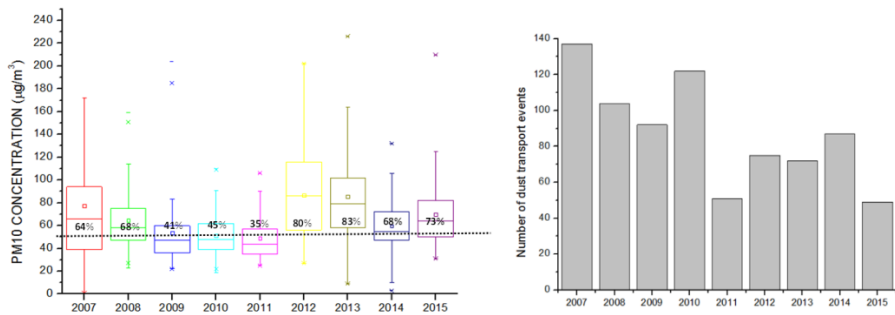


Figure 6. PM₁₀ concentrations (left) during dust transport events (right)

3.3. Influence of desert dust transport on surface PM₁₀ concentrations

Quantification of the impact of desert dust on surface PM₁₀ concentrations was performed with the reference EU method as explained in Section 2.4. On days without the influence of dust transport, PM₁₀ background concentrations were calculated at an urban background station with a 30-day moving percentile. These concentrations were then subtracted from daily PM₁₀ concentrations at the urban station to determine the net desert dust contribution to PM₁₀. Figure 7 shows the yearly PM₁₀ concentrations due to desert dust advectations in Istanbul during 2007-2014. The total percent contribution per year and per season are also observed in Fig. 7. Important contributions to the EU air quality standard attributed to desert dust transport were observed, particularly in 2009, followed by 2008 and 2010 with 72% and 41-42% of PM₁₀ concentrations due to desert dust transport, respectively. Yearly-averaged net desert dust concentrations ranged from 14 to 33 $\mu\text{g m}^{-3}$ in 2014 and 2009, respectively. These yearly-averaged PM₁₀ concentrations represent 22-72% of the yearly-averaged ground-level PM₁₀ concentrations observed in Aksaray, Istanbul.

Clear interannual variations were observed with a decreasing trend from winter (12-54 $\mu\text{g m}^{-3}$) to fall (9-37 $\mu\text{g m}^{-3}$) followed by spring (11-37 $\mu\text{g m}^{-3}$) to summer (4-20 $\mu\text{g m}^{-3}$) which are consistent with a stagnant atmosphere during the winter and the occurrence and intensity of desert dust transport events during the spring and summer. High concentrations during the fall observed in 2008, 2010, and 2011-2013 are caused by increased concentrations in months with prevailing northern winds, except in 2010 with high wind speed southern winds (Fig. 7). These northern and southern winds may be associated to transport from Asian and African deserts, respectively. High concentrations due to desert dust transport of 40-80 $\mu\text{g m}^{-3}$ were observed in Oct 2008 – Mar 2009. These high concentrations were due to a combination of (a) very strong dust transport events with net daily dust load of 0.26-8.97g m^{-2} that covered most of the Mediterranean Region and Europe, (b) strong winds (5.5 m s^{-1}) favoring dust transport to Istanbul, (c) high frequency (43%) of trajectories originating from the Sahara desert at 1500-2200 m effectively moving the dust to the surface, and (d) high frequencies (32%) of short air masses transporting the dust from 2000 m to the surface in Istanbul (Flores et al., 2017). Natural contributions from the African desert may have been enhanced in October and November 2008 with northerly winds with 55% frequency transporting dust from Asian deserts. According to forecasts from the BSC-DREAM8b model, approximately 8×10^6 g of dust were transported between October

2008 and April 2009 (Flores et al., 2017). This condition may be worsened by atmospheric stagnation typically observed during the winter seasons in Istanbul due to the formation of anticyclons (Tayanç, 2000). This analysis provides understanding of occurrence and intensity of dust outbreaks coupled to meteorological conditions that can be considerably worsened by local emissions and long range transport, for appropriate air pollution management strategies, especially in Megacities such as Istanbul.

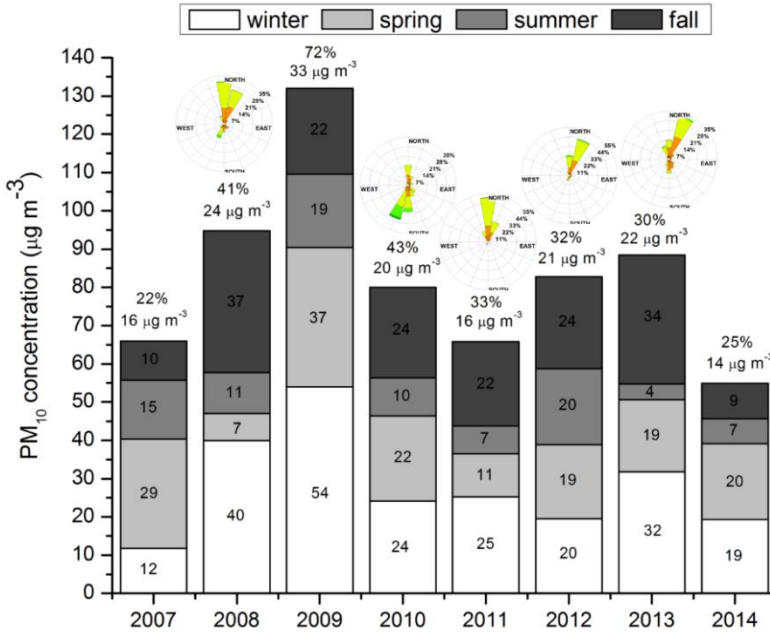


Figure 7. Net desert dust load contribution to surface PM_{10} concentrations at the urban station in Istanbul. Percent values indicate yearly-averaged contribution of desert dust to yearly-averaged surface PM_{10} concentrations. The numbers inside and on top of the columns indicate seasonal- and yearly-averaged PM_{10} concentrations due to desert dust, respectively. Wind roses are for selected months that contribute to high PM_{10} concentrations during the fall season as follows: Oct-Nov 2008, Nov 2010, Nov 2011, Sep-Nov 2012, and Oct-Nov 2013.

3.4. Aerosol optical depth and aerosol index

Daily-averaged aerosol optical depth and aerosol index were provided by NASA-GES DISC with GIOVANNI data analysis and visualization tool. AOD values <0.4 indicate average air quality or clean atmosphere. $AOD > 0.5$ indicate very hazy conditions with 74% extinction of solar radiation. In Istanbul, average AOD is 0.35, except in 2010, 2011, and 2015 with AOD ~ 0.41 . Less than 15% of the AOD is greater than 0.5, except in 2008, 2010, and 2015 with 20, 20, and 16% of the AOD > 0.5 , respectively (Fig. 8). High AOD are observed in February-May, which is when the most intense dust

transport events are found (Fig. 9). Low correlations were found between AOD, surface PM₁₀ concentrations, and dust load. This is due to the physical characteristics of the measurements, PM₁₀ concentrations are obtained at the surface, AOD are the result of the total column of aerosol, and dust loads are forecasted by the DREAM model at 3000 m. Aerosol Index is helpful to identify potential sources of aerosol that will be transported to Istanbul and their short them, seasonal, and long term variations. Figure 10 shows absorption of aerosols in Africa, Arabian Peninsula, and Asian deserts that span from Southeast to Southwest Istanbul and could enhance the already high local PM₁₀ concentrations.

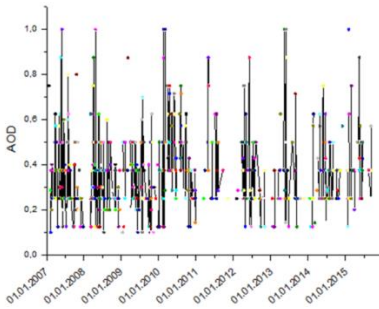


Figure 8. Monthly AOD Dark Target values

Day	ASRY PM10 (µg/m ³)	AOD (dimensionless)	Dust Load (g/m ²)
20-May-07	36	0.875	0.75
31-May-07	56	1.0	0.30
4-Apr-08	109	0.875	0.30
22-Apr-08	138	1.0	4.5
6-Mar-09	204	0.875	0.75
17-Feb-10	106	0.875	1.50
20-Feb-10	51	1.0	2.50
04-Mar-10	75	1.0	1.0
01-May-11	55	0.875	0.50
06-Jun-12	104	0.875	0.50
17-May-13	70	1.0	0.50
29-May-13	97	1.0	1.0
30-May-13	81	0.875	0.50
1-Feb-15	210	1.0	1.0
16-May-15	45	0.875	0.25

Figure 9. Correlation between PM₁₀, AOD, and Dust load during high AOD days

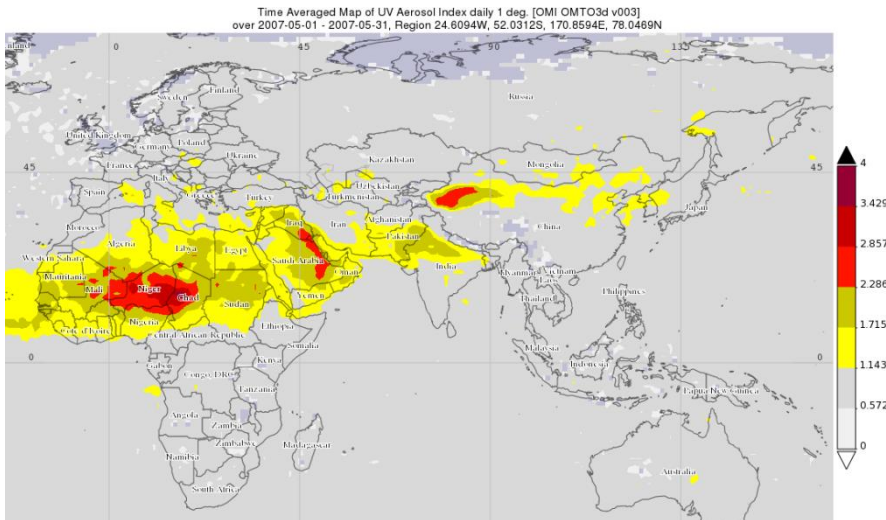


Figure 10. Identification of potential aerosol sources with Aerosol Index (May 2007)

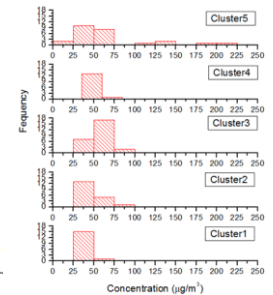
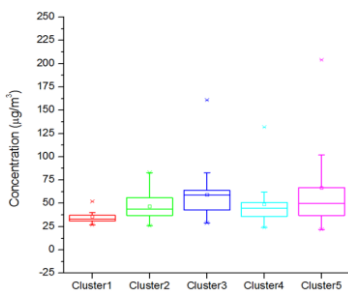
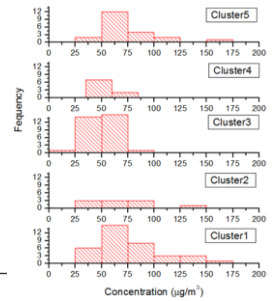
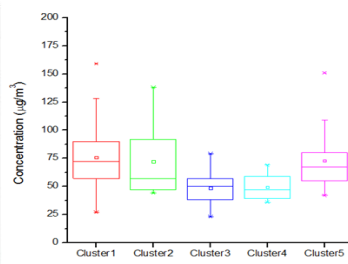
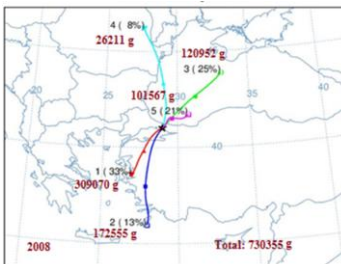
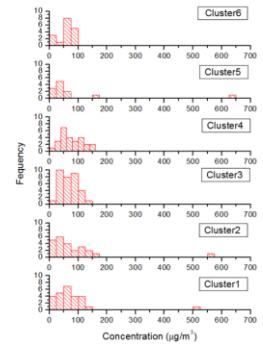
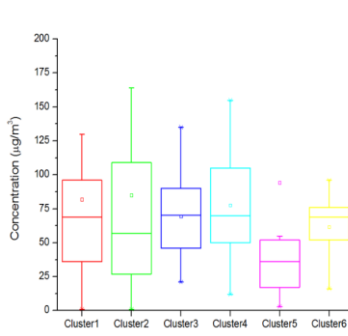
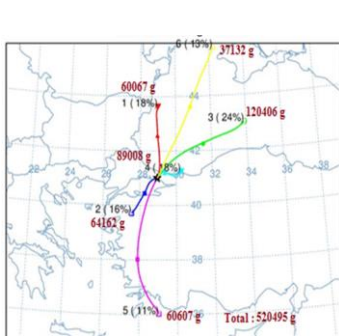
3.5. Cluster analysis

Air mass trajectories and cluster analysis were performed with the NOAA-HYSPLIT model. Overall, 5 mean air trajectories resolved over 75% of the total variation as follows (Fig. 11, Fig 12, left): North (6-18%), NNE (0-35%), NE (12-24%), short local trajectory (10-34%), SSW (0-33%), and S (11-33%). The air mass trajectories can be organized according to average air mass frequencies as follows: southern (38%) > local air masses (23%) > NE (20%) > N (10%) and NNE (8%). The most abundant air masses are also associated to important regional aerosol transport to Istanbul due to African and Asian dust advections (Fig. 10), which enhance PM₁₀ concentrations due to local anthropogenic sources.

Surface PM₁₀ concentrations and dust loadings were calculated according to each resultant cluster to obtain basic statistics (Fig. 11, Fig 12, middle), frequencies (Fig. 11, Fig 12, right), and total dust transported (g) to Istanbul (Fig. 11, Fig 12, left). The highest dust loadings in Istanbul observed in 2007 (520,495 g) and 2008 (730,355 g) are associated to air mass trajectory clusters from African (South) and Asian deserts (North East) and short air masses that recirculate winds in the Black sea region (Fig. 11). The occurrence of desert dust advection and dust loadings decreased in 2009-2011 (147,436 - 342,653 g) which are also consistent with decreased surface PM₁₀ concentrations (Fig. 6). 2010 showed relatively high concentrations compared to 2009 and 2011 due to higher frequency (34%) of air masses and high dust loadings (118,768 g) associated to African dust advection.

High frequencies of southern air mass trajectories (44-51%) were observed in 2012-2015, however, dust loadings from the African desert forecasted by the DREAM model decreased during these years. It is possible that high surface PM₁₀ concentrations observed during 2012-2015, and particularly in 2012-2013 are due to other natural or anthropogenic sources near the sampling site. As can be observed in Fig. 7, approximately 70% of the surface PM₁₀ concentrations in 2012-2013 is due to anthropogenic sources. Main anthropogenic sources of PM₁₀ in Aksaray may be emissions from private and public transportation, residential heating, and ship emissions (Deniz and Durmuşoğlu, 2008; Im and Kanakidou, 2012; Onat et al., 2013; Tayanç, 2000). In 2012, 44% of the dust load (88,735 g) transported to Istanbul is associated to cluster 2 which has southern trajectory and may be associated to African desert dust transport (Fig. 12). Cluster 2 is also associated to high frequencies of PM₁₀ concentrations as high as 125 µg m⁻³ and low frequencies of concentrations as high as 175 µg m⁻³. On the other hand, the highest concentrations in 2012 are associated to cluster 5 (21%)

followed by cluster 3 (16%) which may be associated to regional transport from Northeastern sources such as the Asian deserts and short trajectories that may recirculate local anthropogenic emissions, respectively. In 2013, similar behavior as 2012 was observed. The highest PM₁₀ concentrations of 250 µg m⁻³ were associated to cluster 2 which has a southern trajectory with frequency of 30%. Cluster 1 has short trajectory with frequency of 18% and is associated to high frequency of high PM₁₀ concentrations and also shows the highest averaged PM₁₀ concentrations in 2013 (100 µg m⁻³), which may be associated to local anthropogenic sources.



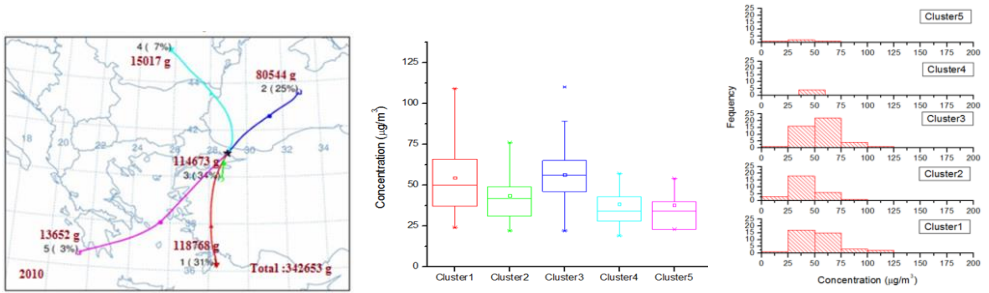
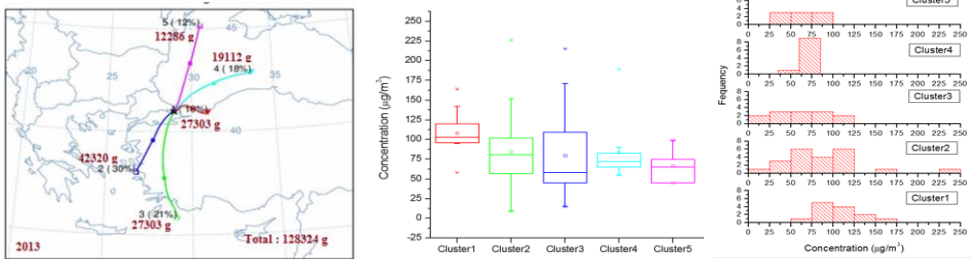
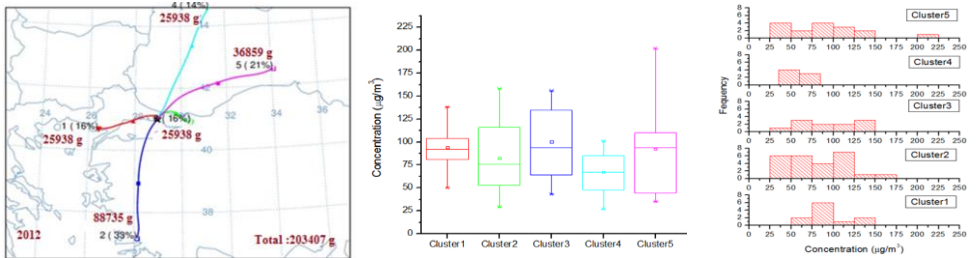
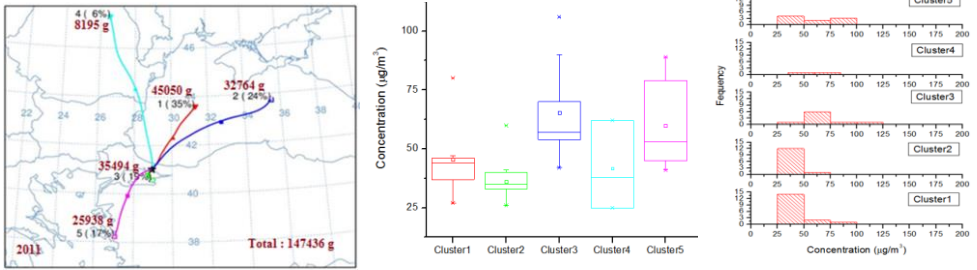


Figure 11. Mean air mass trajectories resulting from cluster analysis for 2007-2010 (left figure). Middle and right figures represent frequency analysis of surface PM₁₀ concentrations associated to each air mass trajectory cluster.



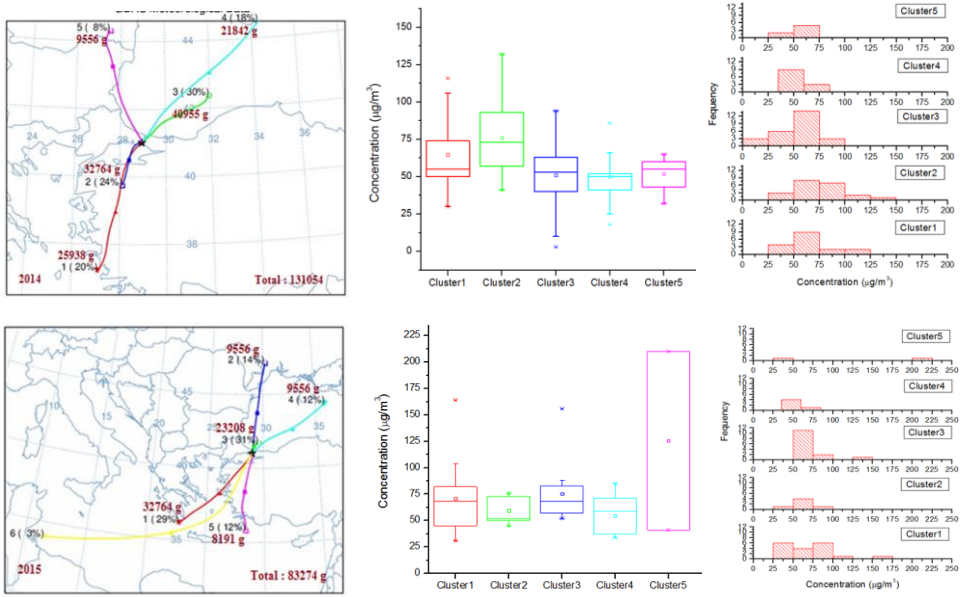


Figure 12. Mean air mass trajectories resulting from cluster analysis for 2011-2015 (left figure). Middle and right figures represent frequency analysis of surface PM₁₀ concentrations associated to each air mass trajectory cluster.

4. Conclusions

Important contributions of African desert dust to surface PM₁₀ concentrations in Istanbul were found. Particularly in 2008-2010, the contribution varied between 41% and 72%. The total number of mineral dust transport events ranged 49-137 during the study period. The largest number of mineral dust transport events was observed in 2007 and 2010. The highest ground-level PM₁₀ measurements were observed in 2007 and 2012-2013 with approximately 70% of the daily average concentrations exceeding the air quality standard of 50 µg m⁻³. Overall, 5 air mass trajectory clusters were able to resolve over 75% of the total spatial variance. These trajectories vary in frequency and direction throughout the years, however, the main trajectories favor aerosol transport from the African and Asian deserts. Increased surface PM₁₀ concentrations in 2012-2015 may be due to a combination of local anthropogenic sources in Istanbul and long-range transport of dust from African and Asian deserts. Evaluation of mineral dust loading and PM₁₀ concentrations is helpful for successful development and implementation of air quality management strategies on local levels, particularly in Megacities such as Istanbul.

Acknowledgements

The authors thank the following institutions: BAPKO (Bilimsel Araştırma Projeleri Birimi) at Marmara University for travel grant. Turkish Ministry of Environment and Urbanization for maintaining facilities and providing PM₁₀ concentrations. NASA, NOAA, and BSC for providing satellite data, backward trajectories, cluster analysis, and dust loading forecasts, respectively.

References

- Agacayak, T. *et al.*, A case study for Saharan dust transport over Turkey via RegCM4. 1 model, *Atmospheric Research* 153(2015), pp. 392-403.
- Aleksandropoulou, V., Lazaridis, M., Identification of the influence of African dust on PM₁₀ concentrations at the Athens air quality monitoring network during the period 2001–2010, *Res* 13(2013), pp. 1492-1503.
- Deniz, C., Durmuşoğlu, Y., Estimating shipping emissions in the region of the Sea of Marmara, Turkey, *Sci. Total Environ.* 390(2008), pp. 255-261.
- EC, Working Group on Particulate Matter. Commission Staff Working Paper: Establishing Guidelines for Demonstration and Subtraction of Exceedances Attributable to Natural Sources under the Directive 2008/50/EC on Ambient air Quality and Cleaner air for Europe. SEC 208 final, (2011).
- Escudero, M. *et al.*, A methodology for the quantification of the net African dust load in air quality monitoring networks, *Atmos. Environ.* 41(2007), pp. 5516-5524.
- Flores, R.M., Kaya, N., Eşer, Ö., Saltan, Ş., The effect of mineral dust transport on PM₁₀ concentrations and physical properties in Istanbul during 2007–2014, *Atmospheric Research* 197(2017), pp. 342-355.
- Im, U., Kanakidou, M., Impacts of East Mediterranean megacity emissions on air quality, *Atmos. Chem. Phys.* 12(2012), pp. 6335-6355.
- Im, U. *et al.*, Study of a winter PM episode in Istanbul using the high resolution WRF/CMAQ modeling system, *Atmos. Environ.* 44(2010), pp. 3085-3094.
- Karaca, F., Anil, I., Alagha, O., Long-range potential source contributions of episodic aerosol events to PM₁₀ profile of a megacity, *Atmos. Environ.* 43(2009), pp. 5713-5722.
- Karaca, F., Camci, F., Distant source contributions to PM₁₀ profile evaluated by SOM based cluster analysis of air mass trajectory sets, *Atmos. Environ.* 44(2010), pp. 892-899.

Kuzu, S.L., Saral, A., Demir, S., Summak, G., Demir, G., A detailed investigation of ambient aerosol composition and size distribution in an urban atmosphere, *Environmental Science and Pollution Research* 20(2013), pp. 2556-2568.

Lloyd, S., Acker, J.G., Prados, A.I., Leptoukh, G.G., Using NASA's Giovanni Web Portal to Access and Visualize Satellite-based Earth Science Data in the Classroom, (2008).

Onat, B., Sahin, U.A., Akyuz, T., Elemental characterization of PM_{2.5} and PM₁ in dense traffic area in Istanbul, Turkey, *Atmospheric Pollution Research* 4(2013), pp. 101-105.

Querol, X. *et al.*, African dust contributions to mean ambient PM₁₀ mass-levels across the Mediterranean Basin, *Atmos. Environ.* 43(2009), pp. 4266-4277.

Salvador, P. *et al.*, African dust contribution to ambient aerosol levels across central Spain: Characterization of long-range transport episodes of desert dust, *Atmospheric Research* 127(2013), pp. 117-129.

Stafoggia, M. *et al.*, Desert dust outbreaks in Southern Europe: contribution to daily PM₁₀ concentrations and short-term associations with mortality and hospital admissions, *Environ. Health Perspect.* 124(2016), p. 413.

Tayanç, M., An assessment of spatial and temporal variation of sulfur dioxide levels over Istanbul, Turkey, *Environ. Pollut.* 107(2000), pp. 61-69.

Theodosi, C. *et al.*, Aerosol chemical composition over Istanbul, *Sci. Total Environ.* 408(2010), pp. 2482-2491.

Viana, M. *et al.*, Assessing the Performance of Methods to Detect and Quantify African Dust in Airborne Particulates, *Environ. Sci. Technol.* 44(2010), pp. 8814-8820.

A 15 years view of Aerosol Dust over the Middle East

Saviz Sehatkashani¹, Sergio Rodríguez²
savizsehat@yahoo.com, srodriguez@aemet.es

¹ Atmospheric Science and Meteorological Research Center(ASMERC), Tehran, Iran

² Izaña Atmospheric Research Centre, AEMET, Tenerife, Spain.

Abstract

Main dust sources over the Middle East have been studied by analysing 15 years (2001–2016) of combination of the aerosol optical depth data - obtained using dark-target and deep blue algorithms measured by the Moderate Resolution Imaging Spectroradiometer (MODIS) - and gridded meteorological National Center for Environmental Prediction/National Center for Atmospheric Research (NCEP/NCAR) re-analysis data. The spatial distribution, potential sources, wind patterns and meteorological scenarios associated with dust events are examined. The spatial distributions present a considerable agreement with the wind field as well as reproduction of the characteristic seasonal dust features over the Middle East. Various atmospheric phenomena including synoptic, regional and local patterns influencing dust genesis include these four types, as shamal, frontal, northerly low level jet formation and convective dust storms over the region leading to different maximum dust seasonal cycle in different dust sources during the year.

Keywords: dust climatology, wind patterns, dust impacts.

Airborne Particulate Matter and Health in the Eastern Mediterranean Region

Mazen Malkawi

WHO Centre for Environmental Health Action (CEHA)

1. Health Impacts of Airborne Particulate Matter (PM)

The evidence on public health impact of PM is consistent in showing adverse health effects at exposures that are currently experienced in all countries of the World. The ranges of health effects are broad, but are predominantly to the respiratory and cardiovascular systems.

Health effects of ambient air pollution are a subject of intensive research in the last decades. One of the main findings is identification of the association of the risk of cardiovascular diseases, such as ischaemic heart disease or stroke and of lung cancer with long term exposure to fine particulate matter, i.e. airborne particles less than 2.5 μm in diameter (PM_{2.5}). Other studies show association of the incidence of respiratory disease and symptoms, including acute respiratory infections, as well as of mortality with short term exposure to suspended particulate matter less than 10 μm in diameter (PM₁₀). The risk increases with the exposure level but is seen also at relatively low concentrations, commonly observed even in relatively clean communities. Already in 2005, the WHO review of available evidence lead to formulation of WHO Air Quality Guidelines, recommending concentration of main pollutants which should be achieved to reduce significantly adverse effects of pollution on health¹. More recently, the review conducted by WHO concluded that the newly completed studies support and strengthen the conclusions of the WHO Air Quality Guidelines². These studies indicate that the effects occur, in some cases, at air pollution concentrations lower than those serving to establish

¹ Air Quality Guidelines – global update 2005. WHO 2016
http://www.euro.who.int/_data/assets/pdf_file/0005/78638/E90038.pdf?ua=1

² Review of evidence on health aspects fo air pollution – REVIHAAP. WHO 2013.
http://www.euro.who.int/_data/assets/pdf_file/0004/193108/REVIHAAP-Final-technical-report-final-version.pdf?ua=1

these guidelines. International Agency for Cancer Research classified ambient air pollution, and especially fine particulate matter, as substances causing lung cancer (Group 1)³. These reviews provide strong scientific arguments for taking decisive actions to improve air quality and reduce the burden of disease associated with air pollution.

Particles suspended in the air have diverse chemical and physical properties. Some are directly emitted from natural or man-made pollution sources, other are created from gases through chemical reactions occurring in the atmosphere. Aerodynamic diameter is an important parameter, determining the ability of particles with less than 10 μm diameter (PM₁₀) to penetrate to the lungs and of finer fraction (diameter less than 2.5 μm , PM_{2.5}) to get from the lungs to the bloodstream and other body organs and systems. Currently developed risk functions for particulate matter use mass concentration of PM_{2.5} or PM₁₀ particles, expressed in $\mu\text{g}/\text{m}^3$, as the universal indicator of exposure, independently of the chemical composition or sources of the particles mixture. An important research question concerns potential differences in the health risk due to various composition or sources of PM_{2.5} and PM₁₀. However, the research on this question is not providing definite answer if, and if yes, what, differences in the toxicity of various particle mixtures present in the atmosphere exist. Therefore risk assessment of PM_{2.5} and PM₁₀ uses the same set of concentration-response functions in settings with various pollution sources⁴.

2. Particulate Matter Air Pollution in the EMR

As indicated by the WHO Global Urban Ambient Air Pollution Database (update 2016)⁵ air pollution is increasing at alarming rates: The annual average concentration of particulate matter of 10 microns (PM₁₀) in Eastern Mediterranean (EM) Region is the highest in the world = 238 microgram/ m^3 (12 times the WHO recommended level). The annual average concentration of particulate matter of 2.5 microns (PM_{2.5}) in some

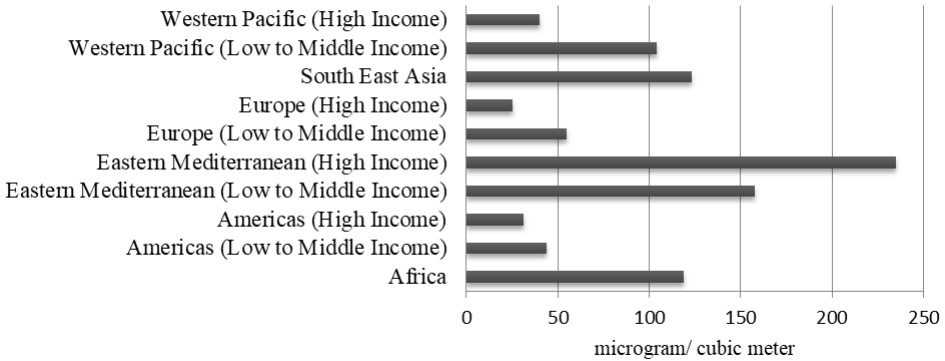
³ Loomis et al. The carcinogenicity of outdoor air pollution. The Lancet Oncology 2013; 14: 1262-1263

⁴ Review of evidence on health aspects of air pollution – REVIHAAP project. WHO 2013. http://www.euro.who.int/_data/assets/pdf_file/0004/193108/REVIHAAP-Final-technical-report-final-version.pdf?ua=1

⁵ http://www.who.int/phe/health_topics/outdoorair/databases/cities/en/

of the EM countries is 2-11 times the WHO recommended level.

PM10 levels for the last available in the period 2008-2015



The 2016 update of WHO’s Ambient Urban Air Pollution data base contains annual mean concentration of particulate matter in ca. 3000 cities worldwide. The data are compiled from official reporting from countries to WHO, official national/subnational reports, and national/subnational web sites containing measurements of PM10 or PM2.5 as well as from national or regional networks, international agencies or programs.

Out of the 22 WHO Member States belonging to the EM Region of WHO, data on particulate matter concentrations are available in the WHO AQ data base from 15 countries. PM10 was monitored in 82 cities or agglomerations with 202 monitoring stations. PM2.5 data come from 21 cities (mostly those where PM10 is also monitored) and 50 monitors.

According to the Database on source apportionment studies for particulate matter in the air (PM10 and PM2.5)⁶, a total of 419 source apportionment records from studies conducted in cities of 51 countries were used to calculate regional averages of sources of ambient particulate matter. Based on the available information, globally 25% of urban ambient air pollution from PM2.5 is contributed by traffic, 15% by industrial activities, 20% by domestic fuel burning, 22% from unspecified sources of human origin, and 18% from natural dust and salt. The situation in the EMR is somehow different from the global situation as more than 52% of urban ambient air pollution from PM2.5 is contributed by natural dust and sea salt, 12% by traffic, 27% by industry, and 9% from unspecified sources of human origin. There are two myths about the health effects of dust: myth 1: Dust particles are large and cannot reach the lungs. Analysis show that only 50%

⁶ http://www.who.int/quantifying_ehimpacts/global/source_apport/en/

of particulate matter is larger than 10 μm (non-inhalable), while about 45% of PM are coarse between 2 and 10 μm (inhalable), and the rest 5% of PM are fine less than 2 μm (penetrate deeply)⁷. Myth 2: Dust composition is similar to that of natural soil, therefore is not toxic. Airborne PM is a mixture: Minerals (e.g., SiO_2 , Al_2O_3 , CaO), Metals (e.g., Fe), Bio-aerosols (e.g., pollen, fungi, bacteria), and Anthropogenic pollutants⁸. Unfortunately partial toxicity of this mixture is not well understood. WHO is currently reviewing the available evidence on this critical issue.

Air pollution with particulate matter is killing more than 200,000 people annually in our Region.

3. Air pollution with particulate matter is a major risk to public health in the Eastern Mediterranean Region⁹

Particles suspended in the air have diverse chemical and physical properties. Some are directly emitted from natural or man-made pollution sources, other are created from gases through chemical reactions occurring in the atmosphere. Aerodynamic diameter is an important parameter, determining the ability of particles with less than 10 μm diameter (PM₁₀) to penetrate to the lungs and of finer fraction (diameter less than 2.5 μm , PM_{2.5}) to get from the lungs to the bloodstream and other body organs and systems. Currently developed risk functions for particulate matter use mass concentration of PM_{2.5} or PM₁₀ particles, expressed in $\mu\text{g}/\text{m}^3$, as the universal indicator of exposure, independently of the chemical composition or sources of the particles mixture. An important research question concerns potential differences in the health risk due to various composition or sources of PM_{2.5} and PM₁₀. However, the research on this question is

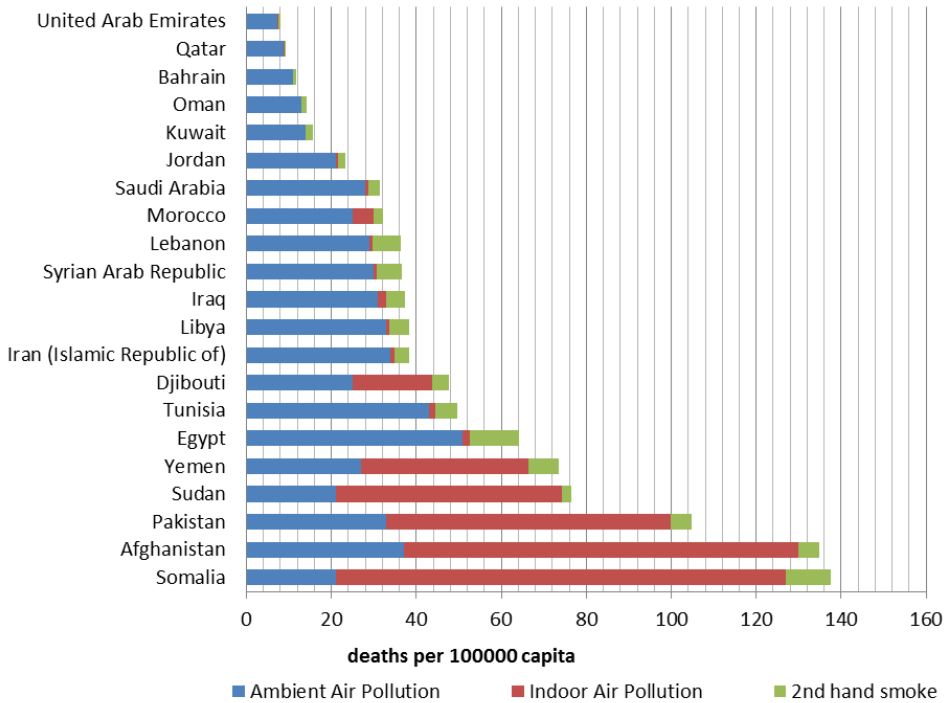
⁷ Goudie, Andrew, Middleton, Nicholas J.; *Desert Dust in the Global System*, Springer, 2006

⁸ Krueger, B. J., V. H. Grassian, J. P. Cowin, and A. Laskin (2004), Heterogeneous chemistry of individual mineral dust particles from different dust source regions: The importance of particle mineralogy, *Atmos. Environ.*,

38, 6253– 6261.

⁹ The Eastern Mediterranean Region includes 22 countries, namely: Afghanistan, Bahrain, Djibouti, Egypt, Iran, Iraq, Jordan, Kuwait, Lebanon, Libya, Morocco, Oman, Palestine, Pakistan, Qatar, Saudi Arabia, Somalia, Sudan, Syria, Tunisia, United Arab Emirates, and Yemen

not providing definite answer if, and if yes, what, differences in the toxicity of various particle mixtures present in the atmosphere exist. Therefore risk assessment of PM_{2.5} and PM₁₀ uses the same set of concentration-response functions in settings with various pollution sources¹⁰. The most recent global analysis of health risks of ambient air pollution has been conducted by WHO in 2016 for 2012¹¹. Available estimates indicate that: more than 200,000 premature deaths could be attributed to outdoor air pollution.



¹⁰ Review of evidence on health aspects of air pollution – REVIHAAP project. WHO 2013. http://www.euro.who.int/_data/assets/pdf_file/0004/193108/REVIHAAP-Final-technical-report-final-version.pdf?ua=1

¹¹ Burden of disease from ambient air pollution for 2012. Summary of results. http://www.who.int/phe/health_topics/outdoorair/databases/AAP_BoD_results_March2014.pdf?ua=1

4. Gaps and Challenges

WHO/EMRO/CEHA systematically reviewed the available information on air quality and health in the region during the period 2000-2017¹². The following gaps were identified:

- lack of available data and communication mechanisms;
- poor commitment; and
- poor coordination between the different related sectors.

UNEP surveyed in 2015 policies and actions that effect air quality in all countries of the world including the 22 countries of the Region. Detailed profiles based on these surveys were prepared and published online¹³. These profiles show that:

- There is clear lack of data and information in almost all countries of the region; and
- Air quality management actions and polices are still far below the levels that controls air pollution in the Region. This is also complicated by absence of information on health impacts of air quality and health at national and provincial levels.

5. WHO Air Quality Guideline update

WHO commissioned a systematic review on the health effects of desert and sand dust (ongoing). This is being done in recognition of the importance of understanding the specific health effects of desert dust, and need for more evidence to support risk assessment. The outcome of this review will be used to update the WHO guidelines on air quality and health with a clear recommendation on the health effects of desert dust. This recommendation will be relevant for countries to move towards mitigation and adaptation measures in relation to desert dust.

¹² Air pollution and health outcomes in the Eastern Mediterranean Region: Knowledge and Research Gaps and Needs: Expert consultation for finalization a regional plan of action for th implementation of the WHO global raodmap for addressing air quality and health, Amman, Jordan, 24-25 May 2017

¹³ UNEP Air Policy Catalogue <http://apps.unep.org/repository/coverage/country>



6. Recommendations of the DSD Working Group

- Need for desert dust assessment and forecasting (lead WMO SDS-WAS);
- Need for standardization of time-series studies on desert dust health effects, i.e. Standard Operating Procedures with minimal requirement
- Existence of local AQ monitoring network measuring PM₁₀ /PM_{2.5} & dust characterization
- Sound morbidity/ hospitalization/ mortality records providing counts of daily health events
- Standard definition of desert dust episode
- Identification of research gaps in the existing assessments (e.g. long term studies on DSD effects, effectiveness of exposure reduction measures)

Evaluation of the Precipitated Desert Dust Effects on the Socioeconomic Activities of the Southeastern Anatolia Region

Dr. M. Taner ŞENGÜN¹, Dr. Harun Reşit BAĞCI²

¹ Firat University, Department of Geography, Elazığ, Turkey, mtsengun@gmail.com

² Ondokuz Mayıs University, Department of Geography, Turkey, hrbagci@gmail.com

Abstract

The effects of natural environment elements on social and economic activities constitute the main field of study of the Geography science. Daily life and economic activities of people living in the regions that are close to the deserts and exposed to desert dust transportation through winds are affected by the desert-derived dusts. This has caused the subject of desert dusts studied primarily by environmental, meteorological and chemical engineers to be included in the area of interest of the Geography science, and the source zones of the desert dusts, their modes of transportation and routes as well as their effects on natural environmental and human factors in the areas where it is dominant have been started to be evaluated in terms of geographical point of view.

In this study, it is aimed to reveal the effects of the desert dust on socio-economic activities on the basis of Adıyaman, Diyarbakır and Şanlıurfa provinces selected from the Southeastern Anatolia which is the region most effected by the desert dust transportation in Turkey. For this purpose, the sources of dusts transported to these provinces and the distribution of dust transportation by months and seasons have been determined by using Satellite images and data obtained from the Turkish State Meteorological Service. Some samples have been taken from the surfaces where the dust settled and then, related analyzes have been carried out by XRF method, thus the elemental structure of the desert dust has been determined. In the sample provinces, the local people have been subjected to interviews and the diseases triggered by the desert dusts have been tried to be determined by examining the data obtained from the Provincial Directorates of Health and hospitals. Besides, the connections of the desert dusts with human and economic activities such as agriculture, transportation, energy production and tourism have been tried to be explained in many ways.



As a result of the study, it is understood that there are heavy metals such as aluminium, chromium, nickel and zinc inside the desert dust particles settled with the precipitation or as dry and that the desert dusts lead to contamination in natural and human environments and cause deterioration and energy loss in ventilation and energy systems. It is determined that when the desert dust transportation is intense, there are problems in air, road and sea transportation and that there are significant increases in the number of people who apply to the outpatient clinics due to chronic respiratory diseases such as asthma and bronchitis. Besides, the fact that the weather is overcast and dirty on dusty days obstructs many touristic and sporting activities organized outdoors and this also causes psychological problems in the local people.

Keywords: *Desert dust, Southeastern Anatolia Region, Socio-economic activity, Heavy metal, Respiratory tract diseases.*

Sand Dust Storms Source Identification and the Mineralogical and Micro-Organisms Effects of Regional Dust Storms - Middle East Region

Moutaz Al-Dabbas¹, Mohammed Ayad Abbas² and Raad Al- Khafaji³

¹ Science college, Uni. of Baghdad, Iraq, profaldabbas@yahoo.com

² Medical City, Ministry of Medicine, Baghdad, Iraq.

³ Education College (Ibn Al-Haitham), University of Baghdad, Iraq.

Abstract

The blowing regional dust storms over Iraq and the Middle East were studied (identified by satellites images), from March 2007 to July 2010, the total studied dust storms were 47 (seven in 2007, twenty in 2008, eleven in 2009 and nine in 2010). The collected dust samples, in the middle and south Iraq, were from Baghdad, Ramadi, Kut, Basra, Najaf, Karbala, Hilla and Sallahaldin. Grain size, shape and mineralogical analyses were determined. Analyses of the heavy elements were performed to determine the heavy metals (Pb, Zn, Cd, Ni, Cu, Co and Fe) concentration. Pollen analyses were performed as well, to identify the pollen concentration in the dust samples. Microorganism's analyses methods for bacterial, fungal, and viral isolates were done. The average means annual rainfall (mm) indicate an increase of the number of days / years of the dust storms reflected the effect of the regional climatic change. The particle size analyses indicate the texture most of samples are ranging from sandy clayey silt (72 %), and clayey sandy silt (28 %). The result of roundness of quartz grains, (20 % rounded, 80 % sub rounded). The clay minerals (Chlorite, Illite, Montmorillonite, Palygorskite and Kaolinite) were recognized. The analyses of heavy minerals percentages by using the microscope were done. The results of pollen distribution, in descending order, were Chenopodiaceae, Gramineae, Pine, Artemisia, Palmae, Olea and Typha, (reach 83%, 70%, 65%, 50%, 15%, 10% and 5% of the counted pollen grains, respectively). The results of microorganism (i.e. isolated bacteria and fungal), in descending order, were the gram – positive *Bacillus* species (40.6 %), *Aspergillus* species plus *Candida albicans* (14.5%), and (7,7%) respectively, the gram-negative rods, *Escherichia coli* (8.4%), the gram-positive *Cocci streptococcus pneumonia* (7.4%), than the gram-negative rod *Enterobacter Cloacae* (5.8%), *Staphylococcus epidermidis* and *Staphylococcus* (4.2%) and (2.6%), respectively. The remaining Gram -negative microorganisms were *Pseudomonas aeruginosa* (2.9%). Regarding the viral etiology; there

is no any viral isolate among the work results. The Uranium concentration average absorbed dose and average external effective dose were calculated for dust storms for both Baghdad and Ramadi. The specific activity of uranium were in range of (5.43-9.56 Bg/kg) and the absorbed dose range (2.19- 5.46 nGy/h) for dust storm at 2-4/7/2009 and the average specific activity of uranium ranging from 7.32 to 18.96 Bg/kg and the average absorbed dose (3.27- 8.98 nGy/h) for dust storm of 3-4/4/2010. All the results were lower than critical dose level, but the culmination of the dose of more than one duststorm may have a damage effect..

Keywords: *Dust Storm, mineralogy, pollens, microorganisms, Radioactive Characteristics.*

1. Introduction

Dust and sand storms are persistent problem in Iraq and Middle East Region. The regional dust storms had bad effects on health of human life which can cause asthma, bronchitis and lung diseases, due to their carrying micro-organisms (such as bacteria, fungi, spores, viruses and pollen), and their sharp edged particle. Several researches have shown that microorganisms mobilized into the atmosphere along with desert soils are capable of surviving long-range transport on a global scale. Dust-borne microorganisms in particular can directly impact human health via pathogenesis, exposure of sensitive individuals to cellular components (pollen and fungal allergens, etc.) and the development of sensitivities (i.e., asthma) through prolonged exposure. The chemical components of dust are affecting the microbial life beside the precipitation, wind direction, time of day, season and atmosphere inversion conditions, all affecting the survival of total culturable bacteria associated with dust particles and the microbes were capable of surviving long distance transport, (Cook, et al., 2005, Garrison et al., 2006, Martiny, et al., 2006). Several studies conducted to investigate the role of dust storms that consists of concentrated crustal particulates have shown an associated allergic, asthma, and silicosis/pulmonary fibrosis risk. Areas impacted by desert dust storms, such as communities in the Middle East, were known to have some of the highest incidences of asthma on the planet, as it was determined that the incidence of asthma increased between 1973 and 2004, due to the increasing dust storms in the Middle East region, (Prospero, 1999). Allergens commonly associated with dust storms include fungal spores, plant and grass pollens, anthropogenic emissions, and organic detritus. *Aspergillus* species is a common soil fungus which was the first pathogen to be identified and proven to cause disease. Moreover, long-range transport

of human influenza virus could occur in the winter months given the prevailing wind pattern and the low dose of virus required for infection, Pneumonia from dust storm exposure has also been reported in the Middle East, especially those cases pertaining to deployed military personnel (Ezeamuzie, et al. 2000, Middleton , 2001, Shoor, et al., 2004, Poschl , 2005, Delfino, et al, 2005, Lohmann, and Feichter, 2005, Griffin, 2007, Griffin, et al., 2007, UNEP, WMO, UNCCD., 2016).

Exposure to uranium and its compounds can cause adverse health effects due to its chemical toxicity and radiologic hazard caused by absorption of radiation emitted from uranium and its decay products. At high levels, uranium may cause chemical toxicity. The low level of radioactivity emitted causes less concern. Exposure to uranium and other heavy metals in large doses can cause changes in renal function, resulting in renal failure, (7,8,9,10,11).

The aims of this research were to study the regional dust storms that blowing over Iraq and the Middle East by using satellites images and GIS Technology. Also, to study the effect of climatic change, source of materials of regional dust storms by analyzing the heavy, light, clay minerals, trace metals, grain size analyses, pollen and the microorganisms include, the bacteria, fungal, viruses and their effect. As well as , to study the radioactive characteristics of dust from sand storms that occurred over Baghdad and Ramadi cities, middle of Iraq, from February 2009 to July 2010, to measure the Uranium concentration average absorbed dose and average external effective dose for dust of sandstorm for both cities Baghdad and Ramadi.

2. Methodology

The dust samples were collected for the period from March 2007 to October 2008 from many IRAQI governorates, Figure 1. The total number of studied dust storm was 27 during (2007-2008), 7 in 2007, and 20 in 2008, Table 1. The collected dust storms samples were from Baghdad (312), Ramadi (77), Kut (46), Basra (33), Najaf (28), Karbala (21), Hilla (27) and Sallahaldin (4) samples. The samples were collected from the roof of high buildings by using either big volume plastic basins, or by using the cyclone, with 1.65 meter high by rotating the air inside the instrument using an electrical motor to pull & suck the air inside the instrument (Al- Khafaji, 2009).The following analysis had been preformed for the collected dust samples:

Method Number One: Grain size and Shape analyses:

Grain size & Shape analyses were performed by using the sieve and pipette technique (Power, 1953, and Folk, 1974).

Method Number Two: Mineralogy analysis:

The mineralogy of dust samples were determined by applying Carver, 1971, method to study the light minerals & heavy minerals, also the mineralogy of dust samples were determined by X-Ray diffraction method as well.

Method Number Three: Analyses of the heavy elements:

Analyses of the heavy elements were performed to determine the heavy metals (Pb, Zn, Cd, Ni, Cu, Co, Fe) concentration in the dust samples by using the atomic absorption spectrophotometer (AAS).

Method Number Four: Pollen analyses: Pollen analyses were performed to identify the Pollen concentration in the dust samples according to Moore, and Webb, 1978, procedure.

Method Number Five: Microorganisms Analyses:

Microorganism's analyses were performed to identify Bacteria, fungi and Viruses analyses according to the international methods for microorganisms analyzed (Al- Khafaji, 2009).

Method Number Six: Radioactive Characteristics: The Uranium concentration average absorbed dose and average external effective dose were calculated for dust of sandstorm at 2-4/7/2009 and 3-4/4/2010 for both cities Baghdad and Ramadi, according to Mahdi ,et al,2011 and Marouf,2012, methods.

Table 1. The studied regional dust storms over Iraq for the years (2007-2010)

No.	Date of dust storm	No.	Date of dust storm	No.	Date of dust storm
1	17-3-2007	17	7-6-2008	33	17-6-2009
2	18-4-2007	18	15-6-2008	34	28-6-2009
3	11-5-2007	19	28-6-2008	35	2-7-2009
4	16-5-2007	20	1-7-2008	36	4-7-2009
5	8-7-2007	21	7-7-2008	37	29-7-2009
6	16-7-2007	22	11-7-2008	38	30-7-2009
7	7-9-2007	23	27-7-2007	39	3-4-2010
8	19-2-2008	24	30-7-2007	40	4-4-2010

9	3-3-2008	25	15-9-2008	41	13-5-2010
10	15-3-2008	26	24-9-2008	42	14-5-2010
11	30-3-2008	27	16-10-2008	43	6-6-2010
12	4-4-2008	28	17-2-2009	44	23-6-2010
13	17-4-2008	29	20-2-2009	45	24-6-2010
14	27-4-2008	30	27-2-2009	46	19-7-2010
15	16-5-2008	31	9-3-2009	47	20-7-2010
16	25-5-2008	32	9-6-2009		

3. Results and Discussion

1. Climate:

Data of 44 meteorological stations records the climatic elements within Iraq were studied ,such as types of dust, and the Average Mean Annual Rainfall for the years 1968- 2010 (Iraqi Meteorological Department, 2012) .

A - The Average Mean Annual Rainfall:

The Average Mean Annual Rainfall were analyzed and the trends show remarkable decrease in the average mean annual rainfall (in mm) with time that may reflect the regional climatic change (Figures 1, 2, 3, and 4).



Figure 1. The Average Mean Annual Rainfall - Baghdad (1971-2000) (Iraqi Meteorological Department, 2012).

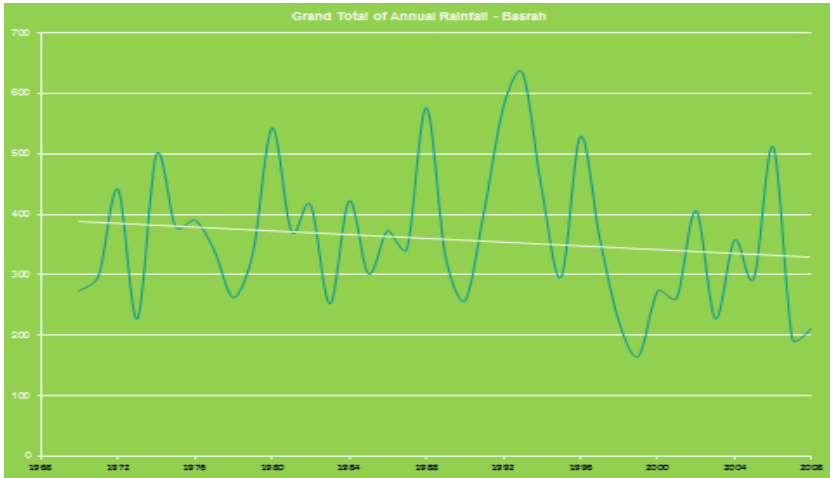


Figure 2. The Average Mean Annual Rainfall - Basrah (1971-2000) (Iraqi Meteorological Department, 2012).

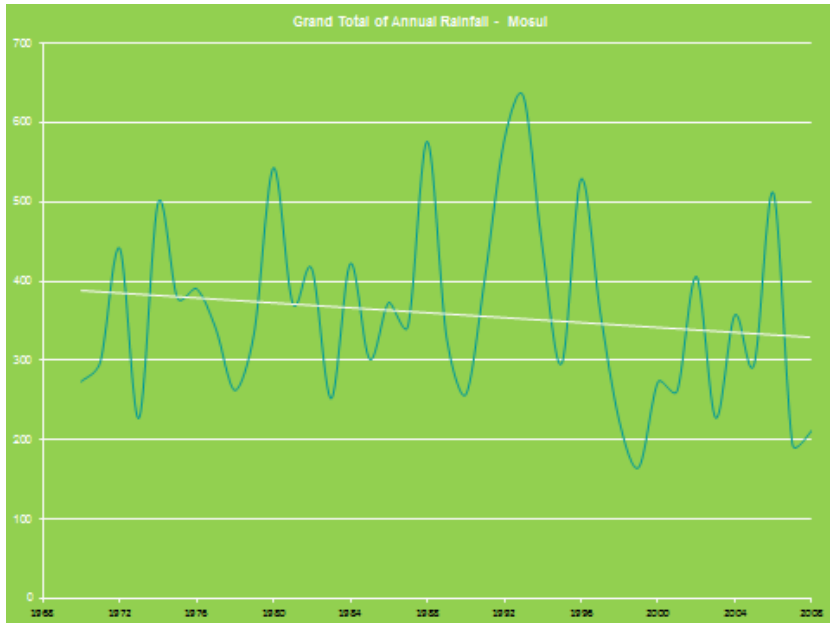


Figure 3. The Average Mean Annual Rainfall - Mosul (1971-2000) (Iraqi Meteorological Department, 2012).

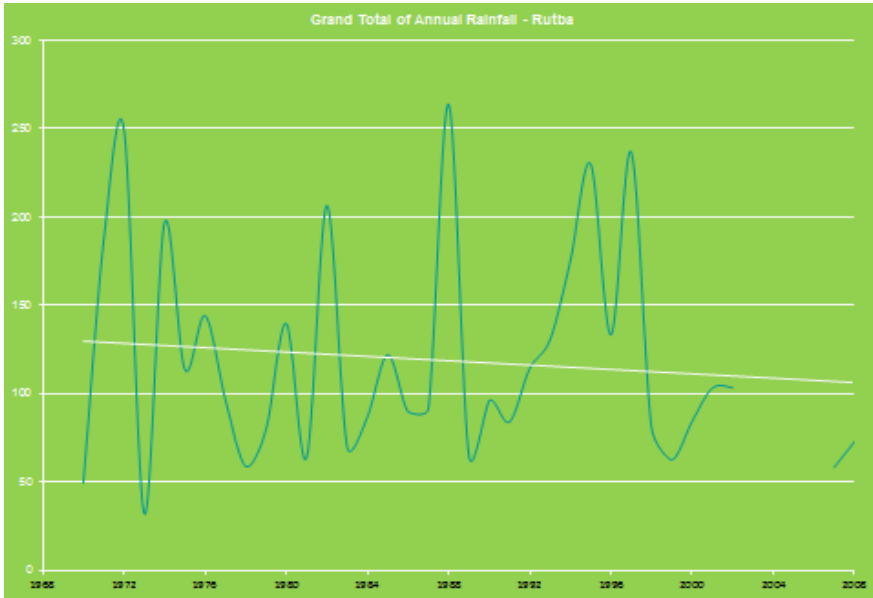


Figure 4. The Average Mean Annual Rainfall - Rutba (1971-2000) (Iraqi Meteorological Department, 2012).

B - Dust Storms

The mean annual number of days with dust storms that distributed over Iraq for seventies years and for millennium were compared (Figures 5 and 6) (Iraqi Meteorological Department, 2012).

The results indicated that Baghdad was within 5-10 numbers of days with dust storms during the seventies that increased to 10-15 numbers of days with dust storms during the millennium years(Figures 5 and 6) .

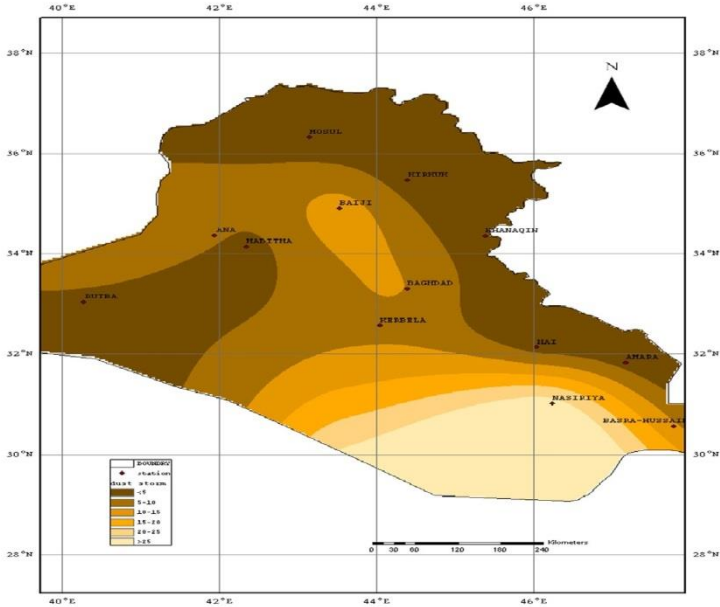


Figure 5. Mean annual number of days with Dust storms that distributed over Iraq for seventies (Iraqi Meteorological Department, 2012).

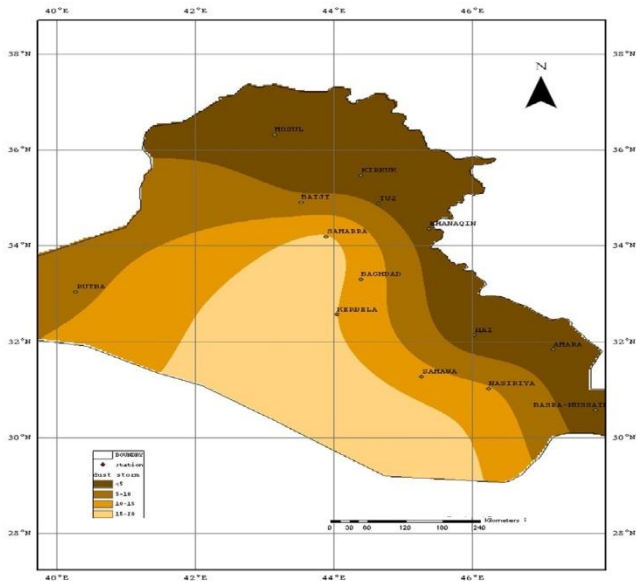


Figure 6. Mean annual number of days with Dust storms that distributed over Iraq for millennium (Iraqi Meteorological Department, 2012).

C - Sand Dust Storms (SDS) Sources

The dust sources were identified over Iraq performed by different authors (Bolorani, et al., 2012 and Alonso-Pérez, et al., 2013) using satellite imagery and other satellite remote sensing data are depicted in Figure 7 .

Three main dust hot point sources were recognized:

1. The Jazera area: This area located in the north west of Iraq and the east of Syria was specified as the main source of dust storms .
2. The Iraqi, Jordanian Syrian borders: that represents parts of Iraqi western desert, parts of Jordanian and Syrian eastern deserts.
3. The Mesopotamian plain of Iraq.

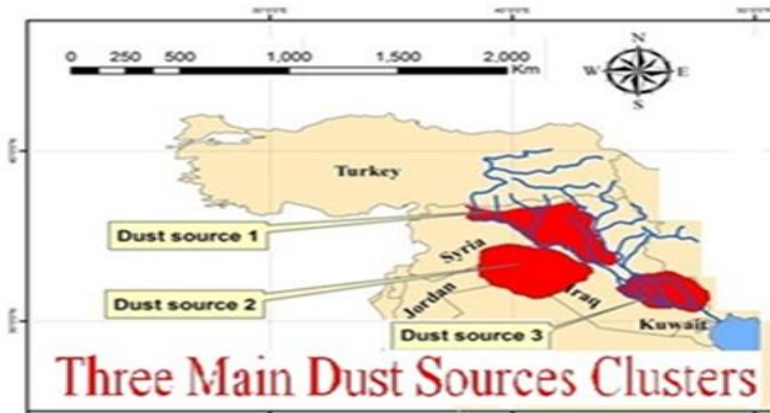


Figure 7. Sand Dust Storms (SDS) Sources over Iraq reflect three dust sources, 1) The Jazera area, 2) The Iraqi, Jordanian Syrian borders and 3) The Mesopotamian plain of Iraq (after Bolorani, et al., 2012 and Alonso-Pérez, et al., 2013).

2-The Size and Shape of Dust Samples:

The results of the particle size analyses indicate that the dust samples composed mainly of Silt (Min.=41%, Max.= 62%, Mean=53%), Clay (Min.=22%, Max.= 30%, Mean= 28%) and Sand (Min.=10%, Max.= 25%, Mean= 19%). However, the texture of samples is ranging from the higher percentages of sandy clayey silt (72%), to the relatively less common clayey sandy silt (28%). The most of dust texture are clay and silt with less quantities of sand.

The roundness of Quartz (reach more than 80% of the sand fraction), in the dust storms samples was studied. The results reflect that the roundness

were mostly ranging from sub-rounded grad of roundness, (80% of all the studied samples), to Rounded grad of roundness, (20% of all the studied samples), that reflect long distance of transportation.

3-The Mineralogy of Dust Samples:

Light and heavy minerals of Dust Samples for sand size fraction were studied by using polarized microscope. The result reflects that the light minerals reach 98% of the sand fraction, while the heavy minerals equal to 2% as a maximum. The light minerals quartz, feldspars, calcite, with little amount of gypsum were recognized. The results of heavy minerals analyses indicated that the highest percentage were opaque heavy mineral, pyroxene, garnet, hornblende, zircon, chlorite, epidote, staurolite, celestite and biotite. The carbonate minerals were studied separately from the bulk dust samples, the result reflect that the carbonate ranging from 4.3% to 53.2 %, with an average 12.1% Carbonate of the total dust samples. The palygorskite, Illite, Kaolinite, chlorite, Montmorillonite, Smectites clay minerals are recognized by X-Ray diffraction method (XRD). The presence of Palygorskite and Kaolinite among the clay minerals reflects the arid and semi-arid climatic conditions. The formation of chlorite mineral reflects arid and semi arid climate with alkaline environment, while, the Illite minerals are very common in desert soils (Al-Dabbas, et al., 2011 and 2012).

4-Toxic Trace Elements Analyses and Their Effect:

Suspended solids are important pollutions which consist of suspended minerals and other suspended solids such as soil, wash off plowed fields, and fertilizers. Inorganic trace elements are commonly present at low levels in nature and there is already a natural level of tolerance. These trace elements pose a threat to human health. Therefore, trace elements should be a priority for evaluation in all dust storms studies. In the present research, seven heavy metals concentration (Pb, Fe, Cu, Co Cd, Ni and Zn) were analyzed by using atomic absorption method, from 47 samples of dust storms which have been collected from many regions of Iraq. It is expected that the heavy metals concentration were varies considerably with the polluted, industrial and contaminated areas, depending on the wind speed and directions. The results reflect that the mean concentration of trace metals of all studied stations are shown in descending order from the highest values, Fe (1419.7 ppm), Pb(226.3



ppm), Zn(209 ppm) , Ni(126.5 ppm), Cu(53ppm) ,Co(39.5ppm) and finally the lowest values of Cd (24ppm) ,while ,their minimum, maximum, and health effects are discussed as follow:

The maximum high value of Fe was in Basrah (2937 ppm) and minimum low value was in Hilla (472 ppm), with the mean concentration of Fe 1419.7 ppm. The iron element is an important to human body and non harmful, it enters in metabolism for human and animals but its increment above the allowed level will be harmful to health which means if level increases over (0.3 Mg/ L). The maximum value of Pb was indicated in Basrah (432 ppm) and minimum low value was in Hilla (149 ppm), with the mean concentration of Pb 226.3 ppm. This element causes stimulation to bronchial mucosa of respiratory system which results cause of allergy and asthma. If it reaches to narrows system through food and drink will result to headache, fatigue and causes bone weakness if its rate increases in human body. The Pb vapors resulting from fuel compounds because of full burn evaporation will complexes in the environment through the vapors produced from cars which get bad negative effects on living bodies. The human body may take the lead through air which ranges between less than (4 Mg /day) and more than (200 Mg/ day) according to area where he lives. The maximum value of Zn was shown in Basrah (374.7 ppm) and minimum low value in Karbala (148 ppm), while, the mean concentration of Zn 209 ppm. Zinc element enter in food metabolism for both plants and animals, zinc regarded important to human growth and animal growth especially in first steps of growth and advances in spite of the need amount is very few decrease of this amount will cause bone damage and damage to skin fertility .Decrease rate of zinc in males will be going with cardiac chronic diseases (Specially arterial). The maximum Ni value was determined in Baghdad (203.1 ppm) and minimum low value in Najaf (58 ppm), with the mean concentration of Ni 126.5 ppm. Nickel element has bad effects on human and cause bronchial carcinoma or Nasal Carcinoma due to nickel gasses . The nickel carbonate (Ni) which results from interaction with carbon monoxide producing complex which is carcinogenic to human and animals which result in respiratory system rapid damage its large doses cause many health affection like infection of other layer of skin beside it effect kidneys and causes vertigo , bronchitis , Asthma .The maximum high value of Cu was reflected in Ramadi (96.2 ppm) and minimum low value in Najaf (29 ppm) with, the mean concentration of Cu 53 ppm. The Copper element is one of the non important elements to human body and will be poisonous if its rate increases. Usually Cu damage

effect will not be oriels present in plenty food because it has high rates in swage substances used for plants, its increment through plants in the human blood and liver tissues will cause the Wilson disease which results in changes in tissues of brain and liver and ophthalmic cornea.

The maximum of Co value was indicated in Basrah (89.6 ppm) and minimum low value in Najaf (12.2 ppm), with the mean concentration of Co 39.5 ppm. Cobalt element is important for human and animals, because it enters in chemical construction of hemoglobin. If cobalt rate decreases it will effect the oxygen transport through hemoglobin but its increase rats will cause disturbances in some important orgasm. The maximum value of Cd was shown in Basrah (61 ppm) and minimum low value in Najaf (8 ppm) with the average mean concentration of Cd 24 ppm.

The cadmium element will be absorbed easily through respiratory and gastro intestinal system in human, when reaches blood will distribute quickly through human tissues like liver, kidneys will take place the useful elements to human body which prevents their absorption through intestine, and this element will increase the effect of Anemia, (Al- Saad and Abed, 2006). Cadmium poisoning result damages the kidneys and hypertension and takes place the calcium. It has accumulative effect to human body and cause bony damage. The highest level allowed for cadmium in air is (0.05 Mg/m³) (Hodges, 1973, WHO, 1996, and 2004).

5-Palynological Analysis:

The dust samples for the pollen grain analysis were collected from many dust storms and many governorates. Accordingly, the results of the studied dust storms samples of Baghdad, Najaf, Ramadi, Wasit, Babel, Basra, and Karbala and Sallahaldin ,reflect that the relatively highest percentages of the pollens are Chenopodiaceae, Graminea, Pine, Artemisia, Palmae, Olea and Typha,(that reach 83%,70%, 65%,50%,15%,10% and 5% of the counted pollen grains from the total studied slides , respectively), with miscellaneous Palynomorphs Cuticle, Fungi, Algae, Lycopodium spores, Sphagnum spores, Unnamed spores and Micro Spines(that reach 80%,60%,20%,75%,8%,6% and 20%, of the counted pollen grains from the total studied slides , respectively),(Table 2). Such results may give good evidence of the regional dust storms that originated in far away places as indicated by the pine pollens that have sacs to keep pollen afloat and carried to great distances by the wind, as it could be from northern Syria , Turkey or transported from the countries near to Iraq which have the same

climate. Some of the fungi and algae may grown, increasing in soil and transportation with regional dust storms that carrying them, Figures 8,9 and 10 (Willard, et al, 2004, Elbert, et al , 2007 , Jassim, 2007).



Figure 8. Micro Spine in the studied dust storms samples of Baghdad, (relatively small at 18 to 25 μm) (Al- Khafaji, 2009).

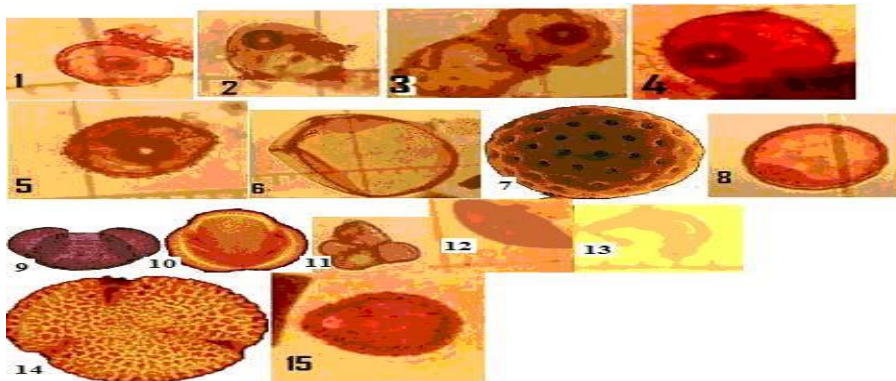


Figure 9. (1-6),cultivated Graminea, (7-8)-Chenopodea,9- bisacate Pinus, 10- Artemisia,11- Typha,(12-13)- Palmae,(14- 15)-Olea(Al- Khafaji, 2009).

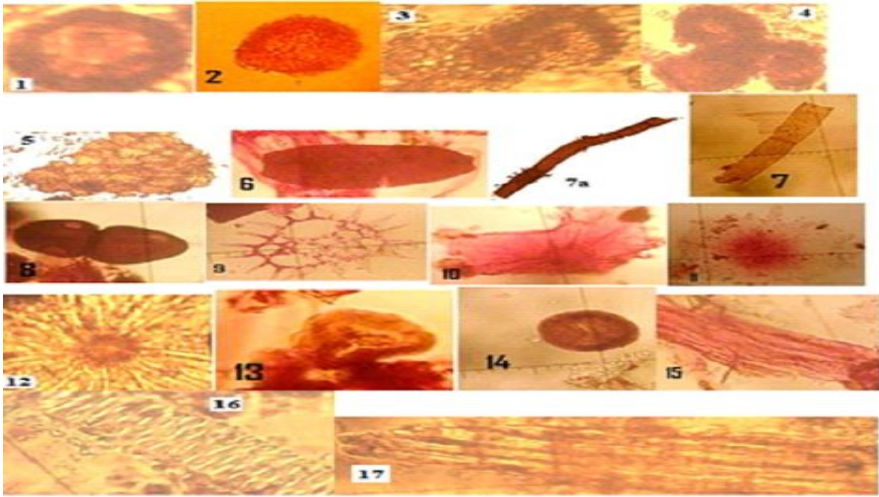


Figure 10. (1)- Sphagnum , (2)-Lycopodium,(4-8)- Fungi, (9-12)-Algae, (13-14)- Unnamed spores,(15- 17)-Cuticle(Al- Khafaji, 2009).

Table 2. Pollens isolates from dust storms in Iraq during March 2007 to October 2008) (Al- Khafaji, 2009).

Identified Pollen Grains	Number of Samples	Range percentages
Chenopodiaceae	21	3-83 %
Graminea	19	5- 70 %
Pine	14	10- 65%
Artemisia	8	0-50%
Palmae	6	0.0- 15%
Olea	4	0- 10%
Typha	3	0-5%
Spores , Fungi , Algae, & Micro Spines		
Cuticle	32	10 – 80 %
Fungi	26	3- 60 %
Algae	5	0- 20 %
Lycopodium	10	5- 75%
Sphagnum	3	0-8 %
Unnamed spores	2	0-6 %
Micro Spines	2	0-20%

6-Microorganisms Analyses for Bacteria, fungi and Viruses:

The Microorganisms in the dust samples were analyzed for Bacteria, fungi and Viruses. The samples were collected from many dust storms and many governorates. Accordingly, the results of the studied dust storms samples of Baghdad, Najaf, Ramadi, Wasit, Babel, Basra, and Karbala and Sallahaldin reflect that the prominent bacterial isolate was the gram-positive bacilli (*Bacillus* species) (40.6 %), then *E. coli* (8.38%), *S. pneumonia* (7.4%), *E. cloacae* (5.8%), *S. epidermidis* (4.1%), *P. aeruginosa* (2.9%), *S. aureus* (2.58%), *E. aerogenes* (1.9%), *P. mirabilis*, *K. pneumoniae* (1.6%) and *P. vulgaris* (0.64%) are all came in consequence respectively (Table 3). The fungal isolates, *Aspergillus* species (14.5%) and *C. albicans* (7.7%) were identified.

Many well - known pathogenic bacteria, fungi, and viruses are transmitted through airborne transport (e.g. the organism causing plague, anthrax, tuberculosis, influenza and Aspergillosis). The closest known association of dust storms and human disease of microbial origin are the out breaks of meningitis such as with *Staphylococcus aureus* (wide range of infections) *Bacillus circulans* (opportunistic), *Bacillus ticheniform* (opportunistic), (Wieser, and Busse , 2000 Kuske, et al., 2006, Drobniewski,1993, Jackson, et al , 1997, Taylor, and Jonsson, 2004) . Fungi are of health concern because many of them are aero allergens as *Aspergillus* and other as allergenic agent. It is clear that the *Bacillus* species were highest during April and May (spring season), may be due to many dust storms events in these months in Iraq and the environment was suitable for microbial growth or it might be due to transportation from the countries near to Iraq which have the same climate. The other dominant microbe isolated was *Aspergillus* species, which had a relatively high percentages at March, April, and May (in 2007) and declined at the same month in the year (2008), the reason may be that a certain elements in the climate in these months help this kind of fungi being in much quantities much more than during summer months (July and September). It was noted that *C. albicans* had a relatively high percentages at May, and July, which is believed to be due to the high temperature, high evaporation, and low relative humidity %, during these months that will assist the fungal growth and increasing in soil and transportation with regional dust storms which carrying them.

Table 3. Microorganisms isolates from dust storms in Iraq during a year period (From March 2007 to June 2008) (Al- Khafaji, 2009).

Isolated microorganisms	Number of isolates	percentage
Gram-positive cocci		
<i>Staphylococcus aureus</i>	8	2.58%
<i>Staphylococcus epidermidis</i>	13	4.19%
<i>Staphylococcus pneumoniae</i>	23	7.4%
Gram-positive rods		
<i>Bacillus species</i>	126	40.6%
<i>Gram-negative cocci</i>	0	0.0%
Gram-negative rods		
<i>Escherichia coli</i>	26	8.38%
<i>Enterobacter cloacae</i>	18	5.8%
<i>Proteus mirabilis</i>	5	1.6%
<i>Pseudomonas aeruginosa</i>	9	2.9%
<i>Klebsiella pneumoniae</i>	5	1.6%
<i>Enterobacter aerogenes</i>	6	1.9%
<i>Proteus vulgaris</i>	2	0.64%
Fungi		
<i>Aspergillus species</i>	45	14.5%
<i>Candida albicans</i>	24	7.7%
Total	310	100%

4. Conclusions

1- The main texture of most dust samples were sandy clayey silt, and to less extent clayey sandy silt, that depend on the energy and velocity of the wind from the regional dust storm which carries these grains. Also, the result of roundness of quartz grain reflects that they were transported over long distances.

2- The studied pollens reflect a wet - moist climate as indicated by the pollen grains. Such results may give good evidence of the regional dust storms that originated in faraway places as shown by the pine pollens that have sacs to keep pollen afloat and carried to great distances by the wind, as it could be from northern Syria, Turkey or transported from the countries near to Iraq which have the same climate. The allergens commonly associated with dust storms include fungal spores, plant and grass pollens, and organic detritus represent an agricultural area pollens grains. Some of the fungi and algae may grow, increasing in soil and transportation with regional dust storms which carrying them.

3- Regarding the bacterial isolates; Bacillus species were more common than others, followed by E.coli, S.pneumoniae, E.cloacae, S.epidermidis, P.aeruginosa, equal values is shared between P.mirabilis and K.pneumoniae, least value reported by P.vulgaris.

4- Regarding the fungal isolates; Aspergillus species was the common, followed by C.albicans.

5- Regarding the viral etiology; there is no any viral isolate among the work results.

6- The highest values of isolates regarding the bacterial and fungal etiology were among the late spring season months and early summer season due to increased dust storms incidence.

7- The Uranium concentration average absorbed dose and average external effective dose were calculated for dust of sandstorm at 2-4/7/2009 and 3-4/4/2010 for both cities Baghdad and Ramadi. All the results were lower than critical dose level, but the culmination of the dose of more than one sandstorm may have a damage effect.

8- During the strong dust storm affected Baghdad, and other Iraqi countries, reports from the Iraqi ministry of health and statistical analyses that have been done by researchers for many cases in many hospitals in

Baghdad and the governorates indicated that many people were taken to hospitals after sustaining breathing problems ,asthma, bronchitis and lung diseases.

References

Al-Dabbas, M., Abbas, M.A. and Al- Khafaji, R., 2011. The Mineralogical and Micro-Organisms Effects of Regional Dust Storms over Middle East Region, International Journal of Water Resources and Arid Environments 1(2): 129-141, 2011.

Al-Dabbas, M., Abbas, M.A. and Al- Khafaji, R., 2012. Dust storms loads analyses /Iraq, Arab J Geosci (2012), Vol .5, Issue 1, pp 121 – 131.

Al- Khafaji, R. M. N., 2009. Effects of Dust Storms on Some Iraqi Territories , Ph.D., thesis, College of Science, University of Baghdad.

Alonso-Pérez, S., Moutaz Al-Dabbas, A. Abd Ali, Tahir H. H. Al-Waeli, 2013. Establishing a National Programme to Combat Sand and Dust Storms in Iraq, Spanish National Research Council (CSIC)/Meteorological State Agency of Spain (AEMET), Spain, Santa

Cruz de Tenerife.

Al-Saad H. T. and Abed S., N., 2006. The contamination Air, Univ. of Basrah, center Science Sea, First edit, p. 84-85 (In Arabic).

BEIR ,2006, Health risks from exposure to low levels of ionizing radiation. BEIR VII-Phase 2 (Free Executive Summary). National Academy of Science, U.S. <http://www.nap.edu>.

Bolorani, Ali Darvishi, Seyed Omid Nabavi, Rasoul Azizi, Mousa Kavosi, Esmail Abasi, Fardin Mirzapour, Hossain Ali Bahrami ,2012. The investigation of dust storm entering the west of Iran using remotely sensed data and synoptic analysis, Recommendations dust and dust

storms Conference (20 to 22 November 2012) State of Kuwait.

Cook, A. G. ; P. Weinstein, and J. A. Centeno , 2005. Health effects of natural dust- role of trace elements and compounds. Biol. Trace.

Craver, R. E., 1971. Procedures in sedimentary petrology, John Willey, New York, p. 653.

Delfino, R. J. ; Sioutas, C. and Malik , S., 2005. Potential role of ultrafine particles in associations between airborne particle mass and cardiovascular health. Environ. Health Prospect. 113:934-946.

Drobniewski, F.A., 1993. *Bacillus cereus* and related species. Clin Microb Rev. 6:324-338.

- Elbert, W. , Taylor, P. E. , Andreae, M. O. and Poschl, U., 2007. Contribution of fungi to primary biogenic aerosols in the atmosphere: wet and dry discharged spores, carbohydrates, and inorganic ions, *Atmos. Chem.. phys.*, 7: 4569-4588 .
- Ezeamuzie, C. I., M. S. Thomson, S. Al-Ali, A. Dowaisan, M. Khan, and Z. Hijazi. 2000. Asthma in the desert: spectrum of the sensitizing aeroallergens. *Allergy* 55:157-162.
- Folk, R.L. , 1974. petrology of sedimentary rocks, Hemphill, Austin, p.182 .
- Garrison, VH. , Foreman, WT. and Genwaldi, S. *et al.*, 2006. Saharan dust-a carrier of persistent organic pollutants , metals and microbes to the Caribbean . *Rev. Biol. Trop. J.* 54(Suppl.3):9 - 21 .
- Griffin, D.W., 2007. Atmospheric movement of microorganisms in clouds of desert dust and implications for human health . *Csm Org.* 13: 450 – 477.
- Griffin, DW. , Kubilary, N. and Kocak, M. ,2007 . Airborne desert dust and aeromicrobiology over the Turkish Mediterranean coastline. *Atmospheric environment* 41: 4050 – 4062 .
- Hodges, L., 1973. Environmental pollution survey emphasizing physical and chemical principles, New York, Holt Rinehart and Winston.
- Iraqi Meteorological Department, 2012.General Climatological Data of all Meteorological Stations, directorate of climatology, and directorate of Hydro- and Agricultural Meteorology, Ministry of Transportation/ Iraqi Meteorological Organization.
- Jackson, N.,O. , Schmiieger, H., Kayiko, M. ,1997. *Bacillus cereus* may produce two or more diarrhea enter toxin. *FEMS ,Microbiol Lett.* 149: 245-248.
- Jassim, S. Y., 2007. Palynological and archaeological evidence for early Mesopotamia during quaternary, Unpub. Ph.D. ,thesis, University of Baghdad.
- Kuske, C. R. ; Barns, S. M. ; Grow, C. C. ; Merrill, L. ; Dunbar, M. S. and Dunbar, J., 2006 . Environmental survey for four pathogenic bacteria and closely related species using phylogenetic and functional genes, *J., Forensic Sci.*, 51: 458- 558 .
- Mahdi , Kh. H., Nasif, R. M. and yassin , K. A. j., 2011. Measurements of radioactivity pollution of dusty storms in middle and west parts of Iraq at 2007 and 2008. *Kufa Univ. Journal of Physics*,2(3).
- Marouf,B.A. ,2012. Assessment of Possible Health Effects of Potential Exposure to Uranium Contamination in the Tuwaitha/Ashtar Village Area, Iraq: Health Effects Due to Uranium Contamination in Iraq,ASTF special publication ,UAE.
- Martiny, J. B. ; Bohannon, B. J. ; H. Brown, J.; Colwell, R. K. ; Fuhrman, J. A. ; Green, J. L.; Horner-Devine, M. C. ; Kane, M.; Krumins, J. A. ; Kuske, C. R.; Morin, P. J. ; Naeem, S.; Ovreas, L.; Reysenbach, A. L. ; Smith ,V. H. and Staley, J. T., 2006. Microbial biogeography: putting microorganisms on the map. *Nat. Rev. Microbiol.*

4:102-112.

Middleton N.J., 2001. Dust storms in the Middle East. *J Arid Environ* 1986,10:83-96.

Moore, P. D. and Webb, J. A., 1978. An illustrated guide to pollen Analysis. , Hodder and Stoughton, London, 133 pages and 48 plates.

Power .M.C., 1953, Anew Roundness Scale for Sedimentary particles. *J. Sed. Pet.* 23:117-119 .

Prospero , J. M. ,1999. Long – rang transport of mineral dust in the global Atmosphere , impact of African dust on the environment of the south east United states , the national academy of sciences colloquium , geology mineralogy and human welfare ,vol. 96 ,issue 7 :3396-3403 .

Taylor, P. E. and Jonsson, H., 2004. Thunderstorm asthma, *Curr. Allergy. Asthm. R.*, 4: 409-413.

UNEP, WMO, UNCCD., 2016. Global Assessment of Sand and Dust Storms. United Nations Environment Program, Nairobi.139p.

WHO, 1996. Air Quality Guide Lines for Europe, Copenhagen, World Health Organization, Regional office for Europe.

WHO, World Health Organization, 2004. Manual for the virological investigation of polio,(4th ed.).

Wieser, M. and Busse HJ. , 2000 . Rapid identification of *Staphylococcus epidermidis* . *International Journal of Systemic and Evolutionary Microbiology* 50:1087 - 1093 .

Willard, D. A. ; Cooper, S. R. ; Gomez, D. and Jensen, J., 2004. Atlas of pollen and spores of the Florida Everglades, *Palynology*, Vol. 28, pp. 175-227.

Review of Dust Control Projects in Ahwaz, Iran and Solutions toward Sustainable Development

Ali Hamidian, Mahsa Abdolshahnejad, Mahin Hanifehpour

National Campaign for Desert, Iran, hamidian_a@ut.ac.ir
University of Tehran, Iran

Abstract

Dust as a climatic phenomenon has led to environmental challenges and impacts even on human health and also economy. Identifying sources of dust is addressed as the first step for management process. In this case, different studies and research projects in Iran such as mineralogy studies, investigating chemical and physical characteristics of sediments, remote sensing projects, dust recognition algorithms and wind erosion susceptibility maps. Ahwaz, a metropolitan city in South-western Iran, has always suffered from dust, desertification and land degradation. In this research, recent projects in this city in order to dust control have reviewed and its outcome have discussed. After identifying source points of dust, different solutions have highlighted. According to the results, source points in the study area according to land use and total area are degraded range lands, rain-fed agricultural fields, bare lands, wetlands, dried out water reservoirs and irrigated farm fields. In order to successful dust control these solutions are recommended: improvement of management techniques, consideration of land capabilities, proper land use schemes, revising in water resources management policies, determining effective techniques for erosion sources fixation and definitely addressing people co-operation and collaboration in all projects..

Keywords: Dust, source points, Ahwaz, desertification

Monitoring of Irrigable Agricultural Lands in Euphrates-Tigris River Basin (Syria-Iraq)

Ayhan ATEŞOĞLU*, Talha Berk ARIKAN, Saffet YILDIZ

Bartın University, Faculty of Forestry, Dept. of Forestry Engineering, Bartın, Turkey

Keywords: *Middle East, Collect Earth, Sand/Dune Source, Euphrates-Tigris River*

Extended Summary

The desert dust resources in the Middle East cause significant problems in the agricultural areas, especially in the countries where they are located and in close neighbors because they cause erosion, especially air pollution (Sivakumar 2005). Soil and vegetation destruction caused by wind-erosion along with Middle East-based dust sources poses a major problem in the context of land management (Stefanski 2007). The Middle East region hosts large dust resources such as Syria-Iraq deserts and Arabia deserts. In Iraq and Syria, where the Euphrates and Tigris rivers pass through and the agricultural activities are conducted in the restricted area, mainly the inefficiency of agricultural areas, losses of livestock farming, soil fertility, transportation, and economic and environmental losses are observed due to the wind erosion caused by dust sources (Sissakian et al. 2013). Middle East region has been chosen as the study area. In the world report of The European Space Agency's (ESA) Global Land Cover Map 2009, the map of Middle East land classification consisting of Turkey, Iraq, Syria, Jordan, Israel, Palestine, Saudi Arabia, United Arab Emirates, Yemen, Oman, Lebanon, Bahrain, Kuwait and Qatar is given in Figure 1.

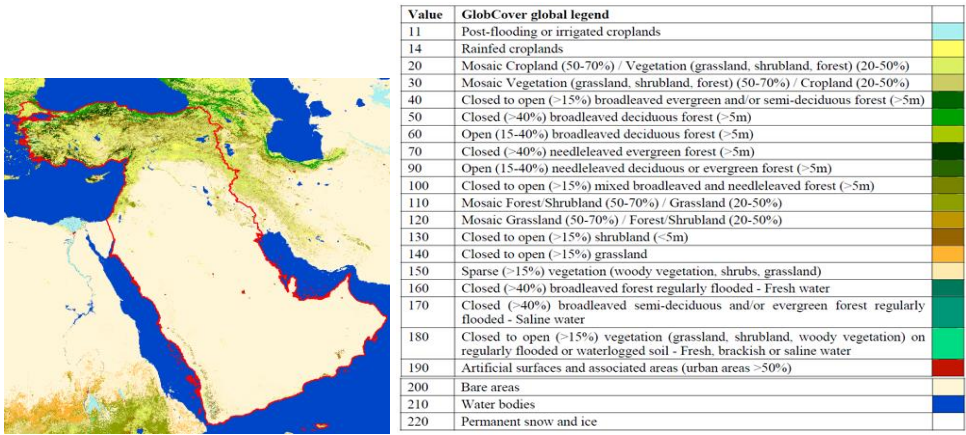


Figure 1. European Space Agency (ESA) 2009 world report Middle East land use classes.

In the ESA land use classes, 11, 14, 20, 30 coded fields illustrate the classes belonging to the agricultural category, and 200 coded fields to bare areas and 210 coded fields to water resources. The data of water and agricultural areas in the Middle East have obtained from the ESA data. Within the context of the "Global Forestry Inventory and Drylands Assessment Project" of the Food and Agriculture Organization (FAO), the status of arid areas was determined using

Collect Earth software, by evaluating primarily forest areas, agricultural areas, shrub areas, pasturelands and other areas. For this purpose, Open Foris Collect Earth software (Open Foris, 2016, Bastin et.al., 2017) was used as the methodology (Figure 2). Using the Collect Earth methodology, approximately 15000 plot areas (0.5 ha) were evaluated in the study done in Antalya / Turkey and a database related to land cover/use classification, greening/desertification was created. In this dataset, there are data on dust sources in both classes called 'sand' and 'dune' as the land class.

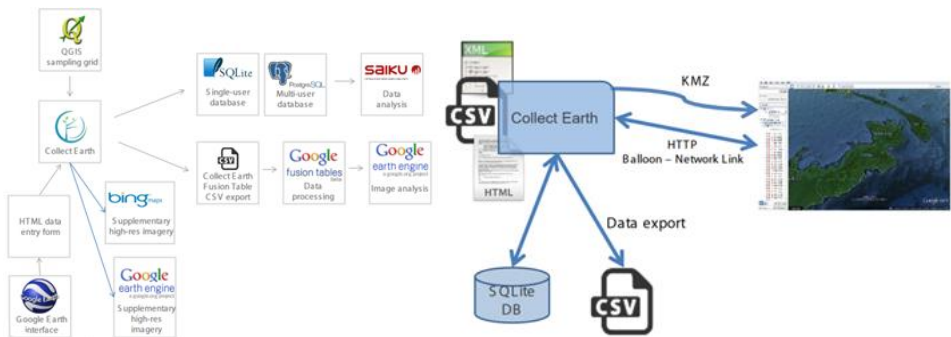


Figure 2. Open Foris Collect Earth.

As a result of the study done;

- 76.47% of the entire Middle East (4362429 km²) is dust resources consisting of sand and desert dune land classes. This high rate threatens vegetation in other land use classes, especially in the Middle East agricultural areas. Considering the current conditions of Iraq and Syria and the changes in land use, the primary factor that causes agricultural areas to become ineffective by exposing them to dust transportation by the influence of wind is the dust resources in the region.
- Using the 'sand/dune' land classes on the basis of the dataset created in the context of FAO's "Global Forestry Inventory and Drylands Assessment Project", a map of risk level classes for the entire Middle East region was created. In the southern part of the Middle East, level 1 and 2 dust resources regions risk classes are located, while the largest dust sources areas in the region are at the level 3 risk class. The countries of Iraq and Syria, which constitute the focal point of the research, are located in the region of the level 3 dust resources mostly. 63.6% of the total area in Iraq, and 53.7% of the total area in Syria constitute level 3 dust resource regions
- **71.3% of the water areas in Iraq, mostly formed by Euphrates and Tigris, are located in the level 3 risky dust resources region. For Syria, these rates are 6% for water areas in the level 3 risky dust resources regions and 27.4% and 25.9% for those in the level 4 and 5 risky dust resources regions, respectively. This requires that the country be sensitive in planning related to water assets and water use. 25.90% of Syria, 10.50% of Iraq is located in the level 3,4 and 5 risky dust resources region. The rest of the agricultural land is threatened by current dust resources and dominant wind directions (Figure 3).**

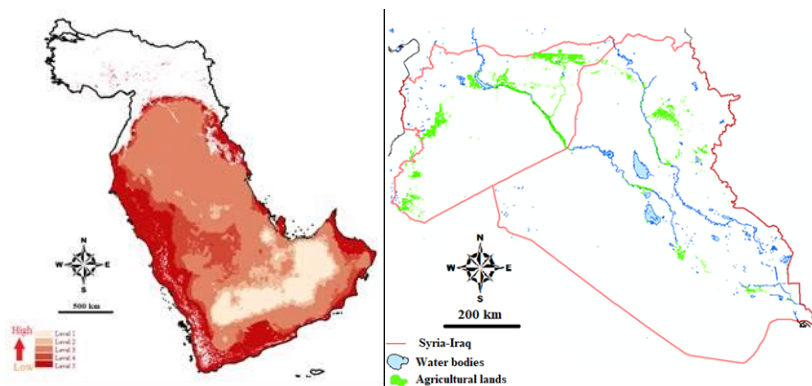


Figure 3. Sand/dune resource regions for the Middle East (left); Agricultural lands within the dust resources regions of Syria and Iraq (right)

In addition to, within General Directorate of Combating Desertification and Erosion in T.C. Ministry of Forestry and Water Affairs, a study was conducted for the detection of desertification-greening trends areas in the buffer zone of 111386.80 km² in Euphrates and Tigris rivers (10 km wide) within the borders of Syria and Iraq with the help of 8152 plot with a size of 0.5 ha by using Collect Earth methodology. As a result of the work carried out in order to monitor and evaluate the vegetation areas, mainly agricultural areas, 193749 ha greening and 73149 ha desertification area were detected between 2001-2016 years (Figure4). A significant increase in the amount of greening, that is vegetation, in the agricultural areas along the Euphrates and Tigris rivers is the evidence of the protection of existing vegetation because the agricultural areas, vast majority of which is located in the third-degree sand/dune resources regions can be irrigated despite the problems of available dust resources and this provides soil aggregates to merge.

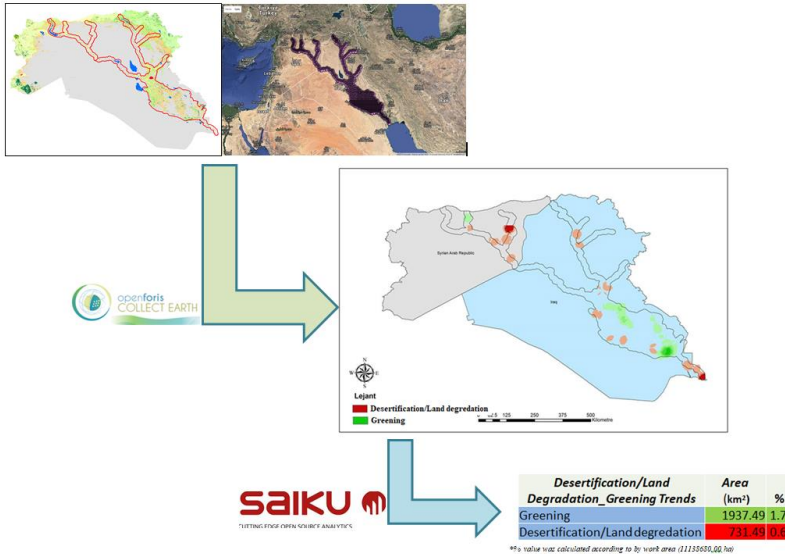


Figure 4. Multi-purpose land monitoring project in Euphrates and Tigris rivers

Acknowledgements

We thank the 20 operators who participated in the Global Drylands Assessment in Antalya/Turkey via General Directorate of Combating Desertification and Erosion; FAO staff who supported it; Danilo Mollicone: Forestry Officer and Project Lead Technical Officer, Forestry Department; Çağlar Başsüllü: FAO's Subregional Office for Central Asia.

References

Bastin J.F., Berrahmouni N., Grainger A., Maniatis D., Mollicone D., Moore R., Patriarca C., Picard N., Sparrow B., Abraham E.M., Aloui K., Ateşoğlu A., Attore F., Başsüllü Ç., Bey A., Garzuglia M., Garcia M.L.G., Groot N., Guerin G., Leastadius L., Lowe A., Momane B., Marchi G., Patterson P., Rezende M., Ricci S., Salcedo I., Diaz P., Alfonso S., Stolle F., Surappaeva V., Castrı R., (2017), *The extent of forest in dryland biomes*, Science, doi: 10.1126/science.aam6527

Open Foris, (2015) Free Open-Source Solutions for Environmental Monitoring, <http://www.openforis.org/> [Accessed 11 July 2017].

Sissakian V.K., Nadhir A., Sven K., (2013), *Sand and dust storm events in Iraq*, Natural Science, doi: <http://dx.doi.org/10.4236/ns.2013.510133>

Sivakumar, M.V.K., (2005), *Impacts of sand storms/dust storms on agriculture*, Natural disasters and Extreme Events in Agriculture: Impacts and Mitigation (Mannava V.K., Sivakumar R.P., Motha H.P.D. Ed,) Springer-Verlag Berlin Heidelberg Press, Netherland, ss.159-177.

Stefanski R., (2007), *Impacts of sand and dust storms on agriculture and potential agricultural applications of a SDSWS*, WMO/GEO SDSWS Meeting – Barcelona, Spain.